# Study on operational characteristics of low power atmospheric pressure microwave plasma spray method

# （低電力大気圧マイクロ波プラズマ溶射法の動作特性の研究）

July, 2016

Doctor of Engineering

AHMAD REDZA BIN AHMAD MOKHTAR

アハマド　レザ　ビン　アハマド　モクタル

Toyohashi University of Technology

別紙４（課程博士）

Date of Submission:
平成　28　年　07　月　15　日

| Department 機械工学専攻 | Student ID Number 学籍番号 | 第 071202 号 |
|---|---|---|
| Applicant's name 氏名 | AHMAD REDZA BIN AHMAD MOKHTAR | |

| Supervisors 指導教員 | 安井　利明<br>福本　昌宏 |
|---|---|

**Abstract**

# 論文内容の要旨　(博士)

| Title of Thesis 博士学位論文名 | Study on operational characteristics of low power atmospheric pressure microwave plasma spray method<br>(低電力大気圧マイクロ波プラズマ溶射法の動作特性の研究) |
|---|---|

(Approx. 800 words)
(要旨　1,200 字程度)


Plasma spraying method is the most versatile coating technique for the deposition of high melting point materials such as ceramics and cermet which is used in the application of wear, corrosion and heat resistance. It uses the heat source generated by direct current, radio frequency or microwave as the power source to melt the spray particles which were injected either axially or radially inside the plasma plume. The accelerated particles will collide and impinged onto the surface of the substrate to fabricate the coating. Conventional plasma spray method possesses very high temperature plasma (above 10000 K) at high power (above 40 kW) which is very useful to fabricate high melting point material coating. However, the excessive heat input from the plasma may influence in deterioration of material phase structure in some material such as ceramics and degraded some functions as well as the difficulty to fabricate coating onto low melting point substrate such as plastics, resin and polymers. Here, the need of using low power plasma to reduce the heat input onto spray and substrate material is being focused and microwave plasma is seen as a good candidate due to its stability in wide range of pressure and easy to be generated at low power. Microwave is rarely been used as the plasma power source due to the unknown mechanism and the stabilization factor of the process. Our research group has managed to generate the plasma with microwave at 1.0 kW of power in atmospheric condition and succeeded to fabricate Cu, Al and Hydroxyapatite coating. However, the mechanism and characteristics of the process is not studied well yet. Thus, the main objective of this research is to study the operational characteristics of low power microwave plasma spray method and its applicability in reducing heat input towards spray and substrate materials as the specialty of this technique. Moreover, the improvements and renovation of the spray device are also studied and presented.

Firstly, the study on operational characteristics of microwave plasma spray in compare to conventional plasma spray is conducted. Here, it is known that the microwave plasma spray method possesses the heat efficiency comparable to the conventional plasma spray which is at the average of 30 %. The microwave plasma can be generated and stabilized down to 0.3 kW as the result received on plasma ignition study. The study on plasma and spray particles behaviour of microwave plasma spray shows that the plasma has the average temperature of over 4000 K and particle velocity of 135 m/s at the maximum parameter. The substrate temperature study shows that the suppression of temperature is able to be achieved for the application onto heat susceptible substrates.

The next study is worked on the applicability of microwave plasma spray in reducing the heat input onto substrate material. Here, the Cr coating onto carbon fiber reinforced polymer (CFRP) was conducted. The CFRP is focused in recent studies due to its property of high strength to weight ratio but due to the polymer matrix, the material surface struggles at wear and corrosion resistance in which the hard chrome coating is crucial to overcome this disadvantage. The conventional method for this coating production is hard chrome plating. However, this method needs control environment due to hazardous waste and slow in production which made the microwave plasma spraying method to be seen as the alternative method. Chromium coating has been successfully deposited onto CFRP substrate with coating microhardness higher than the average in hard chrome plating at above 1100 Hv. The emergence of Cr oxides confirmed by X-ray diffraction analysis is thought to be the factor contributing towards the increasing hardness of the coating. Chrome particles were mostly gathered onto the carbon fiber which appeared after the resin parts were melted by the plasma heat and this suggest that the mechanism of bonding is mostly by the mechanical interlocking.

The research is furthered on the applicability of microwave plasma spraying method at suppressing heat input onto spray materials where the study on coating deposition of $TiO_2$ with low heat effect onto spray material is conducted. Titanium dioxide is a photocatalyst material focused in recent studies because of its magnificent properties where it possesses photocatalytic activity such as the ability to remove the air pollution substance and deodorizing function. Generally, the deposition method of a titanium dioxide coating is carried out by the fixation of titanium dioxide powder with an organic system binder but it will let the degradation of the powerful catalytic reaction of a titanium dioxide. Therefore, thermal spray is thought to be the alternative method but this method will induce transformation from anatase phase with high photocatalyst activity to rutile phase with low photocatalyst activity due to excessive heat. As a result, the maximum of 83 % of anatase content rate is achieved at optimum condition which suggests that the suppression of heat input onto spray materials is successfully obtained by using microwave plasma spray method. From the coating deposited by 99 % of rutile content rate titanium dioxide powder, the anatase content rate increased inside the as-sprayed coating proved that the nucleation of anatase phase occurred during the spray. The anatase content rate inside the as-sprayed coating is increased with the decrease of substrate temperature due to rapid cooling.

In fifth chapter, the research tasks and future perspectives of low power microwave plasma spray device are discussed. Here, the research tasks are divided into three categories which cover the improvement in coating deposition, the device itself and enhancement that should be made. Some of the required optimizations of the current device are particle velocity, powder feeding method, antenna structure, etc. For improvement of particle velocity, electromagnetic pinch thrust by magnetic nozzle is considered and the experimentations as well as the magnetic field simulations are conducted. Simulation results help in obtaining the structure of magnetic nozzle and experimentation results show some improvement in particle velocity and plasma temperature by the use of magnetic nozzle. However, due to the elevated particle velocity is still low, further investigation should be made.

In conclusion, this newly investigated method proved its specialty in low power plasma spray at extremely low power and its efficiency to deposit coating with suppress heat input effect onto substrate and spray materials. Future research should be conducted to improve some of its feature towards realizing this method in the mainstream of thermal spray technique.

# Table of Contents

**Page No.**

## Chapter 3

**Deposition of coating with supress heat input effect onto substrate materials**



## Chapter 4

**Deposition of coating with supress heat input effect onto spray materials**

## Chapter 5

**Research tasks and future perspectives**



## Chapter 6

**General conclusions**

# Chapter 1

# Introduction

## 1.1 Surface engineering

There are numerous products which resulted from a touch of surface engineering process. The bulk material is usually been surface engineered for some desired purposes. Originally, it has been directed to improve some properties of bulk component such as wear resistance, corrosion and oxidation resistance, reduce degradation rate due to environmental affect, thermal insulation and electrical properties, catalytic function, etc. [1]. But nowadays, the competitiveness in surface engineering technologies not only requires good properties but also the component with good appearance, artistic, aesthetics and low cost in manufacturing. Coating technology is one of surface engineering method which can be used for substituting the desired properties in application. Coating technology is a modification treatment of surface by adding new materials on the surface of substrates [1]. There are a lot of variety of coating processes, in which some of them are; CVD (chemical vapor deposition), PVD (physical vapor deposition), spraying, electroplating, cladding and etc. Each process has its own advantages and disadvantages, hence the chosen process depends on several factors and purposes, cost, aesthetics, etc.

## 1.2 Fundamentals of thermal spray method

Thermal spray is one of the methods to fabricate thick coatings by utilizing the thermal energy which produced from the combustion of gas plume, electrically formed thermal arc etc. Thermal spray processes are mostly used to obtain metallic and non-metallic coatings, and include four major groups of processes: spray combustion processes, electric arc spray process, cold spray and the plasma spray

process [2]. Plasma spray is the most versatile of the thermal spray processes. Plasma is capable of spraying all materials that are considered spray-able. Figure 1.2.1 shows the schematic of plasma spray process. The coatings is fabricated by involving the following mechanisms, which is started by heating and acceleration of spray particles inside the plasma plume, then the melted particles are impinged onto the surface of the substrates, and finally flattened particles are then rapidly solidified to form the coatings. Plasma spray process is generally been represented by direct current (DC) plasma where the plasma is generated by direct-current arc electric discharge and radio frequency (RF) plasma, where the plasma is generated by the discharge of radio-frequency. Microwave (MW) is the third plasma source power which is very similar in process to RF power source, but with increase in the frequency for plasma discharge. These plasma spray technology are able to produce approximately 5000~20000K of extremely high temperature plasma. This feature of the thermal plasma made it possible to melt even the high melting point materials such as ceramics and cermet (such as WC-Co), in order to fabricate the coatings [3].

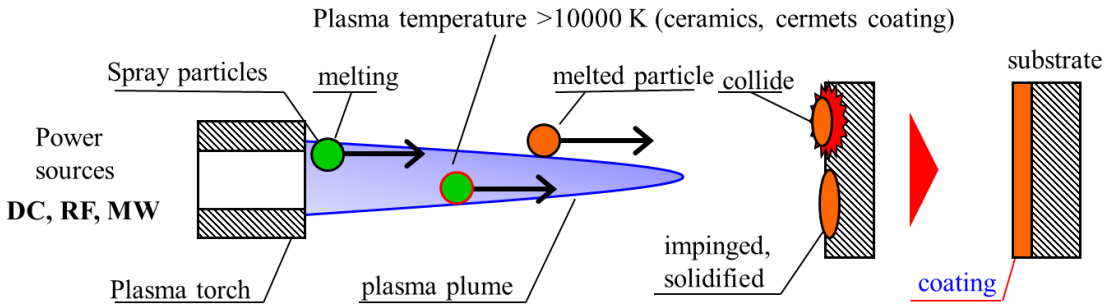


Fig. 1.2.1 Schematic of plasma spray process.

The factors effecting the thermal spray coating process is listed in Table 1.2.1. From this, it is known that there a various factors which will contribute towards achieving the target coating in thermal spray method. Among these factors, the particle velocity and particle temperature are the parameters deem to be the utmost important in plasma spray process. For conventional plasma spray method, particle velocity of above 100 up to several thousand m/s is needed to obtain quality coating

enough for the desired purposes [4]. However, the microwave plasma spray device of our laboratory is still struggling to achieve such speed and the modification and study towards realizing it is still on pursuit. The measured particle velocity obtained up until now is approximately 60 m/s [5]. Particle temperature need to be known to get the idea of what kind of state the particle was inside the plasma where the particle temperature of above the melting temperature of the particular materials may lead to the assumption that it already reached fully melted state. This will result to better impingement of the spray particles onto substrate's surface.

Table 1.2.1 Factors effecting the plasma spray coating process

| Spray stream | Material feed | Gun | Substrate |
|---|---|---|---|
| 1. Temperature<br>2. Velocity<br>3. Spray distance<br>4. External environment<br>5. Turbulence | 1. Particle size/shape<br>2. Injection method and geometry<br>3. Carrier gas, flow and velocity<br>4. Chemical and physical properties | 1. Nozzle geometry<br>2. Power<br>3. Gas flows<br>4. Gas composition | 1. Surface contamination<br>2. Surface profile<br>3. Temperature<br>4. Chemical and physical properties |

However, it has been mentioned as a problem of the conventional plasma spray where the excessive heat input from plasma will cause a remarkable change of material structure to the spray materials, both spray particles and substrates, which delivered towards difficulties in obtaining the target coatings. For an example, hydroxyapatite, which is a biomedical material, could be decomposed to a harmful phase by the thermal spray deposition using high input power at 40 kW [6, 7]. Thus, the thermal spray method which is able to control the change of the material micro-structure of these thermal spray materials is called for. Therefore, the research of the low input power plasma spraying process which expects the control of the heat input to the spray material is advancing in recent years [8, 9].

## 1.3 Low power atmospheric pressure microwave plasma spray

Low power plasma spray method [10] is defined as a thermal spray method generated with low input power of below 5 kW in the heat source. The effects of lowering the input power of the thermal spraying equipment by the plasma production at low electric power as well as the effects of controlling the heat input to the spray material (control of the significant change of material structure) by low input power plasma are expected and the research is advancing in recent years. However, the input power of Cu coating deposited by conventional DC plasma spray method under atmospheric pressure condition which was reported is approximately 5 kW [11, 12] while deposition of coating by using RF plasma spray under atmospheric pressure condition is reported to be difficult due to the difficulty in stabilizing the plasma [13]. On the other hand, with the input power of several kilowatts or less, thermal plasma generation under atmospheric pressure is possible for microwave plasma spray method. For this reason, it is thought that the coating deposition with controlled heat input to the thermal spray material is possible by applying microwave plasma as a low input power plasma spray process. Moreover, this microwave plasma does not require electrode for electric discharge, which made it possible to generate plasma from chemically reactive type of gases if being compared to DC plasma in which the electrodes are needed for electric discharge. Furthermore, compared to DC plasma arc, microwave plasma has a lot of features such as plasma can be produced with relatively low input power, discharge power, plasma intensity, discharge frequency are wide, etc. [14]. Since it has such a feature, in recent years, microwave plasma was applied in a wide range of fields, such as decomposition processing of harmful gas, heat treatment of waste, sterilization of medical material, and deposition of thin film [15]. However, since the efficiency of microwave plasma discharge is bad and the difficulty of producing high temperature plasma, there are only few examples of the application towards plasma spraying method. On the other hand, in our laboratory, the problem of the microwave plasma in the afore-mentioned was solved, and the low input power atmospheric pressure plasma spraying device which used microwave power for the heat source was investigated [16]. Detailed explanation of this thermal spraying equipment is specified in Chapter 2. In our laboratory, research is advancing in order to make an appeal for the low input power

atmospheric pressure microwave plasma to be applied to the mainstream of plasma spraying process.

## 1.4 Mechanism of plasma spray methods

A. Ganguli et. al. made a thorough study on the difference of plasma sources [17]. They also included the breakdown mechanisms of DC plasma in compare to RF/MW power source. The mechanism of RF and MW is discussed to be quite similar due to the existence of high frequency wave to the breakdown mechanism and the only difference is MW discharge use much higher frequency at the range of between a few GHz and several GHz, the frequency 2.45 GHz being the most common while RF discharge at 1 to 100 MHz. The summary of the mechanism of plasma generation by these plasma sources are as follows.

DC Breakdown mechanism: A schematic of the set-up used for obtaining a DC discharge is shown in Fig. 1.4.1. The operation of the discharge in steady state can be understood as follows [18, 19]. Imagine an electron leaving the cathode surface. Let $\alpha$ be the probability that this electron will ionize a gas atom as it travels 1 cm along the discharge tube (a is the first Townsend coefficient). This results in an amplification factor of $\exp(\alpha d)$, i.e. $\exp(\alpha d)$ electrons are released as the primary electron reaches the anode at distance d. This also implies that $\exp(\alpha d)$ ions are produced by the primary electron. To preserve charge neutrality in steady state, these ions have to be given up at the cathode. On striking the cathode the ions produce secondary electrons with efficiency g (g is the second Townsend coefficient.). Thus $g \exp(\alpha d)$ electrons are released by the bombarding ions. It is assumed that one electron leaving the cathode, which had eventually been lost by recombination at the anode. Thus, to compensate for the loss of this electron and to keep the discharge going, the ions bombarding the cathode must release at least one secondary electron. It is to be noted that the continuous loss of electrons to the anode represents a rather severe loss to the system. It renders the dc discharge quite inefficient, since the lost electrons have to be constantly replenished by the release of secondary electrons into the system, i.e. by ion bombardment of the cathode. Thus, the plasma densities obtained in the dc discharge are rather modest.

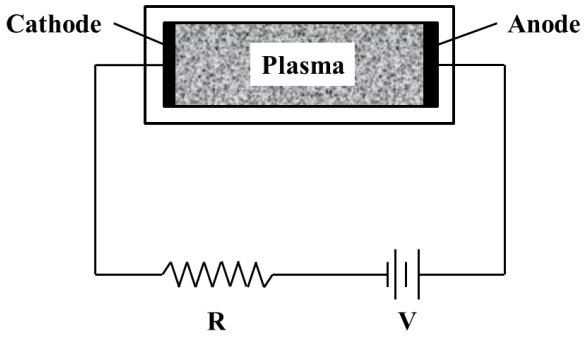


Fig. 1.4.1 Schematic of a DC discharge system.

Figure 1.4.2 shows the schematic of a DC plasma spray system. In DC plasma spray, a high current arc is used to generate a thermal plasma jet [20]. The arc is started by high frequency high voltage ignition and maintained by DC power supply. Inert gases passing the gap between the electrodes are heated up by the arc. Thereby monoatomic gases like argon or helium are partially ionized and molecular gases like hydrogen or nitrogen are dissociated prior to ionization. During recombination of ions and electrons and reformation of molecules, energy is set free and results in temperatures of the plasma jet up to 10000 K in the core at the gun exit. Due to the extreme increase in temperature, there is strong acceleration of plasma gases inside the plasma torch.

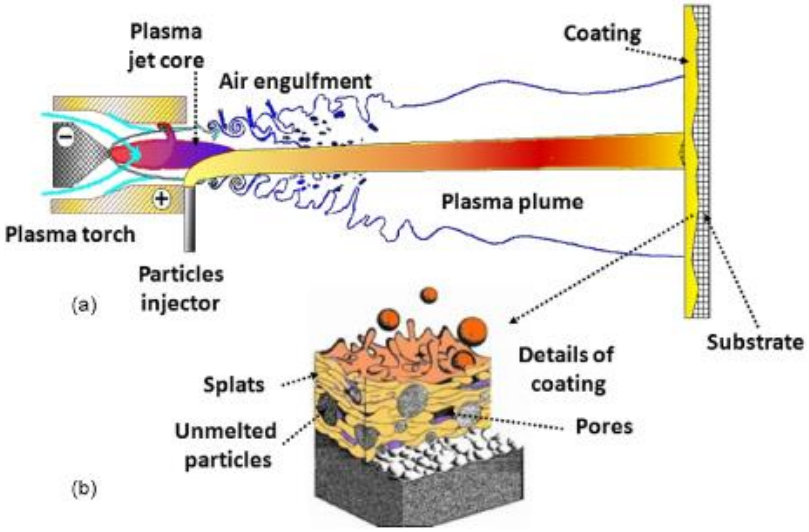


Fig. 1.4.2 Schematic of a DC plasma spray system [20].

RF/MW breakdown mechanism: In the presence of a DC electric field, an electron can keep gaining energy continuously till it has sufficient energy to ionize a gas atom. Collisions (elastic), therefore do not play any significant role in the ionization process in such discharges, except to retard the motion of the electrons. In RF/MW discharges on the other hand, the electrons can only gain oscillatory energy from the ac fields. In the absence of collisions, the electron motion is coherent and no power can be absorbed from the RF/MW fields once the oscillatory motions have acquired their steady-state values. For moderate field strengths, this oscillatory energy could be far short of the ionization energy, so that the ionization efficiency should be poor. This however is not the case, since even for moderate RF/MW powers fairly modest plasma densities can be obtained. The latter feature is primarily due to the role played by the collisions in the ionization process. When an electron suffers a collision, its oscillatory motion is disturbed and its momentum randomized. In steady state, the average value of the random energy is such that the energy imparted to the neutral gas atoms in a collision equals the energy gained by the electrons in the time between two collisions.

Figure 1.4.3 shows the schematic of RF plasma spray system. Radio frequency plasma spray utilizes a plasma jet that is generated by inductive coupling of electrical energy into a gas stream [21]. The advantage of this method is the generation of thermal plasma jet without contact of the generating components with the plasma gases. Therefore, even highly reactive gases, including oxygen and gas mixtures without the concern of eroded electrode materials into the coatings like the one in DC plasma spray. These days systems with powers typically between 25 to 100 kW are available. The temperature inside the plasma jet usually does not exceed 10000 K. In contrast to DC plasma spray, highest temperature is not achieved in the plasma jet core due to maximum temperature shifts to the jet fringes as a consequence of the skin effect. For spraying under atmospheric condition, particle velocity are relatively low (<50 m/s) and plasma is difficult to be stabilized. Gravity is commonly used to achieve the highest possible velocity. Therefore, the RF plasma spray systems are commonly operated in vacuum condition. For vacuum plasma spraying with RF plasma torches, even supersonic flow conditions are possible. However, the plasma jet diameter is reduced accordingly and the reduced chamber pressure results in significantly decreased energy density.

The main shortcomings of RF plasma spray are the poor flexibility concerning handling of the torch, the stiff power supply design and the strong electromagnetic fields that prevent use of electronically controlled substrate handling system. Therefore, the most important applications of RF plasma spray are the spheroidization of powders [22-23] and the analysis of materials by emission spectroscopy after complete evaporation in the thermal plasma jet [24].

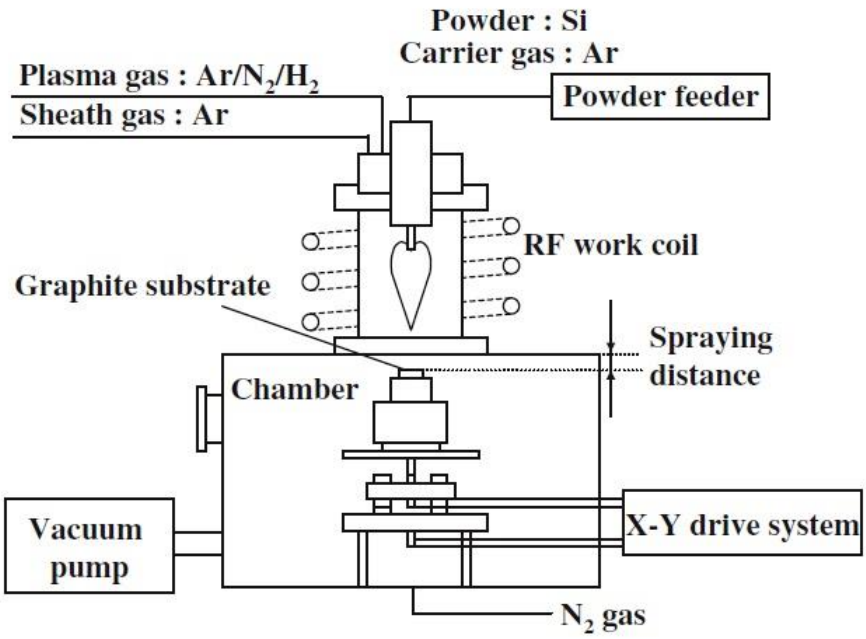


Fig. 1.4.3 Schematic of an RF plasma spray system [21].

As in RF discharges, MW discharges can be operated both with and without external magnetic fields. When operated without external magnetic fields, MW discharges usually use frequencies between a few GHz and several GHz, the frequency 2.45 GHz being the most common. Due to the high frequencies involved, the power is almost invariably coupled through radiation, which bypasses all sheath losses. The antenna can be located either inside the vessel or outside. (In either case, the entire set-up has an electromagnetic (EM) shield to avoid radiation hazard.) On penetration into the plasma, the microwave couples to a mode of the plasma and it is the absorption of this mode by the plasma particles that helps maintain the plasma. The power absorption

depends on the pressure. At moderate pressures the absorption is through electron–neutral collisions. When the chamber dimensions are comparable to, or smaller than the microwave wavelength, the modes in the system are guided-wave modes of the plasma column loaded inside the plasma chamber (with the latter acting as a waveguide). These guided modes may be either EM or quasistatic Trivelpiece-Gould (TG) modes for small diameter plasma vessels. Somewhat higher densities are possible in the latter case, since the TG modes also propagate as surface waves and can be absorbed efficiently over several skin depths near the surface. It was pointed out earlier that the oscillation amplitude for electrons in MW discharges is about 10–100 microns, so that both electron loss and plasma potentials are much lower than in RF discharges. Electron losses are primarily by diffusion in these discharges.

Figure 1.4.4 shows the schematic of MW plasma spray system used in our research. Microwaves with the frequency 2.45 GHz are transmitted through a rectangular waveguide and oscillated into a cylindrical resonant cavity with a hollow antenna resided on the axis. Working gas of Ar is mixed with spray particles in an aerosol chamber and axially feed through the antenna. The system generates high intensity electric field on the tip of the antenna, induces electrical breakdown of working gas, and plasma plume is generated at the outlet point of the antenna through the downstream. The spray particles are heated and accelerated by the plasma plume, and the coating is deposited by the impact of spray particles onto substrate surface at the downstream of the plasma. In our current research, the input power down to 0.5 kW can be utilized to produce coatings.

The comparison of main plasma spray methods which is DC, RF and MW power source is shown in Table 1.4.1. Compared to other plasma power sources, MW plasma spray has the advantages of being able to be generated at atmospheric condition, relatively need very low input power, electrodeless discharge and due to the low power, the size of plasma become narrow at approximately 3 mm in diameter which contribute to the possibility of on demand coating at much narrow area.

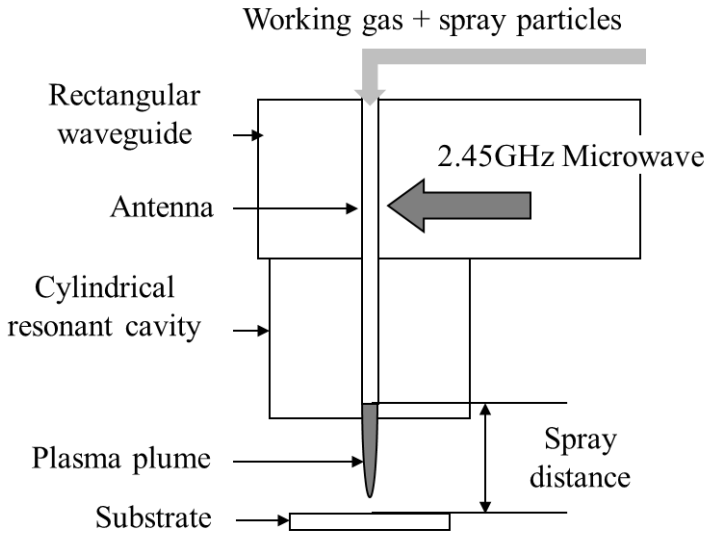


Fig. 1.4.4 Schematic of a MW plasma spray system.

Table 1.4.1 Comparison of main plasma spray methods

| | DC plasma spray | RF plasma spray | MW plasma spray |
|---|---|---|---|
| Atmospheric | ○ | △ | ○ |
| Input power | High (>20 kW) | High (> 20 kW) | Low ( ~ 1 kW) |
| Electrode | Yes | No | No |
| Coating width | Wide (>20 mm) | Wide (>20 mm) | Narrow (~3 mm) |

## 1.5 Characteristics evaluation and the expected application field of low power atmospheric pressure microwave plasma spray

Under atmospheric pressure, the plasma production of approximately 1 kW of low input power is made possible by the atmospheric pressure microwave plasma spraying device at our laboratory. Compared with plasma called DC plasma and RF plasma which are used conventionally, the generated plasma is about 3 mm in diameter, and small in shape. As the characteristics evaluation of atmospheric pressure microwave plasma spraying device, the investigation of plasma production conditions, the

measurement of the temperature of plasma plume and the coating deposition of metallic material which are copper and aluminium has been made. From the plasma temperature measurement result by optical emission spectroscopy measurement, the microwave plasma of approximately 1 kW of input power had the hollow structure where the luminescence of excited Ar atom did not exist in the central axis of the upper stream part, and the plasma changed to solid structure in the downstream part with average temperature of 5000K. From these findings, it was clear that the structure is different with the plasma currently used for the conventional plasma spray. Moreover, in order to investigate whether the heat input reduction to the spray substrates is possible, the metal (Cu) coating onto low melting point material called carbon fibre reinforced plastics (CFRP) and fibre-reinforced plastic (FRP) which are susceptible to heat, and it already been clarified that the deposition of copper coating onto low melting point substrate is possible. In case of coating deposition of hydroxyapatite as a biomedical material, emergence of decomposition phase harmful to human body caused by the heat input from the plasma will occur for the conventional plasma spray process [6, 7]. However, it turned out that it is possible to control the emergence of the decomposition phase by using this plasma spraying method [25].

Because of the deposition of coating with suppressed heat input into the spray material is possible, coating deposition of spray material that were difficult to be obtained by conventional plasma spray results in the widening of expected field of application for microwave plasma spray.

### 1.5.1 *Deposition of coating with suppressed heat input onto substrate material*

Functional hard chrome plating is a critical process associated with manufacturing and maintenance operations on aircraft, vehicles and ships, both in civilian and military sectors. Hard chrome electroplating is commercially used to produce wear-resistant coatings, but the plating bath contains hexavalent chromium, which has adverse health and environmental effects. For this reason, the use of hexavalent chromium has been limited. As a results, the European Parliament and the Council on end-of-life vehicles expressly prohibits the use of lead, cadmium, hexavalent chromium and mercury in all vehicles put on the market after 1$^{st}$ July 2003 (passenger

cars and commercial vehicles up to 3.5 tonnes) [26]. The total permissible amount of hexavalent chromium is limited to 2 g per vehicle. This directive must be implemented as national law in the Member States of the European Union [26].

The types of coatings that are most widely viewed as being capable of replacing hard chrome plating are the thermal spray technologies [27]. Plasma spray method is the most versatile in the thermal spray technologies where even high melting point materials such as ceramics coating can be deposited. However, the conventional plasma spray method generates high heat input (8000 ~ 15000 K in plasma region) to both substrate and spray materials especially to the heat susceptible materials [28]. For this reason, the research of depositing hard chrome coating by low power plasma spray method has been brought upon.

However, the input power of Cu coating deposited by conventional DC plasma spray method under atmospheric pressure condition which was reported is approximately 5 kW [11, 12], while deposition of coating by using RF plasma spray under atmospheric pressure condition is reported to be difficult due to the difficulty in stabilizing the plasma. On the other hand, with the input power of less than 1 kW, thermal plasma generation under atmospheric pressure is possible for microwave plasma spray method [5]. For this reason, it is thought that the coating deposition in which the heat input to the thermal spray material can be suppressed is achievable by applying microwave plasma as a low power plasma spray process. Moreover, this microwave plasma does not require electrode for electric discharge, which made it possible to generate plasma from chemically reactive type of gases if being compared to DC plasma in which the electrodes are needed for electric discharge. In comparison to DC plasma, microwave plasma has a lot of advantages such as plasma can be produced with relatively low input power, high plasma density and electrodeless gas discharge [15]. Therefore, in recent years, microwave plasma was applied in a wide range of fields, such as decomposition processing of harmful gas, heat treatment of waste, sterilization of medical material, and deposition of thin film [29]. In our laboratory, the low power atmospheric pressure microwave plasma spraying device which used microwave plasma for the heat source was successfully being applied [30].

Under atmospheric pressure, the plasma production of approximately 1 kW of low input power is made possible by the atmospheric pressure microwave plasma

spraying device. Moreover, in order to investigate whether the heat input reduction to the spray substrates is possible, the metal (Cu) coating deposition onto low melting point material called carbon fiber reinforced plastics (CFRP) and fiber reinforced plastic (FRP) which are susceptible to heat, is already clarified [31]. In case of coating deposition of hydroxyapatite (HA) as a biomedical material, emergence of decomposition phase harmful to human body caused by the heat input from the plasma will occur for the conventional plasma spray process [6, 7]. Hydroxyapatite coating with suppressed decomposition phase is also successfully able to be deposited [25].

Here, we deposit a hard chrome coating onto heat susceptible substrate, CFRP by using low power microwave plasma spray. For comparison, a hard chromium coating was also deposited onto SUS304. Morphologies and structural characteristics were measured by using X-ray diffraction (XRD) and scanning electron microscope (SEM).

### 1.5.2 *Deposition of coating with suppressed heat input onto spray material*

Titanium dioxide is photocatalyst material which has been focused in recent studies because of the magnificent properties of this material where it possesses photocatalytic activity such as the ability to remove the water pollution substance as well as the deodorizing function [32, 33]. Photocatalyst is a material that alters the rate of a chemical reaction when exposed to light [34]. There are various materials that show photocatalytic capability, and titanium dioxide is said to be the most effective. From the high photocatalytic activity that it possesses, this material is being used for wide area of applications, from the construction field to the medical field.

Generally, the deposition method of a titanium dioxide coating is carried out by the fixation of titanium dioxide powder with an organic system binder. However, due to the powerful photocatalytic reaction of a titanium dioxide, it will let the fast degradation of the organic binder. Therefore, from the recent studies, thermal spray is taught to be the alternative method to fabricate titanium dioxide coating with high photocatalytic activities. However, this method will cause high heat input and induces transformation from anatase phase with high photocatalyst activity to rutile phase with low photocatalyst activity. The coatings made from plasma spray of input power 28 kW

consists of low anatase content rate at 40% [35], and the study of the coating deposition methods which are able to restrain the phase change of spray particle is advancing [36].

Since our microwave plasma spraying device is operable using low power (below 1 kW) comparing with conventional plasma spraying equipment, the control effect of the heat input to the particles at the time of spraying can be considered, and coating deposition with high rate of anatase phase is expected. Therefore, in this research, the coating deposition by controlling the heat input into the spray particle which can be resulted in high rate of anatase phase with high photocatalyst activity was conducted.

## 1.6 Research objectives

The main research objective is to study the operational characteristic of low power atmospheric pressure microwave plasma spray method. The focus is showered on overcoming the major problem of conventional plasma spray which is suppression of heat input onto substrate and spray materials.

In order to study the suppressing effect of heat input onto substrate materials, high carbon steel and CFRP substrates were used as the candidates in which high carbon steel possess the higher phase transformation temperature. Chrome was selected as the spray powder in order to make comparison between Cr coating deposited by microwave plasma spray and hard chrome plating method.

Subsequently, in order to investigate the suppressing effect of microwave spray towards spray materials, $TiO_2$ coating was fabricated onto SUS304 substrate and the anatase content rate of coatings were evaluated. Here, the effect of substrate temperature, anatase content rate of in-flight particles and the nucleation of anatase phase were studied and presented.

## 1.7 Scope of the thesis

This thesis consists of six chapters. Each chapter are introduced briefly and summarized as below:

In Chapter 1 (Introduction), the fundamentals of plasma spray method, the progress of research by using low power microwave plasma spray device, the expected application field of the device, and the research objectives were included.

In Chapter 2 (Characteristics evaluation of low power atmospheric pressure microwave plasma spray), the study of plasma production conditions by using input power below 1 kW, temperature distribution of the plasma torch, the measurement of substrates temperature, and the characteristics study of the microwave plasma spray below 1 kW of input power were conducted. The details of the characterization of microwave plasma and the spray particles behaviour is also discussed in this chapter.

In Chapter 3 (Deposition of coating with suppress heat input onto substrate materials), high hardness material, Cr coating was deposited onto SUS304, high carbon steel and CFRP substrates, and the evaluation of the coating obtained by the experimentation was conducted.

In Chapter 4 (Deposition of coating with suppress heat input effect onto spray materials), the deposition of $TiO_2$ coating was tried and the evaluation of the coating obtained by the experimentation was conducted.

In Chapter 5 (Research tasks and future perspectives), the problems realized after the research being done were summarized and problem-shooting method was discussed align with further studies needed for microwave plasma spray method.

In Chapter 6 (General conclusions), all of the results obtained from this research are concluded and summarized.

# Chapter 2

# Characteristics evaluation of low power atmospheric pressure microwave plasma spray

## 2.1 Introduction

In this research, plasma spray device that use low input power microwave plasma in which is able to be operated in atmospheric pressure was invented. The main objective of this chapter is to investigate the characteristics of the atmospheric pressure microwave plasma torch. The plasma ignition conditions and the thermal efficiency of this microwave plasma spray device were investigated. Furthermore, measurement of substrate temperature, plasma temperature by optical spectroscopic measurement and particle velocity measurement by using high speed camera were conducted.

## 2.2 Low power atmospheric pressure microwave plasma spray device system

The schematic diagram of the low input power atmospheric pressure microwave plasma spraying system used for this research is shown in Fig. 2.2.1. Microwave is oscillated by microwave generation equipment (MICRO-DENSHI, MMG-213V-2P) on the frequency of 2.45 GHz, and then transmitted in the $TE_{10}$ mode through rectangular waveguide (with cross-sectional size: 109.2 mm x 54.6 mm). The maximum continuous output of microwave generator equipment is 1.3 kW. The matching of the impedance between microwave generation equipment and plasma torch and also the turning down of the reflect power ( $P_r$ ) that came from the plasma torch is controlled by the use of an E-H tuner. In the rectangular waveguide, through a directional coupler, the incident wave and reflected wave of microwave are separated, and forward power ( $P_f$ ) and

reflect power are measured with a wattmeter. By ignoring the power attenuation in the transmission line, electric power consumed by the plasma source is calculated as $P_f - P_r$. When this reflective power becomes the minimum, the dielectric breakdown of the gas can be carried out at the optimum electric power efficiency.

Generation of plasma is attained by carrying out the dielectric breakdown of the plasma working gas using an E-H tuner, after supplying Ar which is the plasma working gas to the plasma torch. The plasma working gas was directly supplied from the gas cylinder, and the gas mass flow was adjusted using the mass flow controller (KOFLOC, 3655) with the maximum flow of 20 l/min for Argon gas. Table 2.2.1 shows the details specification of the mass flow controller used in this study.

Table 2.2.1 Detail specification of mass flow controller (KOFLOC 3655)

| | |
|---|---|
| Flow range ($N_2$ equivalent, 20℃/1 atm) | 10 SCCM–20 SLM (freely selectable) |
| Sensor | Thermal mass flow sensor |
| Valve type | Proportional solenoid valve (closed when not energized) |
| Control range | 2–100% (F.S.) |
| Response | 2 sec. or less (0–100% within ±2% typical) |
| Accuracy | ±1.0% F.S. (25℃) |
| Temperature coefficient | ±0.1 F.S./℃ (15–35℃) |
| Repeatability | ±0.5%F.S. |
| Allowable operating pressure | 500 kPa (G) or less |

* SCCM: standard cubic centimeters per minute

* SLM: standard liter per minutes

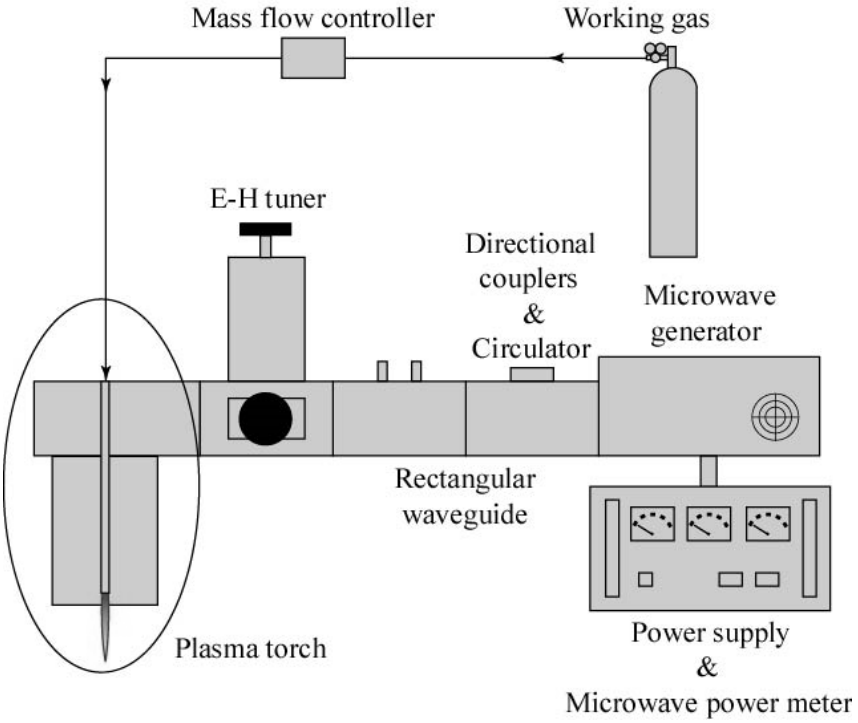


Fig. 2.2.1 Schematic diagram of low power atmospheric pressure microwave plasma spray system.

The photograph of the 1ow power atmospheric pressure microwave plasma spraying system used in this experiment is shown in Fig. 2.2.2, while the schematic diagram of the system is shown in Fig. 2.2.3. In this system, the spray particles were aerosolized by the flow of the working gas inside the aerosol chamber and were supplied into plasma. This is because of it is difficult to use the supply method of projecting a spray particle from the outside of the plasma which are widely used by other thermal spray method since size of plasma plume generated with this equipment is small. The aerosol reaction was produced by the mixing and agitation of the spray particles and the working gas which was supplied into the aerosol chamber. Moreover, in this research, vibration was given to the aerosol chamber in order to assist the generation of the aerosol reaction activity by the use of vibrating machine with the maximum vibration of 2500 rpm. The stage in which a spray substrate is installed is enabled to provide the movement (a maximum of 300 mm/s) of the spray substrate at 1 shaft orientations using a 1 axis electric actuator (IAI, ERC2-SA6C). Moreover, the

distance between the endpoint of the antenna and the substrate surface is defined as spray distance.

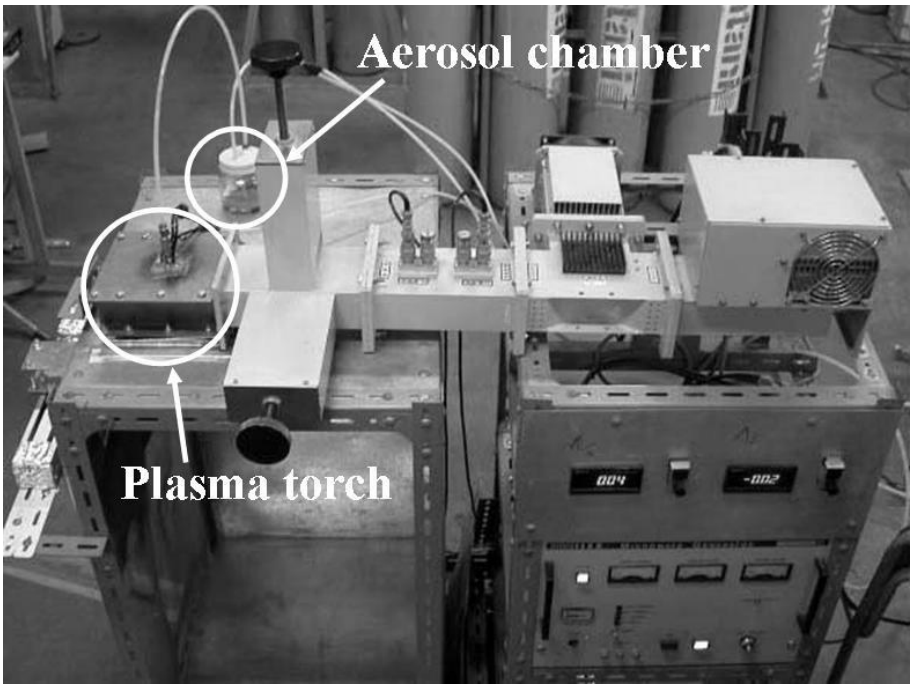


Fig. 2.2.2 Photograph of low power atmospheric pressure microwave plasma spraying system.

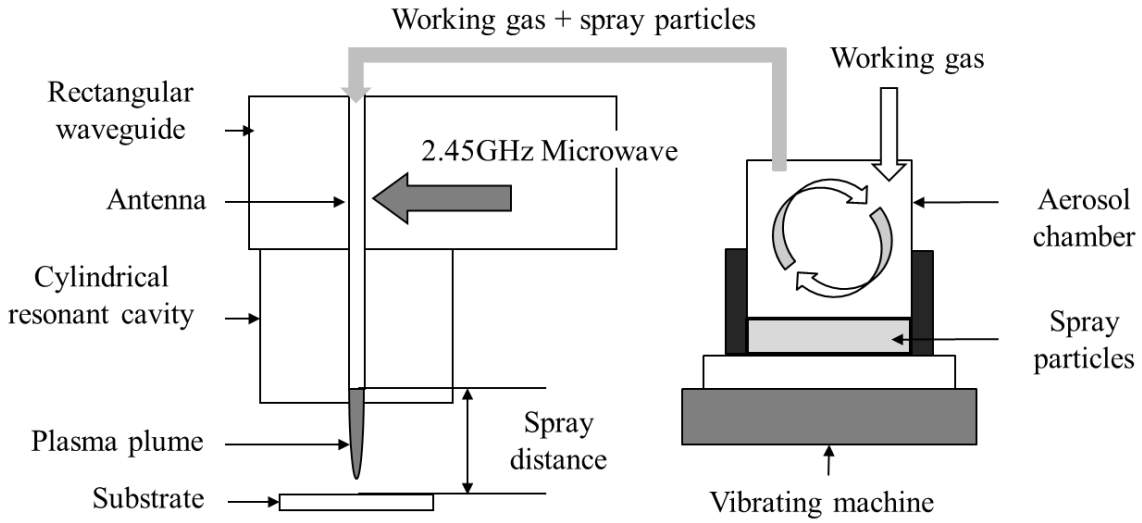


Fig. 2.2.3 Schematic diagram of low power microwave plasma spray system

## 2.3 Structure of plasma torch of atmospheric pressure microwave plasma spray

The schematic view of an atmospheric pressure microwave plasma torch is shown in Fig. 2.3.1. Microwave oscillated from microwave generation equipment is transmitted in a cylindrical resonant cavity ( $\phi$ 120 x L 113), and an antenna which is a metal pipe is arranged on the central axis of the resonant cavity in which the microwave electric field concentrates on the apical portion. Moreover, the plasma working gas blows off from the antenna apical portion, the dielectric breakdown of the plasma working gas is carried out by the microwave electric field concentrated at the antenna apical portion, and the plasma is generated. The photograph of the antenna used for this equipment is shown in Fig. 2.3.2. The side linked to the rectangular waveguide of the antenna was made of Cu-Zn, while the side of antenna apical portion was made of Cu-W which is excellent in heat resistance. For the outside diameter and inside diameter of Cu-Zn is fixed to 6.0 mm and 4.0 mm, while for the Cu-W antenna apical portion, outside diameter is fixed to 4.0 mm, but the inside diameter of 2.5 mm, and 1.5 mm is prepared for the experimentation. As for the reason of changing the inside diameter of the antenna is because it can be thought that by the change of antenna diameter, at the same working gas flow rate, the rise of the gas flow can be expected, which resulting in the effect of the increase in particle velocity. This is thought to be due to Venturi effect occurs when fluid flows to the decreasing end of antenna which results in increasing velocity of the fluid as explained by Bernoulli's principle. The schematic diagram of the structure of the antenna end point which made from Cu-W is shown in Fig. 2.3.3.

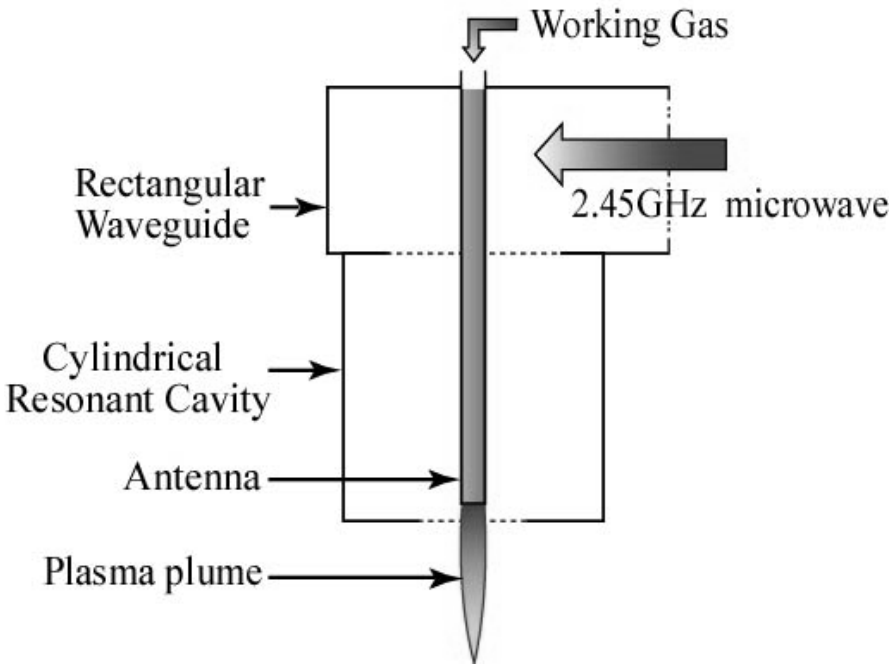


Fig. 2.3.1 Schematic view of atmospheric pressure microwave plasma torch.

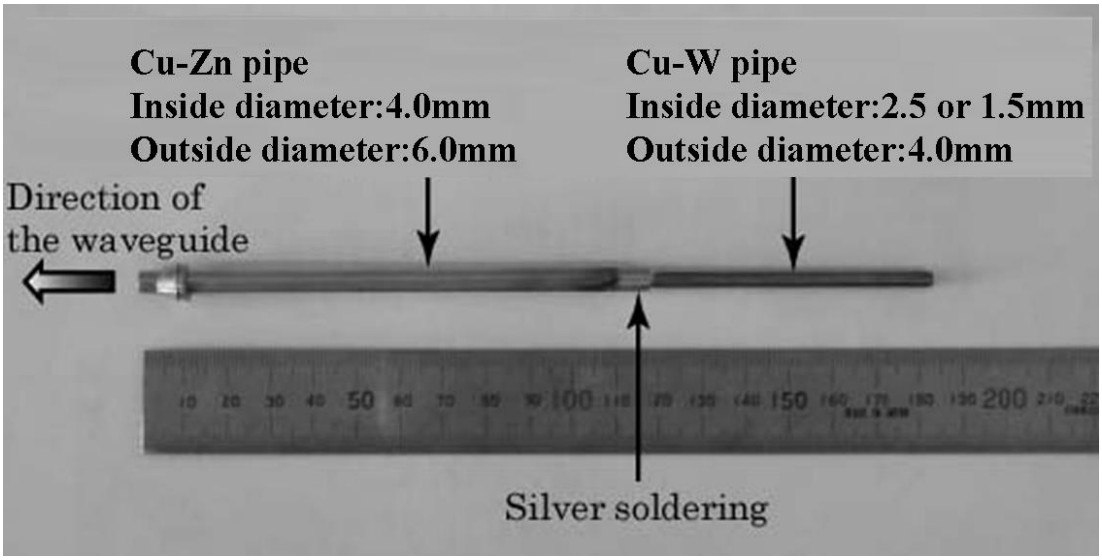


Fig. 2.3.2 Photograph of the antenna.

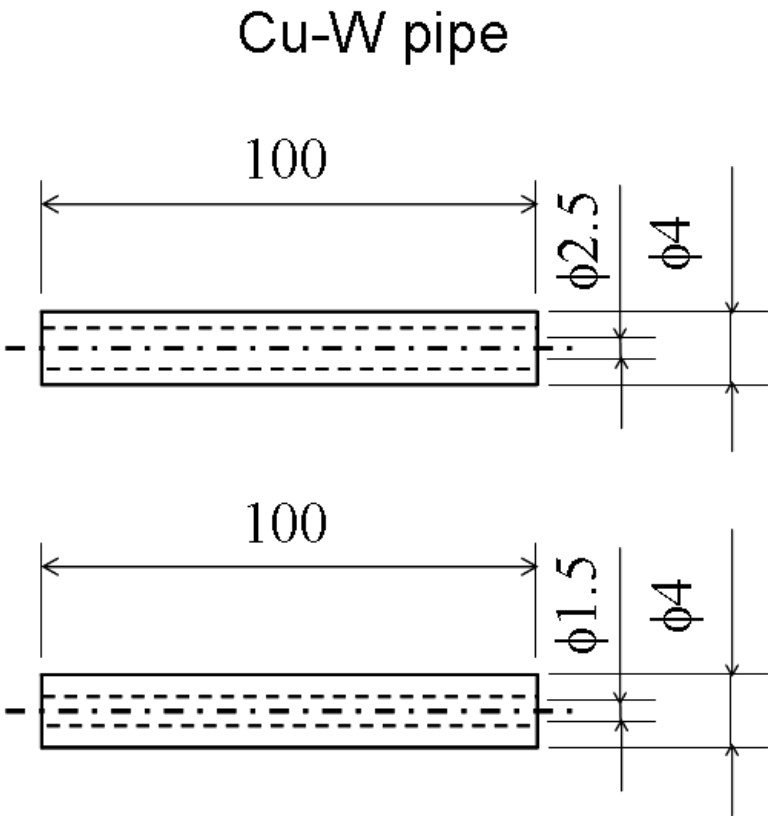


Fig. 2.3.3 Schematic diagram of Cu-W pipe parts of the antenna.

## 2.4 Investigation of plasma ignition conditions of plasma torch

### *2.4.1 Experimental method*

This experiment investigates the plasma ignition conditions of the low power atmospheric pressure microwave plasma torch. The optimal condition of the plasma ignition in which this experiment defines is the generation (ignition) of plasma is easy (plasma can be lit and stabilized in a short time), and it is considered as the conditions which are stable. The first objective of the definition given beforehand is because when the plasma ignition is not occurred for a long time with the $P_f$ - $P_r$ states remain high, plasma torch might be damaged by the heat cause by the microwave. Moreover, and for the latter objective is because of the aim of finally using this equipment as a thermal spraying equipment, it becomes more unstable by supplying a spray particle into plasma

when the generated plasma is unstable, and it is expected that the maintenance of the plasma becomes difficult.

As the plasma production method, after generating the plasma at 1 kW, the possibility of maintaining the plasma was investigated by performing operation which lowers input power to meet the experimental conditions. The ignition conditions of plasma are shown in Table 2.3.1. Two conditions of plasma working gas flow rate, two size of inside diameter of an antenna and three conditions of input power were prepared to investigate the production and the maintenance of plasma. The trial of plasma production of each condition was done 5 times and the propriety of the maintenance of plasma production was judged. The reason of the experiment time was made into a maximum of 3 minutes is because the damage to the antenna by microwave when plasma cannot be generated or maintained in the state where the reflect power was made small as much as possible, was taken into consideration. Argon gas was used as the plasma working gas due to the reason that it is a monoatomic gas, ionization potential is low and the generation of plasma is comparatively easy. The stability of plasma was evaluated from the existence of plasma and the observation of the appearance of the generated plasma. Furthermore, the investigation of the coupling efficiency on each condition was also conducted simultaneously.

Table 2.4.1 Experimental conditions for plasma ignition

| | |
|---|---|
| Forward power (kW) | 0.1, 0.3, 0.5, 1.0 |
| Working gas flow rate (l/min) | 10, 15, 20 |
| Antenna outlet diameter (mm) | 1.5, 2.5 |
| Operating time (s) | 300 |

### *2.4.2 Results and discussion*

Result of the investigation of plasma production conditions is shown in Fig. 2.4.1. Plasma ignition that was able to be produced 5 out of 5 times and maintained for 5 minutes are shown as ● mark. ○ mark shows that 3～4 times out of 5 times of the plasma production, plasma was able to be maintained for 5 minutes, △ mark shows that 1～2 times out of 5 times of the plasma production, plasma was able to be maintained for 5 minutes, ×mark shows that 5 times out of 5 times of the plasma production, plasma was not able to be maintained. From the results, although it was confirmed that the plasma is stabilized and maintained on the conditions of input power 0.5 kW, and antenna outlet diameter 2.5 mm, the maintenance of plasma is difficult at antenna inside diameter 1.5 mm. From the results, it can be clarified that the maintenance and stabilization of plasma is difficult with reduction of the antenna outlet diameter. On the input power 0.3 and 0.5 kW of the plasma ignition conditions, it became clear that the generation and maintenance of plasma is possible even to such low power of microwave input. However, on 0.1 kW of input power, plasma production and maintenance cannot be performed and the maintenance of plasma becomes difficult on the input power of 0.3 kW, antenna outlet diameter 1.5 mm, and the ignition conditions of working gas flow rate 20 l/min. Coupling efficiency is above 99% at the time of the plasma has been stabilized and it is clarified by this study that the microwave generated plasma possesses high coupling efficiency.

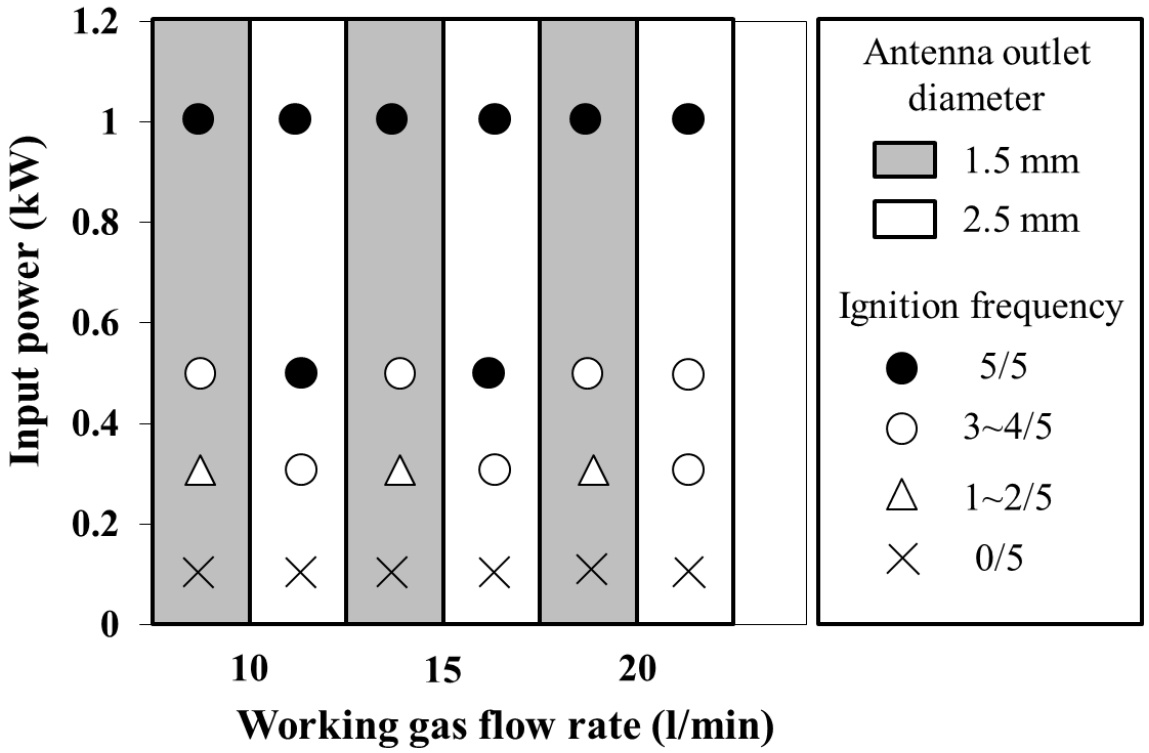


Fig. 2.4.1 Result of plasma ignition experiment.

## 2.5 Thermal efficiency of microwave plasma spray torch

*2.5.1 Experimental method*

In this experiment, the objective is to evaluate the characteristics of the thermal efficiency of low power atmospheric pressure microwave plasma spray torch. Thermal efficiency of the plasma torch is defined as an index which shows the rate of the energy (the amount of heat transfer) used for heating of material to the energy used for the plasma ignition, and it shall be effective to the evaluation of the thermo-physical properties of plasma [1]. In this experiment, thermal efficiency（$\eta_T$）is defined as the formula shown below, and the schematic diagram of thermal efficiency measurement system is shown in Fig. 2.5.1.

$$\eta_T = \frac{Q_2}{Q_1} = \frac{(T_2 - T_1)C_w S}{P_f - P_r} \times 100 \qquad (2.5.1)$$

$Q_1$ : Energy used for the plasma ignition [W]

$Q_2$ : Recovered energy by heat exchanger [W]

$T_1$ : Water temperature of the entrance of heat exchanger [K]

$T_2$ : Water temperature of the exit of heat exchanger[K]

$C_w$ : Specific heat of water [J/kgK]

$S$ : Flow rate of water [$m^3$/s]

$P_f$ : Forward power [W]

$P_r$ : Reflect power [W]

Cu plate was heated by the plasma, and the temperature change of the water flowed inside the Cu pipe that was set at the lower side of the Cu plate was used to calculate the heat efficiency of the plasma. The temperature of the water flowed at the entrance and the exit of the Cu pipe was measured by K-type thermocouple. The photograph of the thermal efficiency measurement experiment of atmospheric pressure microwave plasma torch is shown in Fig. 2.5.1, while Fig. 2.5.2 shows the schematic diagram of the thermal efficiency measurement system. The ignition conditions are shown in Table 2.5.1. Working gas flow rate was made as the changing parameter and the heat efficiency was measured. Furthermore, measurement position was set to 30 mm from the tip of the antenna in which the plasma was produced, and the Cu plate is fully heated by the contact to the plasma.

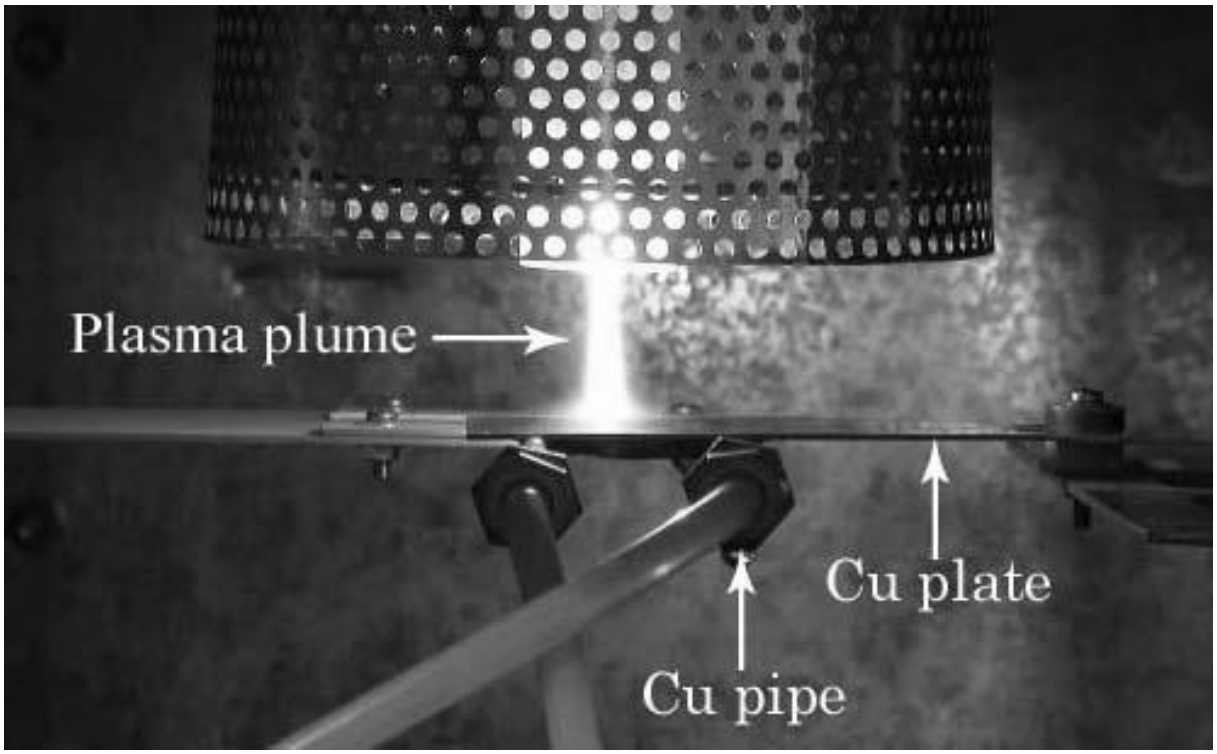


Fig. 2.5.1 Photograph of thermal efficiency measurement system.

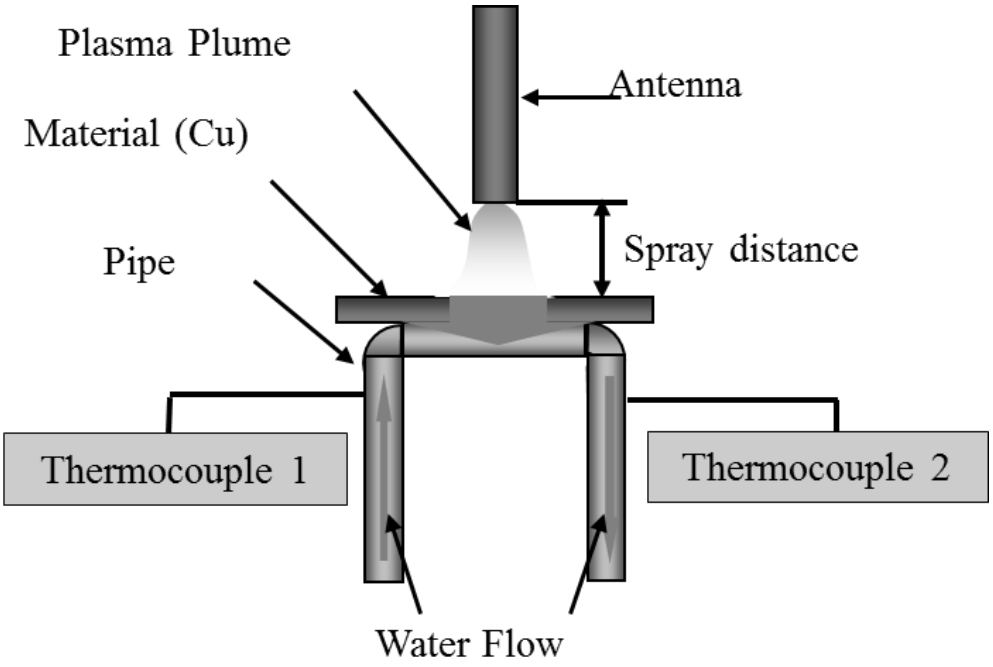


Fig. 2.5.2 Schematic diagram of the thermal efficiency measurement system.

Table 2.5.1 Experimental conditions for thermal efficiency measurement

| | |
|---|---|
| Forward power (kW) | 0.5 |
| Working gas | Ar |
| Measurement distance (mm) | 40 |
| Working gas flow rate (l/min) | 10, 15, 20 |
| Operating time (s) | 300 |
| Antenna outlet diameter (mm) | 1.5, 2.5 |

*2.5.2 Results and discussions*

The result of thermal efficiency measurement is shown in Fig. 2.5.3. From the result in Fig. 2.5.3, the highest thermal efficiency is at antenna inside diameter 2.5 mm and working gas flow rate 10 l/min, where the average of the heat efficiency is 28.1 %. It is also known from the result that there is no significant change of heat efficiency by the change of antenna outlet diameter size from 2.5 mm to 1.5 mm. This may result in the almost significant heat transfer even by small size of antenna outlet diameter. From this result, it is confirmed that the heat efficiency of this microwave plasma spray is at comparatively at the same level of the heat efficiency of atmospheric pressure DC plasma torch (plasma gun) which is widely and generally used where the heat efficiency are about 10～40% *[2, 3]. Furthermore, from the results, the thermal efficiency of the plasma torch is decreasing with the increase of working gas flow rate. This can be considered that there is the influence of plasma temperature, in which plasma temperature rises with the increase of the energy given per working gas unit volume under atmospheric pressure. From this, it is thought that plasma temperature fell by the increase in a working gas flow rate, and thermal efficiency fell because of the decrease of the amount of heat input into the Cu plate.

It is clarified from the results obtained above that this equipment has thermal efficiency comparable to conventional DC plasma spray. For this reason, the application as a heat source for plasma spray coatings is expected from this device.

*[2, 3] The thermal efficiency value was obtained by the experimental conditions shown below.

*[2]

| | | |
|---|---|---|
| Device | : | Atmospheric pressure DC plasma torch |
| Thermal efficiency | : | 10 ～ 25 % |
| Plasma working gas | | |
| Primary | : | Ar（66.3 l/min） |
| Secondary | : | He（35.7 l/min） |

Arc current : Current 275A

Arc voltage : Voltage 175V

*[3]

Device : Atmospheric pressure DC plasma gun

Thermal efficiency : 40 %

Plasma working gas : Ar

Arc current : Current 1000A

Arc voltage : Voltage 40V

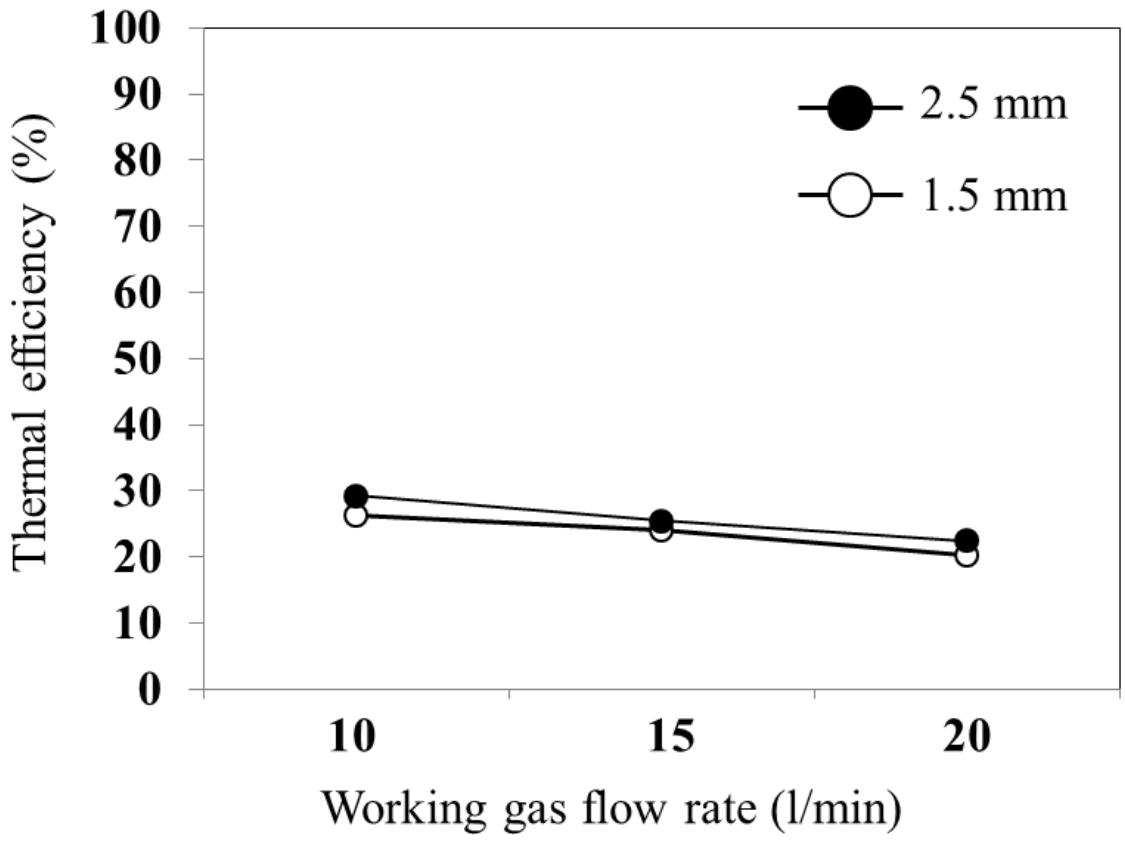


Fig. 2.5.3 Results of thermal efficiency measurement of microwave plasma spraying device.

## 2.6 Measurement of substrates temperature

### 2.6.1 *Experimental method*

In this experiment, the effect of the heat input from the plasma plume to the substrates was investigated by measuring the temperature of substrates during plasma spraying was performed. For the measurement of substrates temperature, the temperature is measured with the sheath type thermocouple (K-type) by collecting the signals from the thermocouple by the data logger GR-3000 (KEYENCE CORP). The substrate material was SUS304 with the dimension size of 20 x 20 x 3 mm. The thermocouple with ϕ1.5 mm in diameter was inserted inside the slit opened in the substrates with the distance of 1 mm from the surface of the substrates and 2mm width. By this positioning of the thermocouple, inside temperature of the substrates are able to be measured.

Experimental conditions of substrates temperature measurement are shown in Table 2.6.1, while Fig. 2.6.1 shows the measurement method. In this experiment, substrate temperature by the change of spraying distance, working gas flow rate, and input power were measured. Spraying distance is the distance from the antenna tip to the substrate surface. Generally, for the conventional plasma spraying method which consumed high input power, to protect the substrates from excessive heat, cooling device is normally installed at the spray stage. However, by using low input power plasma spraying method, spray substrates are able to be protected against the excessive heat without the cooling device and this will also widened the type of spray substrates materials to be applied with. Measurement time is set to the time the measurement started until the temperature is stable which is approximately 120 s. The reason of spraying distance is set to be at least at 30 mm is because at the spraying distance below 30 mm, it was observed that the spray particles which collided with the substrates and not impinged onto the substrates surface will soars in the direction of the antenna with the reflected working gas. This results in the difficulty for the plasma to be stabilized. Therefore, in this research, the distance of above 30 mm which has little influence by the un-impinged spray particles on the plasma was used as the experimental condition. The maximum temperature was measured, and the average value was calculated from 3

times of measurements.

Table 2.6.1 Experimental conditions for substrate temperature measurement

| | |
|---|---|
| Forward power (kW) | 0.5 |
| Working gas flow rate (l/min) | 10, 15, 20 |
| Spray distance (mm) | 30, 35, 40 |
| Traverse speed (mm/s) | 5 |
| Antenna outlet diameter (mm) | 1.5, 2.5 |

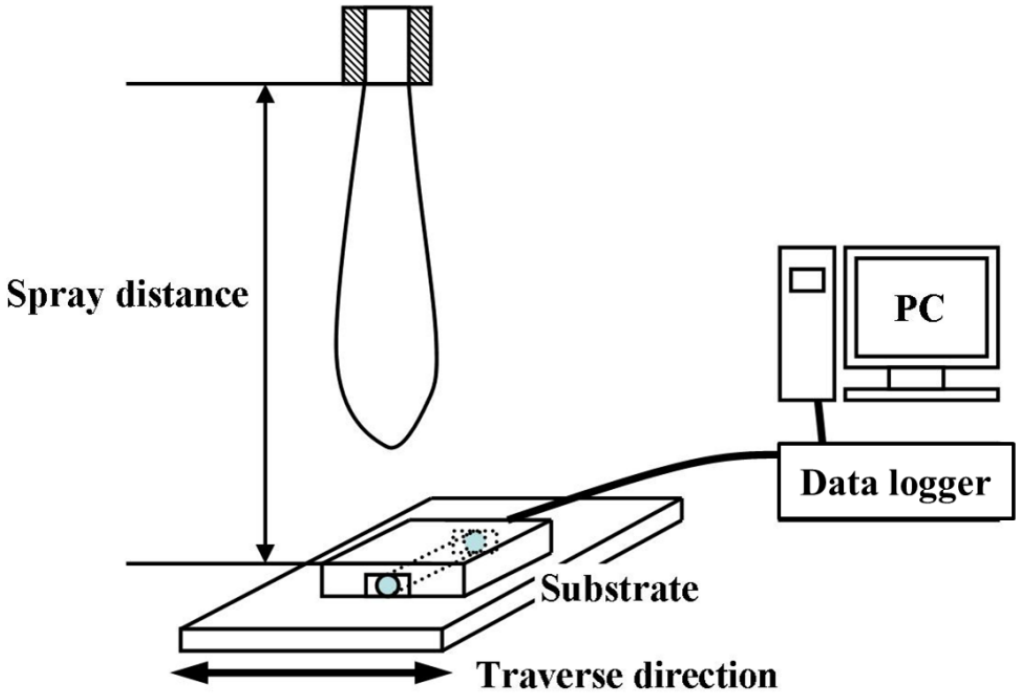


Fig. 2.6.1 Schematic drawing of substrate temperature measurement.

### *2.6.2 Results and discussions*

The results of substrate temperature at experimental conditions of Table 2.6.1 at 2.5 mm of antenna outlet diameter are shown in Fig. 2.6.2. Figure 2.6.3 shows the photograph of the plasma at the time of measurement. Furthermore, the plasma length results which were derived from the photograph of the plasma are shown in Table 2.6.2. From the results, the substrates temperature is decreased with the increase of working gas flow rate and the increase of spray distance. As a result, at working gas flow rate 10 l/min and spray distance 30 mm, the substrates temperature was at the highest at the temperature of 678 K while the lowest substrate temperature was at spray conditions of working gas flow rate 20 l/min and spray distance 40 mm at 389 K. In the reduction of the plasma length by the increase in working gas flow rate, it is thought that the energy given per unit working gas volume is decreased with working gas flow rate while the energy from microwave was constant, and plasma length decreased by the pinch effect [4]. With the plasma generated using the antenna with 2.5 mm of antenna outlet diameter, the experimental result shows that at any conditions of working gas flow rate, the highest substrates temperature is shown at 30 mm of spray distance.

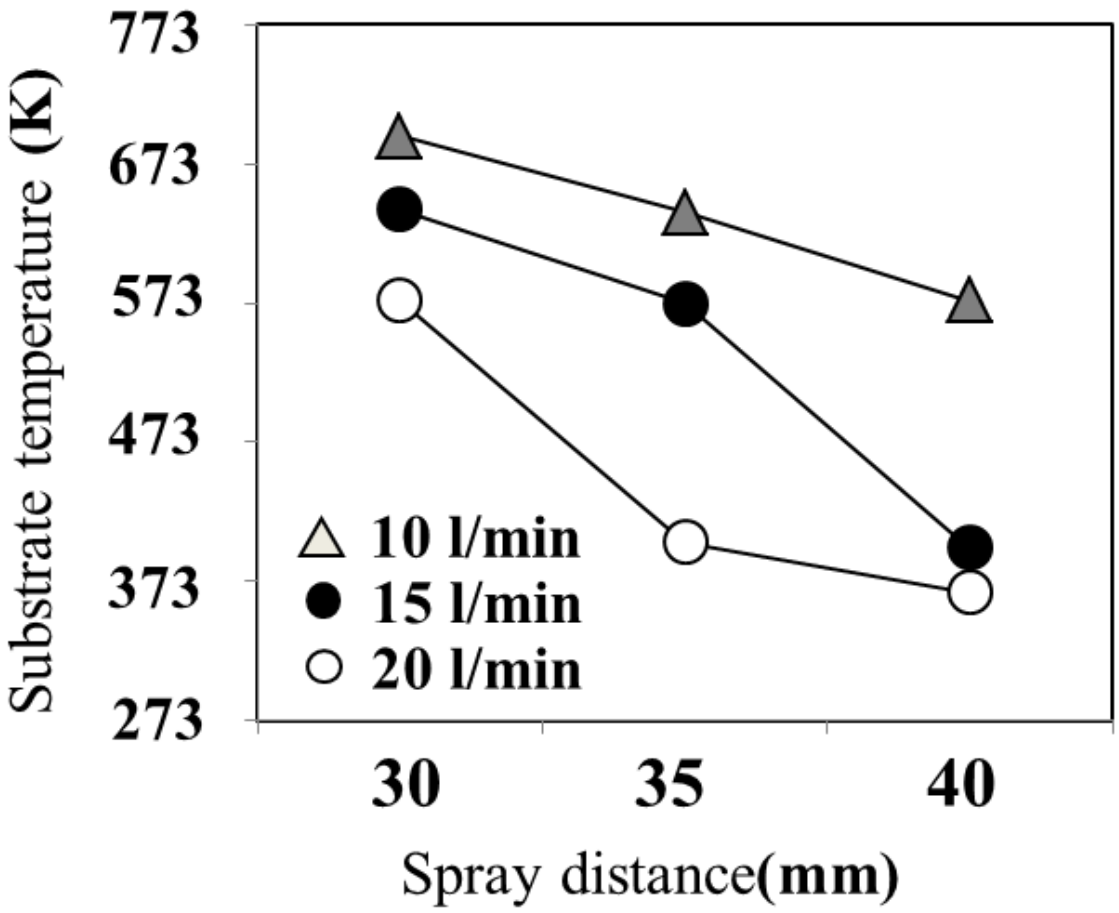


Fig. 2.6.2 Effect of working gas flow rate and spray distance on substrate temperature at antenna outlet diameter 2.5 mm.

| | 1.5 mm | 2.5 mm |
|---|---|---|
| 10 l/min | 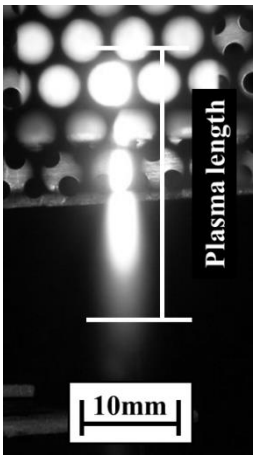  | 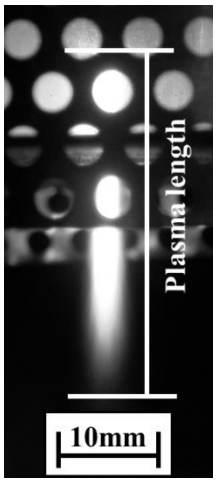  |
| 15 l/min |  | 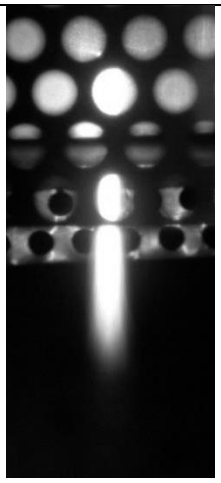 |
| 20 l/min |  |  |

Fig. 2.6.3 Photographs of the plasma generated by microwave plasma torch for each experimental conditions.

Table 2.6.2 Plasma length (mm) of each experimental condition

| | | Working gas flow rate (l/min) | | |
|---|---|---|---|---|
| | | 10 | 15 | 20 |
| Antenna diameter (mm) | 1.5 | 33.1 | 30.9 | 27.4 |
| | 2.5 | 34.3 | 32.6 | 28.3 |

The result of the measurement of substrates temperature obtained by the plasma generated at antenna inside diameter 1.5 mm is shown in Fig. 2.6.4. From the result, by reducing the antenna inside diameter, it is confirmed that the substrates temperature are able to be decreased further comparing to antenna inside diameter 2.5 mm. Moreover, even at 1.5 mm of antenna outlet diameter, the decrease of plasma length with working gas flow rate is observed. It can be thought that the reason of this phenomenon is because of the decreasing of the plasma length as the result of the reduction of antenna size from the observation of the photograph of plasma in Fig. 2.6.3. In this research, in third chapter, the objective of the study is to deposit coating by controlling the heat input onto the substrates by using low input atmospheric pressure microwave plasma spraying method. From the results shown in Fig. 2.6.4, the melting point temperature of CFRP is 523 K, means that by choosing the spray conditions, the deposition of coating with controlling heat effect onto CFRP substrates is also able to be conducted.

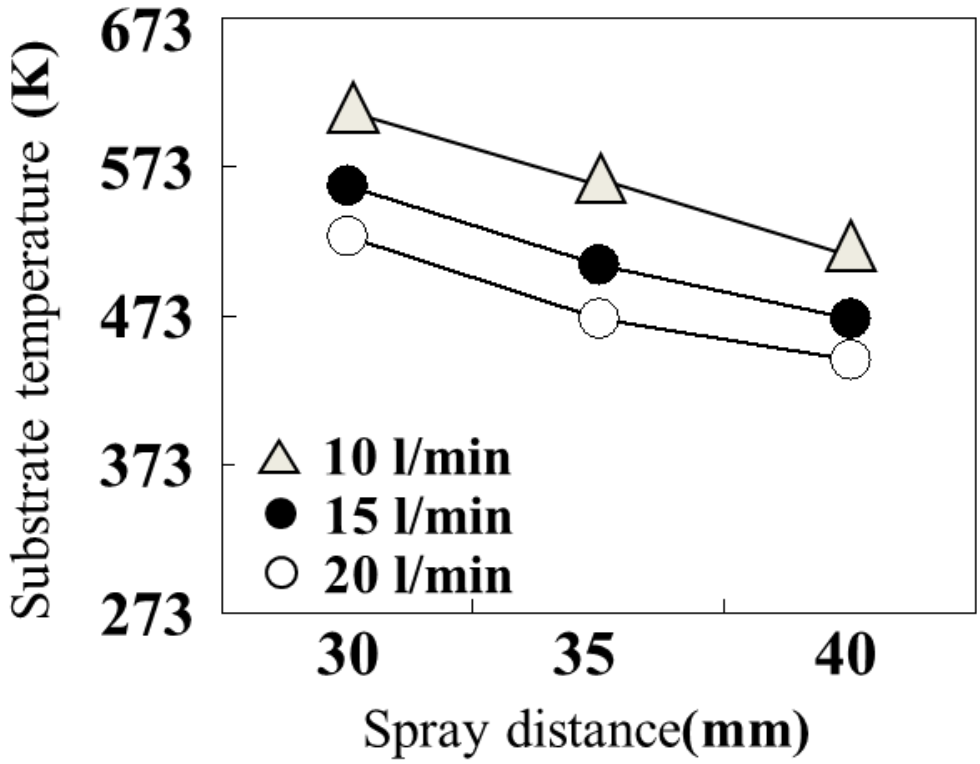


Fig. 2.6.4 Effect of working gas flow rate and spray distance on substrate temperature at antenna outlet diameter 1.5 mm.

## 2.7 Study on Plasma Behaviour

### 2.7.1 *Introduction*

Plasma spraying is an effective and practical way for the deposition of thick coatings with different functionalities in corrosion, wear, and heat resistance application. Conventional atmospheric pressure plasma spray systems are operated by direct current (DC) arc discharge with high power (>20kW) as the heat source. Spray powder are introduced into the plasma jet, melted or partially melted during the residence time in the plasma jet, accelerated towards a substrate, and the impingement by collision of the spray particles with the substrate surface will gradually fabricate the coating. These plasma jet show high flow velocity (up to 2500 m/s) and high temperature (up to 1400 K) [5]. These features are advantageous for deposition of ceramic materials with high melting point. However, it is difficult to fabricate coating on low temperature substrate due to high heat flow from the plasma jet [6]. Thus, low power atmospheric pressure plasma spraying is a promising way to fabricate coating on low temperature substrate. However, atmospheric pressure plasma spraying with low power (< several kW) is difficult for DC arc discharge.

Microwave easily generates high electric field and efficiently ignites discharge at atmospheric pressure condition under several kW. Moreover, this microwave plasma does not require electrode for electric discharge, which made it possible to generate plasma from chemically reactive type of gases if being compared to DC plasma in which the electrodes are compulsory for electric discharge. In comparison to DC plasma, microwave plasma has a lot of advantages such as plasma can be produced with relatively low input power, high plasma density, wide discharge frequency and the previously mentioned electrodeless gas discharge [7]. Therefore, in recent years, microwave plasma was applied in a wide range of fields, such as decomposition processing of harmful gases, heat treatment of wastes, sterilization of medical materials, and deposition of thin films [8]. However, there has been no practical plasma spray system using microwave plasma so far. From the characteristics that it possesses,

atmospheric microwave plasma has a possibility to be applied as the low power atmospheric pressure plasma spraying with microwave power of not more than 1kW. In this laboratory, atmospheric pressure microwave plasma source was developed for atmospheric pressure plasma spraying [9-11] and coatings of high melting point materials such as Cr [12] and even ceramics materials such as $TiO_2$ [13] are able to be fabricated at 0.5 kW of microwave power. However, the operational characteristics and the behavior of the plasma as well as the spray particles during the process are not studied very well. This study is important in order to optimize the controlling factors of the process. Therefore, the study of the operational characteristics of plasma spraying were investigated and presented in this report. Cu particles were used as the test subject to easily elucidate the particle behavior with lower melting point metallic material.

### 2.7.2 *Experimental procedure*

Microwaves with the frequency 2.45 GHz are transmitted through a rectangular waveguide and oscillated into a cylindrical resonant cavity with a hollow antenna resided on the axis. Working gas of Ar is mixed with spray particles in an aerosol chamber and axially feed through the antenna. The system generates high intensity electric field on the tip of the antenna, induces electrical breakdown of working gas, and plasma plume is generated at the outlet point of the antenna through the downstream. The spray particles are heated and accelerated by the plasma plume, and the coating is deposited by the impact of spray particles onto substrate surface at the downstream of the plasma. Feedstock powder materials with two different sizes were used for this investigation: atomized pure copper with spherical shape (Cu-HWQ φ5μm and φ20μm, Fukuda Metal Foil and Powder, Japan). Figure 2.7.1 shows the morphology of the feedstock powders. Spraying conditions are shown in Table 2.7.1. In this experiment, the working gas flow rate, antenna outlet diameter and particle size which are important parameters in the spraying process were investigated. Microwave power was set to 0.5 kW. Here, traverse speed is defined as the moving speed of the substrate under the plasma for coating deposition. The feed rate was controlled by the mass flow rate of working gas. The substrate was placed at 40 mm downstream from the tip of antenna.

Cu coating was deposited onto grit blasted SUS304 substrates with dimension of 20 x 20 x 2mm to improve the adhesion between coating and substrate surface. To observe the flattening and deposit behavior of an individual particle, the particles were collected on the stainless steel substrate which was mirror polished prior to spraying. For the powder collection on the substrate surface, substrate plates were traversed at about 300 mm/s with the angle perpendicular to the torch axis to get a small number of the particles onto the substrate surface individually. Splat and cross-sectional morphology of Cu particles for each spraying condition was determined by scanning electron microscopy (SEM) (JSM-6390TY, JEOL Co. Ltd., Japan).

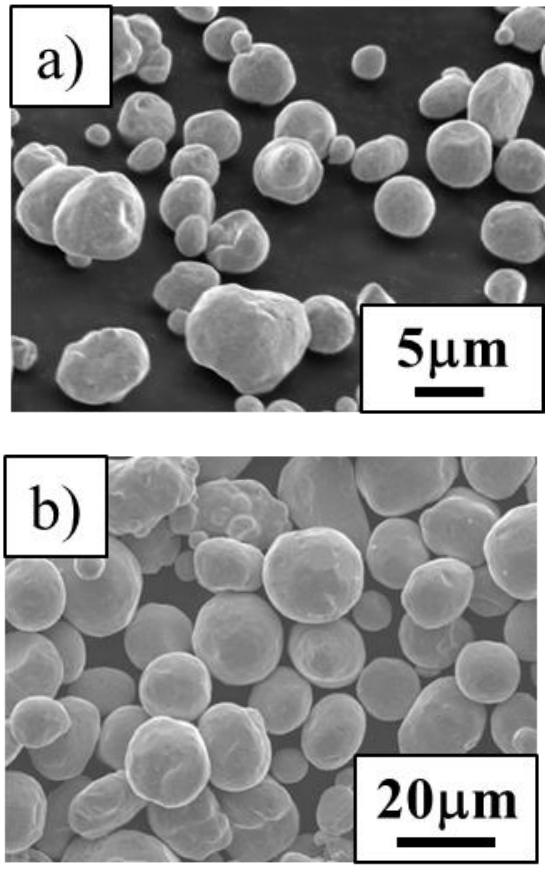


Fig. 2.7.1 Feedstock powder morphology of a) 5 μm and b) 20 μm of Cu particles.

Table 2.7.1 Spraying conditions

| | |
|---|---|
| Microwave power | 0.5 kW |
| Antenna outlet diameter | 1.5, 2.5 mm |
| Working gas | Ar (10, 15, 20 l/min) |
| Spray powder | Cu (φ5, φ20 μm ) |
| Spray distance | 40 mm |
| Traverse speed | 5 mm/s |
| Spray time | 60 s |
| Vibrating speed | 1500 rpm |
| Substrate | SUS304 |

2.7.3 *Plasma temperature*

Optical emission spectroscopy was used as the plasma temperature diagnosis method. Here, optical emission spectroscopy is a non-contact type of plasma diagnosis method, in which by the measurement of the intensity of the light emitted by the plasma, the identification of ionic species and the measurement of the temperature of the plasma become possible. Figure 2.7.2 shows the schematic diagram of optical emission spectroscopy measurement method used in this experiment. After the light emitted from the plasma was condensed by a quartz lens (Sigma opto-mechanic, lens diameter = 50mm, focal length = 120mm), it is then taken into the spectroscope (Ocean Optics, HR4000 (H3)) through fiber optic. The spectroscope is able to measure the intensity of light in the wavelength range of 370～810 nm. Figure 2.7.3 shows the spectral

measured in this study and from the result, it is known that the the spectral peak of Ar I is recorded at all peaks. Furthermore, the fiber optic was fixed to X-Z stage where the distribution of axial and radial direction of plasma was measured accordingly. The direction of the plasma flow is considered as Z-axis, the tip of the antenna is set to be Z=0, and the brightest region of the plasma which is Z=15 mm is measured. In order to measure the plasma temperature in radial direction, the reflected image of the plasma which is 6 times the actual size was divided into 17 points with the distance of 0.5 mm (0.083 mm in actual size) with the starting point measured from the center of the plasma towards the peripheral parts. Moreover, after the measurement of luminescence intensity of Ar atom in Ar plasma was taken place, spectral analysis by the Abel inversion and the Boltzmann plot was conducted, and the excitation temperature of Ar was derived based on the findings reported by R. Alvarez et.al. [14, 15]. The schematic diagram of the Abel inversion method is shown in Fig. 2.7.4. The plasma is assumed to be asymmetric in all direction for the Abel inversion to be conducted successfully. The equation for the Boltzmann plot is

$$\ln\left(\frac{I_{v'v''}\lambda_{v'v''}{}^{4}}{Re^{2}(\bar{r}_{v'v''})\,q_{v'v''}}\right) = \left(-\frac{G_{(v')}hc}{kT}\right) + C \qquad (2.7.1)$$

where $I_{v'v''}$ is the measured intensity in (a.u), $\lambda_{v'v''}$ is the wavelength in (nm), $Re^{2}(\bar{r}_{v'v''})$ is the electron transition moment in which $\bar{r}_{v'v''}$ is core distance between the atoms, $q_{v'v''}$ is Planck-Condon coefficient, $G_{(v')}hc$ is the energy, k is the Boltzmann coefficient and C is the constant for a given atomic species. The parameters used for this study is derived from the research done by S. Y. Moon et. al. [16].

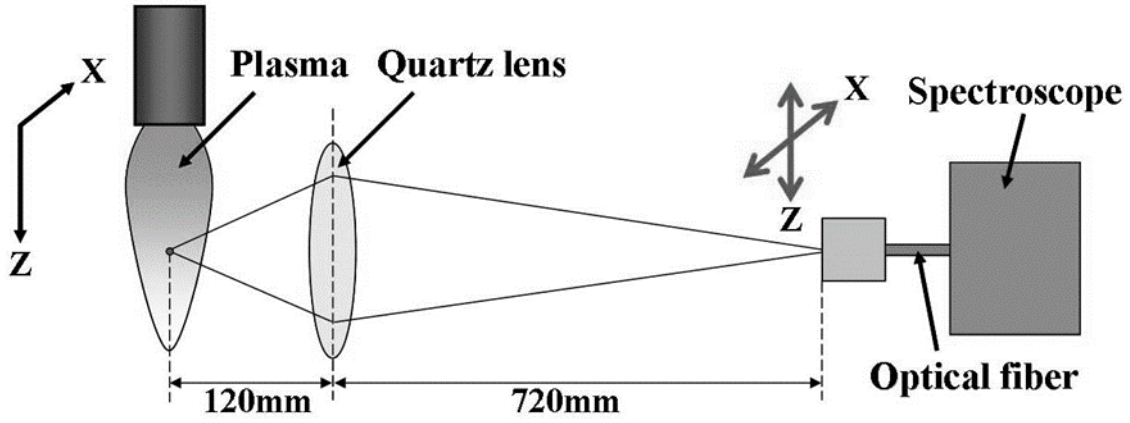


Fig. 2.7.2 Schematic diagram of optical emission spectroscopy measurement method.

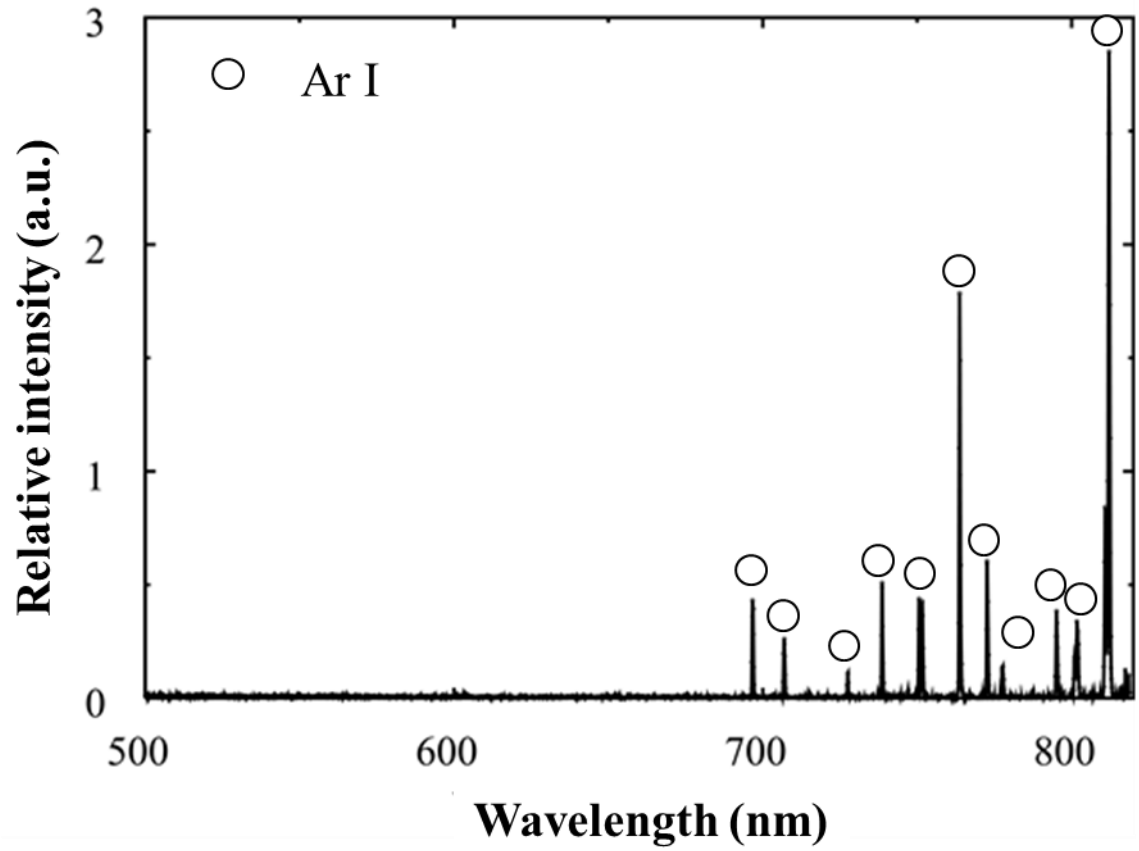


Fig. 2.7.3 Measured spectra.

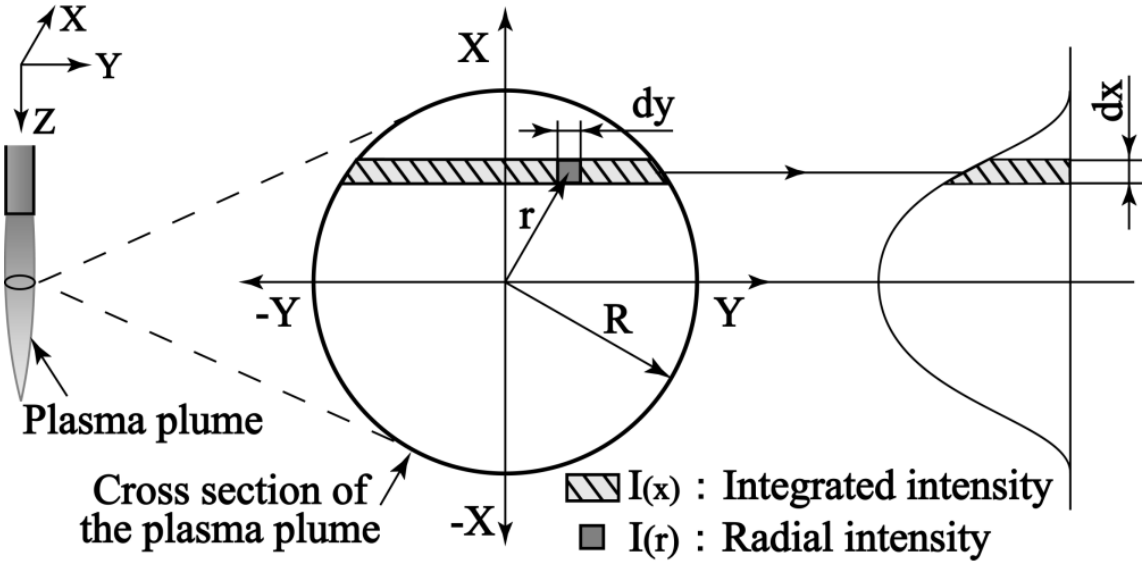


Fig. 2.7.4 Schematic diagram of Abel inversion.

2.7.4 *Results and discussion*

Figure 2.7.5 shows the result of plasma temperature by the change of antenna outlet diameter and working gas flow rate. From the results, the generated plasma had about 4000 K uniform thermal field in the measurement position of 15 mm. Furthermore, it is known that the radial size of plasma decreases with the increase of working gas flow rate at both antenna sizes. This is due to the increase of thermal pinching effect with the increment of working gas flow rate [4]. At the same radial position, the plasma temperature increase by approximately 300 K at any working gas flow rate at smaller antenna outlet diameter. This is thought to be due to the increase of energy per volume of the plasma plume and the mechanical pinching effect. From the radial distribution, it is known that the plasma temperature is higher in the peripheral side of the plasma which is the result of swaying motion of the plasma. The maximum temperature of 4500 K was obtained at 10 l/min of working gas flow rate and 2.5 mm of antenna outlet diameter.

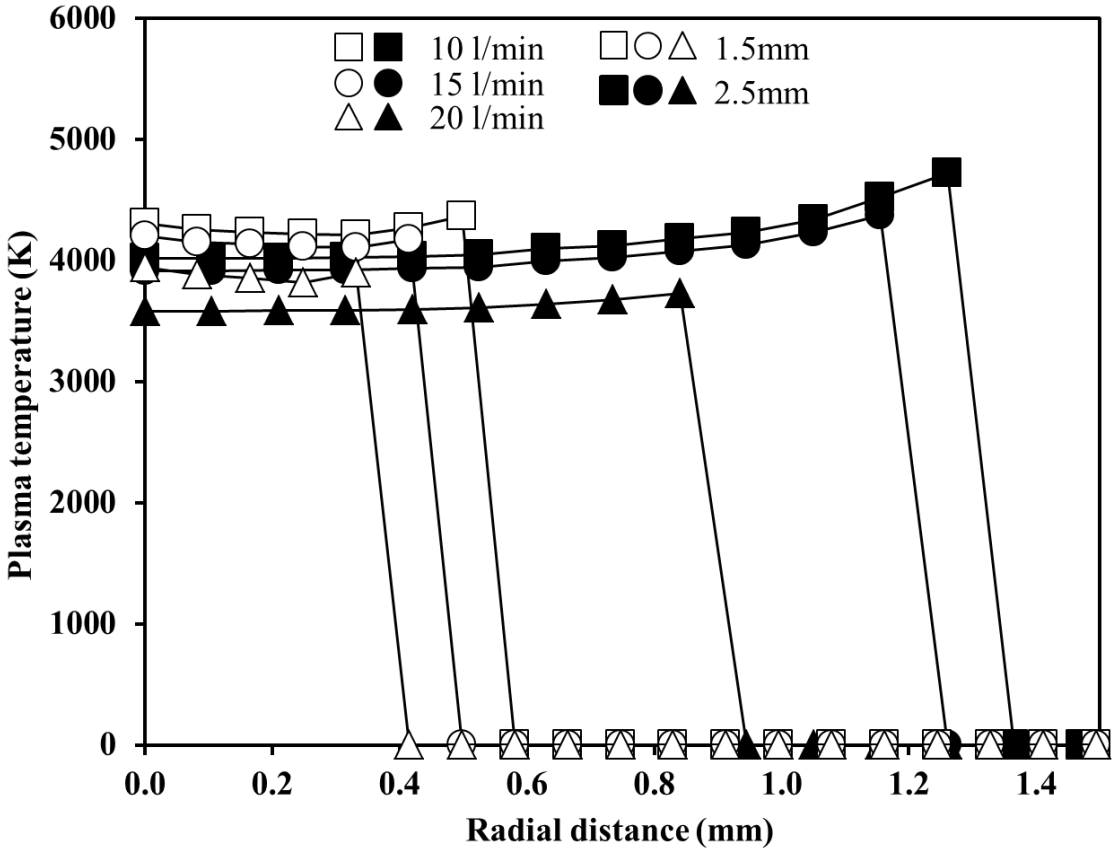


Fig. 2.7.5 Radial distribution of Ar plasma temperature at different working gas flow rate and antenna outlet diameter at Z =15 mm.

## 2.8 Study on spray particles behaviour

The increase in speed of the spray particle by plasma is known for the coating deposition film method using a plasma spray process. The in-flight speed of spray particle (particle velocity) is the factor which influences the structure of a spray deposit greatly [17]. It is generally known that when the particle velocity is high, the coating with low porosity and densely structured is able to be deposited. Therefore, in this section, the investigation was made in order to clarify the influence on the particle velocity by the change of working gas flow rate and antenna inside diameter.

### 2.8.1 *Measurement of particle velocity*

Particle velocity measurement of spray particles during spray was measured by high speed camera (Photron FASTCAM Mini AX 200) at 50000 frames per second. Figure 2.8.1 shows the still image of particles trajectory used for the particle velocity measurement. From the figure, the plasma area is defined as the area of the plasma swaying from left to right during the spray. In order to clarify the particle velocity during the collision to the substrate, particles trajectory at 40 mm of spray distance was used for the measurement. Image was captured without the substrate. The particle velocity was derived from the length of the trajectory of particle inside the plasma. The average of 10 particles trajectory was used for each measurement. The equation use for the derivation is as follows:

$$V\ (m/s) = L\ (m) \times \text{frame rate}\ (1/s) \qquad (2.8.1)$$

where v is particle velocity and L is length of trajectory.

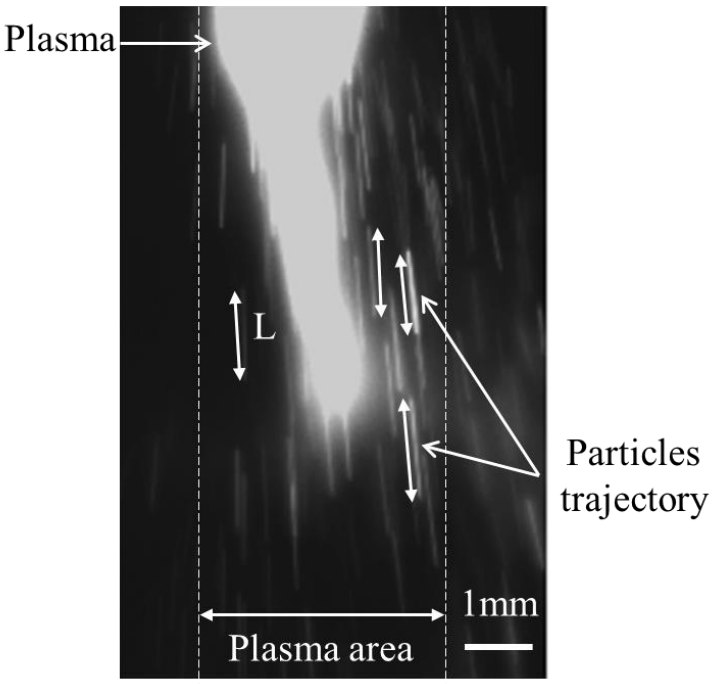


Fig. 2.8.1 Still image of particle trajectory captured by high speed camera.

2.8.2 *Results and discussions*

Figure 2.8.2 shows the results of particle velocity as a factor of working gas flow rate by the change of particle size and antenna outlet diameter. From the results, there is significant increase of particle velocity with the decrease of particle size. Smaller particle is easy to be flown by the working gas flow due to the lower weight. There is also significant increase of particle velocity with the smaller antenna outlet diameter at any spray conditions. This is thought to be the result of increasing gas velocity at smaller antenna outlet diameter. This is supported by the gas velocity simulation results obtained in the previous sub-chapter. The maximum velocity for 5 μm and 20 μm of spray particles at 1.5 mm of antenna outlet diameter were 135 m/s and 85 m/s, respectively. It is also known from the results that the particle velocity of low power microwave plasma spray is relatively low compared to conventional plasma spray where the particle velocity of the conventional easily exceeds 150 m/s even at the lowest parameter [18].

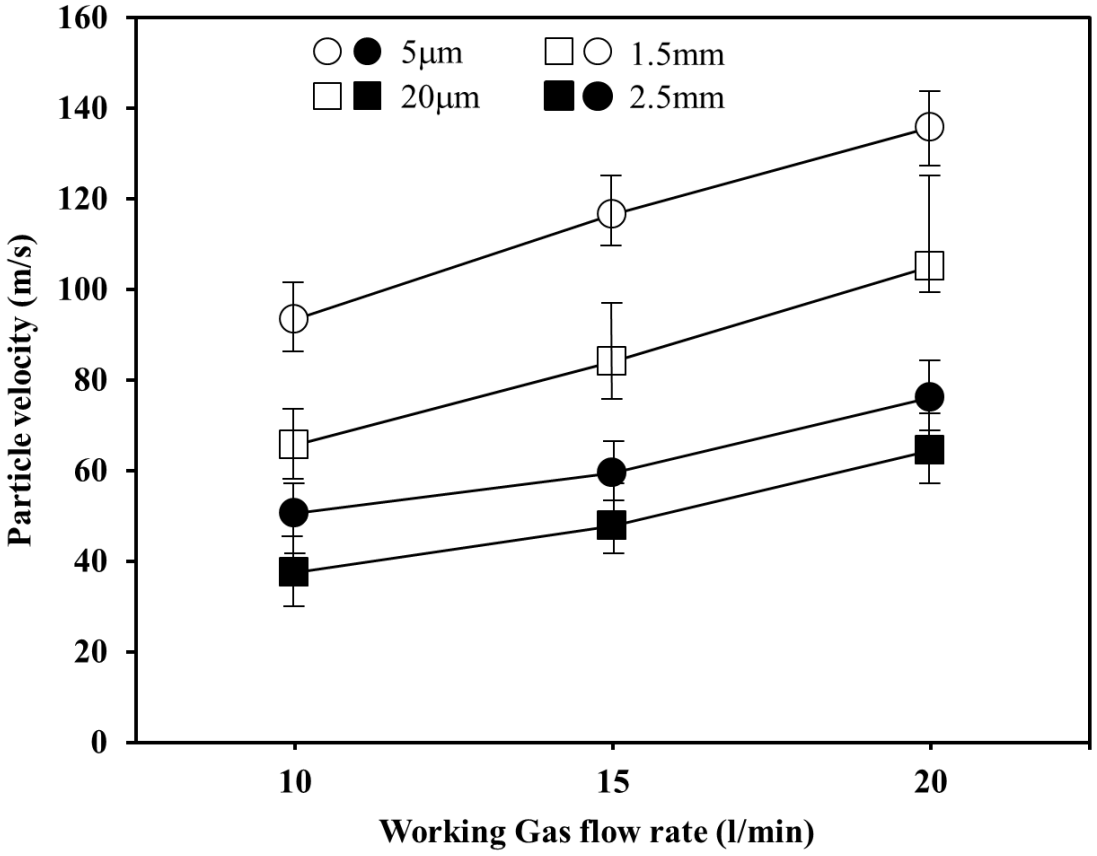


Fig. 2.8.2 Particle velocity measurement as a function of working gas flow rate on different antenna outlet diameter and particle size.

2.8.3 *Flattening behaviour of collected particles*

Figure 2.8.3 shows the results the flattening behaviour of single splat collected at each spray parameters by the use of 1.5 mm of antenna outlet diameter. From the results, the splat particles show splashing splat condition at 20 μm of particle size irrespective of any working gas flow rate. The particles collected only turned to disk splat shape at 15 and 20 l/min of gas flow rate at 5 μm of particle size. These results seem to correspond directly to the result of particle velocity in which the particle splat shows the tendency of turning to disk splat at particle velocity condition at higher than 15 l/min of gas flow rate where the particle velocity value is at above 110 m/s. As the reason of this phenomenon, by the increase of working gas flow rate, not only the particle velocity appeared to be increased, consequently, the plasma length decreased due to the thermal pinching effect. This results in increasing in-flight dwelling time of particles inside the plasma source. The increasing heat input towards the spray particles contributes to the formation of splashing splat. Furthermore, in the result of the particles turning to splashing splat, the shape are in annular ringed shape, where the ring area of the splat seems to bounce far from the center of the particles. As the details explanation of this phenomenon, study should be made on the effect of particle velocity towards the splat formation of particles whereas quite a number of researchers are focusing on the effect of substrate temperature [19, 20].

In general, however, it is well known that the breakup phenomenon of the liquid film generated by the collision of the particle to the solid surface can be evaluated by the splashing parameter, K, in the fluid dynamics field [21]. K is defined as $We^{0.5}Re^{0.25}$ and it is based on the in-flight kinetic information of the liquid particle. Here, We= $\rho$ dv2/c, and Re = qdv/g and $\rho$ : density, d: diameter, v: velocity, c: viscosity, g: surface tension, respectively. K has a critical value, and if the K value of the particle exceeds Kc, the liquid film show the break-up after the collision onto the solid surface. Here, if the density and surface tension are considered constant due to the same material, the splashing parameter depends mostly on particle's diameter, velocity and viscosity. Viscosity is inversely proportional to the temperature of the plasma where the melting of the particles occurred. Hence, the splashing parameter will be lower in the case of high gas flow rate in microwave plasma spray method where it is already explained in

the results of plasma temperature and particle velocity. From the equation theory, it can be explained from the result of 20 μm of Cu particle size where the splash splat occur in all conditions in compare to the ones with smaller diameter size, 5 μm particles. Hence, focus should be made on the appearing of disk splat in the result of 5 μm of particle size. Here, it can be explained that even though the velocity of particle is higher with increasing gas flow rate, the plasma temperature as well as dwelling time of the particles in plasma is decreased due to the decrease of plasma length which has been discussed earlier.

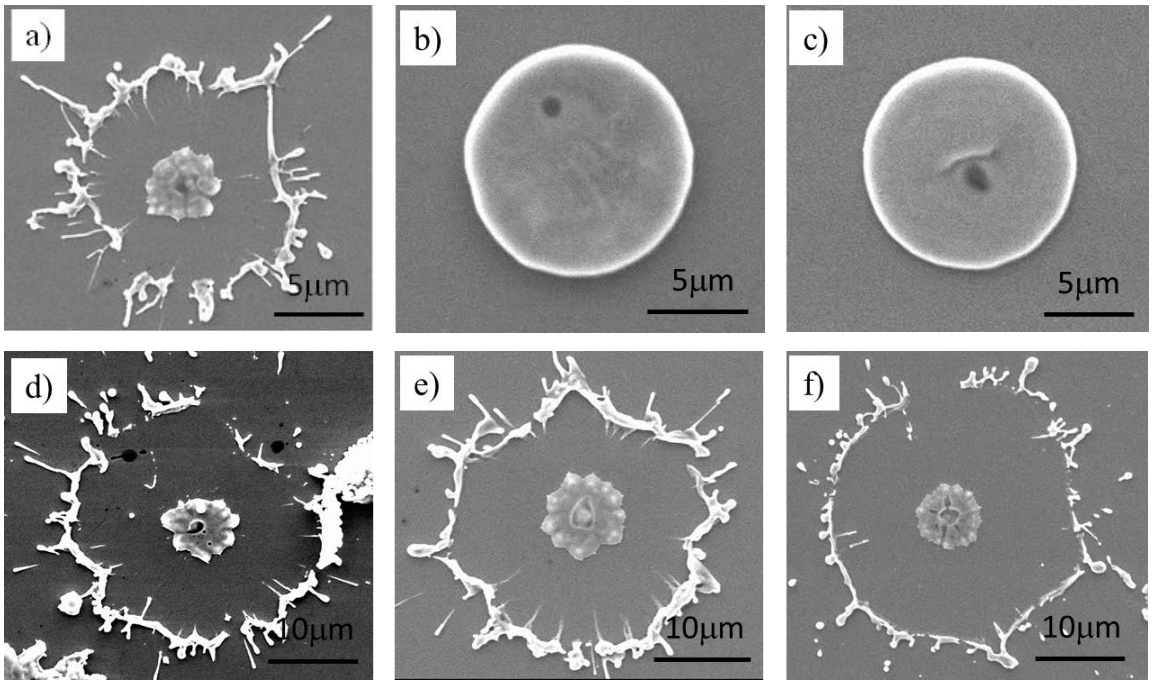


Fig. 2.8.3 Flattening behaviour of Cu particles at 1.5 mm of antenna outlet diameter and different particle size where (a), (b), (c) are 10, 15, 20 l/min of working gas flow rate respectively at 5 μm while (d), (e), (f) are 10, 15, 20 l/min respectively at 20 μm.

### 2.8.4 *Deposition of Cu coating*

Figure 2.8.4 shows the cross sectional morphology of Cu coating by the change of working gas flow rate and particle size at 1.5 mm of antenna outlet diameter. From the result, it can be observed that the thickness of the coating increase with working gas flow rate and with the decrease of particle size. This is due to increase of amount of particles by the change of working gas flow rate and the increase of particle velocity helps in increasing the impingent of the particles to fabricate the coating. Apparent porosity can also be observed to be reduced by the increase of working gas flow rate and decrease of particle size by the same reason on increasing particle velocity. Increase of particle velocity results in the further flattening of the particles which contributes to the deposition of coating with higher density. In this result, the formation of splashing splat is also can be thought as the reason of increasing apparent porosity of the coating. The splat splashing phenomenon may distribute the particles in much smaller size where the smaller sub-particles that solidify rapidly and may formed void in the middle of the ringed shape of the splat. The continuity of this phenomenon may increase the porosity inside the coating as the particles mount up to form the coating.

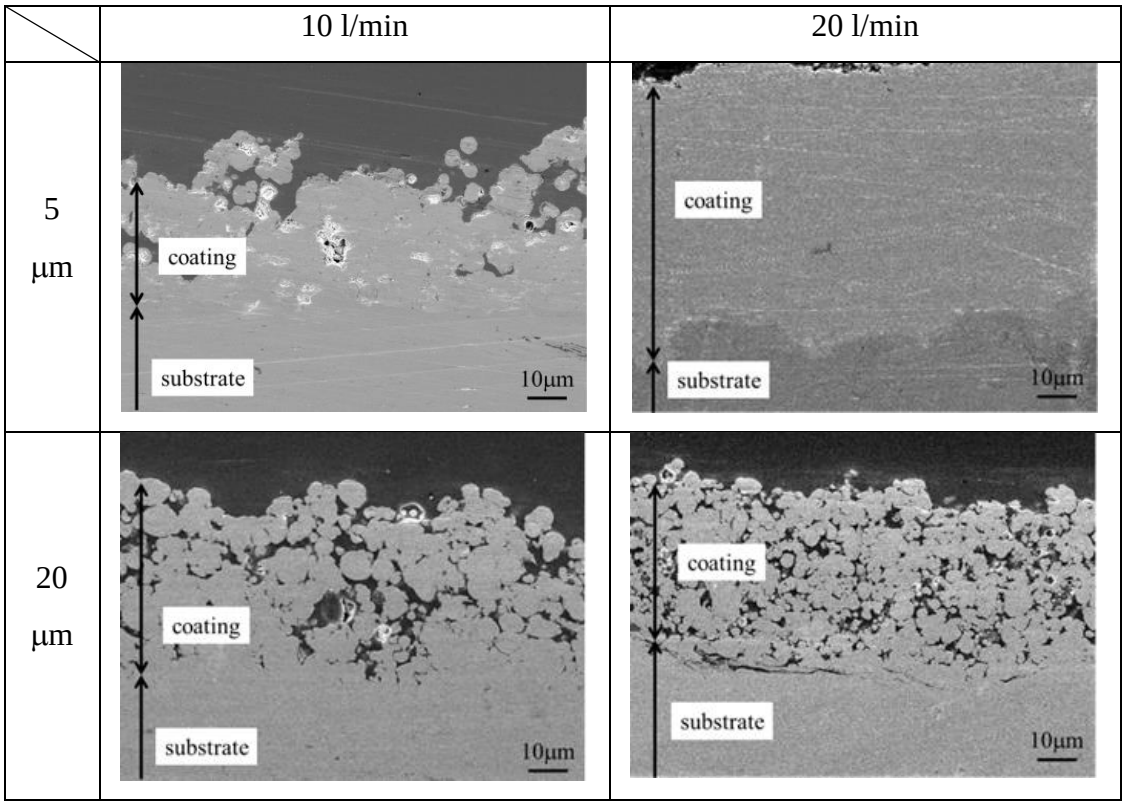


Fig. 2.8.4 Cross-sectional morphology of Cu coating deposited at 1.5 mm of antenna outlet diameter at changing gas flow rate and particle size

Meanwhile, Fig. 2.8.5 shows the cross sectional morphology of Cu coating by the change of working gas flow rate and particle size at 2.5 mm of antenna outlet diameter. The same tendency as observed in the result of 1.5 mm of antenna outlet diameter is recorded in the results. In overall result in compare to smaller antenna diameter size, the apparent porosity and coating thickness is appeared to be higher in the case of 2.5 mm due to the decrease of particle velocity.

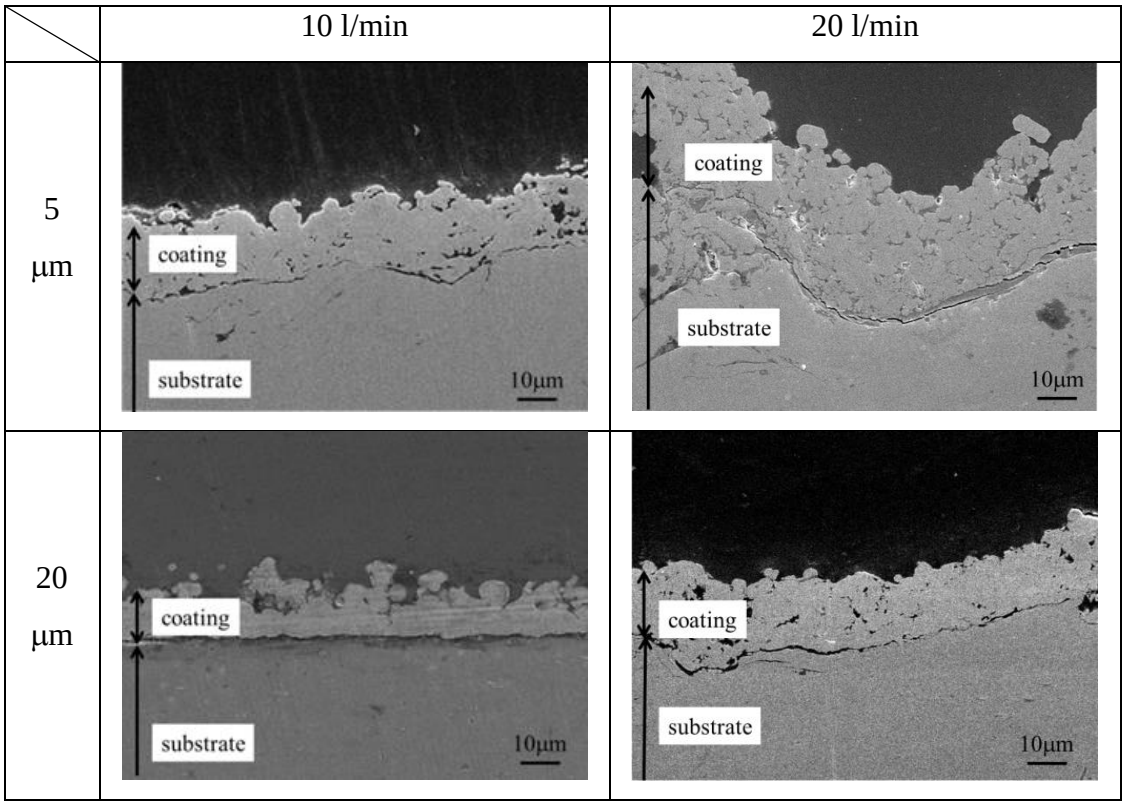


Fig. 2.8.5 Cross-sectional morphology of Cu coating deposited at 2.5 mm of antenna outlet diameter at changing gas flow rate and particle size

## 2.9 Conclusions

The summary of the things that had been clarified from the study of the operational characteristics evaluations of the low input power atmospheric pressure microwave plasma spraying device are listed below.

- At input power 0.5 kW of the plasma production conditions, it is clarified that the generation and maintenance of plasma is possible. However, on 0.1 kW of input power, plasma production and maintenance could not be performed and the maintenance of plasma becomes difficult on the input power of 0.3 kW, antenna outlet diameter 1.5 mm, and the ignition conditions of working gas flow rate 20 l/min.
- Substrate temperature decreased by the reduction of input power, the increase in a working gas flow rate, and the reduction of the antenna outlet diameter, in which the substrate temperature in 0.5 kW of input power, working gas flow rate 20 l/min, and antenna outlet diameter 1.5 mm was 381 K.
- Plasma length decreased with the increase in the working gas flow rate and antenna outlet diameter where the maximum plasma length on 34.3 mm was measured at antenna outlet diameter 2.5 mm.
- The maximum temperature of 4500 K was obtained at 10 l/min of working gas flow rate and 2.5 mm of antenna outlet diameter.
- The maximum velocity for 5 μm and 20 μm of spray particles at 1.5 mm of antenna outlet diameter were 135m/s and 85m/s, respectively.

# Chapter 3

# Deposition of coating with supress heat input effect onto substrate materials

## 3.1 Introduction

Hard chrome plating has been a trusted industry solution for wear, erosion, corrosion resistance and dimensional reclamation for many years. It can be applied at a reasonable cost per unit of surface area, but has limitations on thickness build-up, part size, and in some instances performance in service.

Over the past few years, costs have been steadily escalating due to the growing environmental pressures and legislation imposed on the chrome plating process and the disposal of its by-products. It has therefore become critical to industry to find alternative processes that offer similar characteristics to hard chrome plating, but without the consequent risks. Thermal spraying technology is increasingly offering a viable alternative to this technology, and could provide the chrome plating industry with complimentary processes for part protection and reclamation [1]. When comparing the two processes, a consideration of the economics involved in establishing and maintaining both types of facilities can be made. The following factors make thermal spraying commercially competitive with hard chrome plating.

1) Capital Cost - The relative capital expenditure for establishing facilities with the same production capability is much greater for chrome plating than thermal spraying.

2) Space - A thermal spray facility requires significantly less floor space than an equivalent plating facility.

3) Energy Cost - For plating, approximately 15 watts of energy are required per square inch. As part size increases, so do the energy costs. For thermal spraying,

part size affects coating application time, and depending on the process used, energy costs are similar.

4) Waste Disposal - Disposing of effluents from the plating process is becoming more and more costly. State and Federal regulations on pollution control require that each facility make substantial investments to adequately provide for waste treatment. Thermal spraying produces hazardous waste in the form of metallic dust, whose disposal is relatively easy.

5) Materials Diversity - A chromium plating facility is a total commitment to one coating, whereas a thermal spray facility provides the capability of producing a broad range of coatings.

Hard chrome plating is a crucial process associated with manufacturing and maintenance operations on aircraft, vehicles and ships, both in civilian and military sectors. Hard chrome electroplating is commercially used to produce wear-resistant coatings but the plating bath contains hexavalent chromium, which has adverse effects on health and environment. For this reason, the use of hexavalent chromium has been limited [2]. The types of coating methods that are most widely viewed as being capable of replacing hard chrome plating are the thermal spray technologies [3, 4]. Plasma spray method is the most versatile in the thermal spray technologies where even high melting point materials such as ceramics coating can be deposited. However, the conventional plasma spray method generates high heat input (8000 ~ 15000 K in plasma region) to both substrate and spray materials especially to the heat susceptible materials [5]. For this reason, the research of depositing hard chrome coating by low power plasma spray method has been brought upon.

Low power plasma spray method [6] is defined as a thermal spray method which used the thermal plasma generated with low input power (less than 10 kW) in the heat source. The effects of lowering the input power of the thermal spraying equipment by the plasma production at low electric power as well as the effects of controlling the heat input to the spray material (control of the significant change of material's microstructure) by low input power plasma are expected and the research is advancing in recent years. However, the input power of Cu coating deposited by conventional DC plasma spray method under atmospheric pressure condition which was reported is approximately 5kW [7, 8], while deposition of coating by using RF plasma spray under

atmospheric pressure condition is reported to be difficult due to the difficulty in stabilizing the plasma. On the other hand, with the input power of less than 1 kW, thermal plasma generation under atmospheric pressure is possible for microwave plasma spray method [9]. For this reason, it is thought that the coating deposition in which the heat input to the thermal spray material can be suppressed is achievable by applying microwave plasma as a low power plasma spray process. Moreover, this microwave plasma does not require electrode for electric discharge, which made it possible to generate plasma from chemically reactive type of gases if being compared to DC plasma in which the electrodes are needed for electric discharge. In comparison to DC plasma, microwave plasma has a lot of advantages such as plasma can be produced with relatively low input power, high plasma density, wide discharge frequency and electrodeless gas discharge [10]. Therefore, in recent years, microwave plasma was applied in a wide range of fields, such as decomposition processing of harmful gas, heat treatment of waste, sterilization of medical material, and deposition of thin film [11]. In our laboratory, the low power atmospheric pressure microwave plasma spraying device which used microwave plasma for the heat source was successfully being applied [12].

Under atmospheric pressure, the plasma production of approximately 1 kW of low input power is made possible by the atmospheric pressure microwave plasma spraying device. Moreover, in order to investigate whether the heat input reduction to the spray substrates is possible, the metal (Cu) coating deposition onto low melting point material called carbon fiber reinforced plastics (CFRP) and fiber reinforced plastic (FRP) which are susceptible to heat, is already clarified [13]. In case of coating deposition of hydroxyapatite (HA) as a biomedical material, emergence of decomposition phase harmful to human body caused by the heat input from the plasma will occur for the conventional plasma spray process [14]. However, the HA coating with suppressed decomposition phase is also successfully able to be deposited [15].

Here, we deposit a hard chrome coating onto heat susceptible substrate, CFRP by using low power microwave plasma spray. For comparison, a hard chromium coating was also deposited onto SUS304. Morphologies and structural characteristics were measured by using X-ray diffraction (XRD) and scanning electron microscope (SEM).

## 3.2 Test materials

3.2.1 *Feedstock powder materials*

In this experiment, high hardness metal material, Cr which possesses the melting point of 2176 K is used as feedstock powder to deposit coatings. Chrome powder (ATP100-10μm, KOJUNDOKAGAKU Research Centre) has the average size of 10 μm with the purity of above 98 %. SEM image of Cr powder is shown in Figure 3.2.1. The particle shape, diameter and melting point is shown in Table 3.2.1. The X-ray diffraction analysis result of the Cr powder is shown in Fig. 3.2.2.

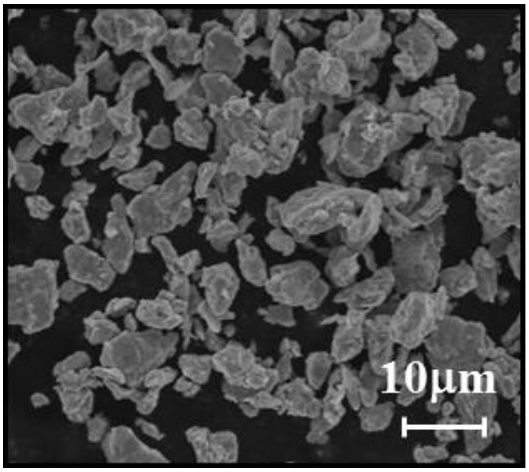


Fig. 3.2.1 SEM image of Cr particles.

Table 3.2.1 Material properties of Cr particles

| Particle shape | Grid form |
|---|---|
| Particle diameter (μm) | 10 |
| Purity (%) | > 98 |
| Melting point (K) | 2176 |

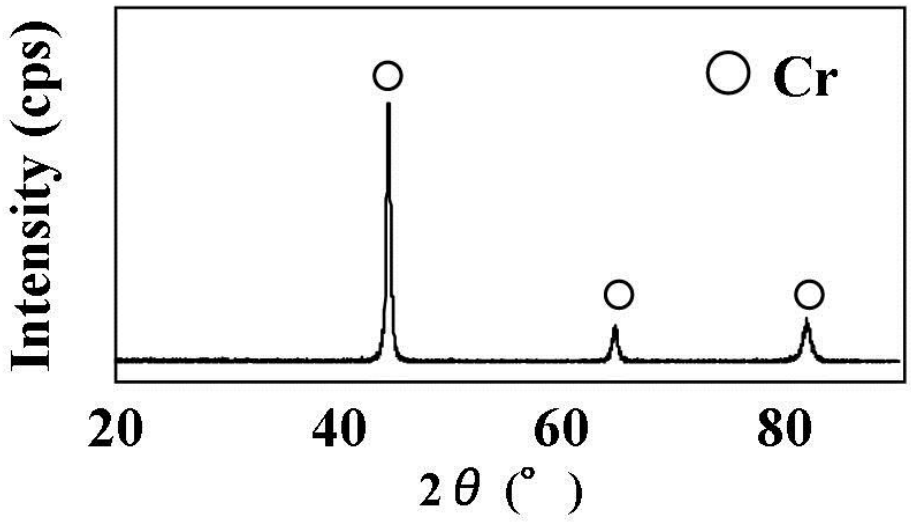


Fig. 3.2.2 X-ray diffraction pattern of Cr particles

### *3.2.2 Substrates materials*

#### *3.2.2.1 SUS304*

Firstly, in order to test whether the Cr coating is able to be deposited by microwave spray device at our lab, SUS304 was used as substrate material, and the experimentation as well as the investigation of the coating was conducted. Due to the reason that the heat susceptible substrates such as high carbon steel and CFRP are easy to be affected by the heat input of the plasma, some of the evaluations of the coating were conducted on the SUS304 substrates. As the pre-treatment for the substrates before spraying, substrates were grit blasted to roughen the surface and then the substrates were cleaned by acetones. Size of substrate is fixed at the dimension of 20 x 20 x 3 mm. In order to observe the deposition of particles on the substrate, the observation of every single particle of collected splat was done after sprayed using the substrates with mirror finished.

#### *3.2.2.2 High Carbon Steel*

High carbon steel substrates used in this research are manufactured by KANAI JUYO Corporation. The substrate is unconnected oblong ring in shape with the

dimension of 5 mm length and 2 mm width. Figure 3.2.3 shows the photograph of high carbon steel substrate used in this experimentation. The deposition of Cr coatings was applied at the area shown in the figure.

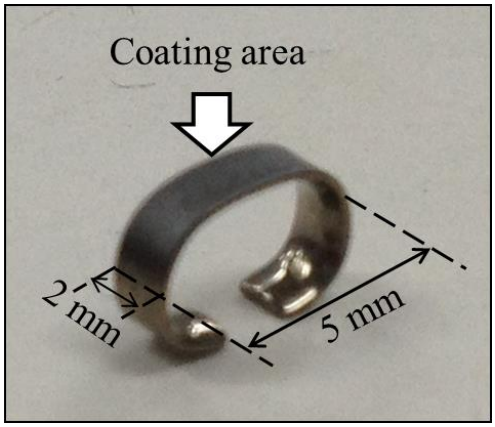


Fig. 3.2.3 Photograph of high carbon steel substrate.

*3.2.2.3 CFRP*

After the experimentation of the coatings deposited onto SUS304 substrates and high carbon steel substrates, coating deposition onto low melting point substrate, CFRP at the most optimum condition was tried. The heat-resistant temperature of CFRP used in this experiment is about 523K. As the pre-treatment for the substrates before spraying, the surface of the substrates was cleaned by ethanol. Moreover, carbon fibre uses the base material by which multi-stage lamination was carried out, and is horizontally laminated to the direction of the substrate. Size of substrate was set at the dimension of 20 mm x 20 mm x 3 mm.

## 3.3 Experimental method

In this study, the experimentation of coating deposition and the observation of as-sprayed coating in which Cr powder was used as the spray particle, the observation of splat shape, measurements of the hardness of coatings were performed. Experimental condition is shown in Table 3.3.1. Antenna inside diameter of 1.5 mm was selected in order to expect the reduction of porosity and the increase of density of the coating. Moreover, in order to investigate the effect of working gas flow rate influencing the particle velocity, 3 conditions was set which are 10, 15 and 20 l/min. From the past research findings, although it was known that the porosity in the coating decreases with the increase in working gas flow rate , however on the other hand, sufficient heat input to particles was not able to be transferred resulting in the difficulty of depositing the coatings. The reason of the input power to be set at 0.5 kW is to lower the input power used by this plasma spray equipment and the plasma is also reported to be more stabilised at 0.5 kW. Coating was first deposited onto high melting point substrates which is SUS304, then onto the heat susceptible substrates, high carbon steel and finally onto CFRP.

Table 3.3.1 Experimental conditions for the deposition of Cr coating

| | |
|---|---|
| Input power (kW) | 0.5 |
| Working gas flow rate (l/min) | 10, 15, 20 |
| Antenna diameter (mm) | 1.5, 2.5 |
| Spray distance (mm) | 30, 35, 40 |
| Traverse speed (mm/s) | 5 |
| Operation time (s) | 300 |

## 3.4 Evaluation method

*3.4.1 Observation method of spray particles, coating and the splat shape*

The observation of spray particles, coating and the splat's shape of the Cr feedstock powder used in this experiment were conducted by the scanning electron microscope (JSM-6390TY, which will be mentioned afterwards as SEM) is manufactured by NIPPON DENSHI CORP. For the cross-sectional observation of the coating, substrates were mounted into the cold mounting resin, polished with the emery paper (starting from the rough #80 until #2000), then buffing was performed using 1 μm and 0.3 μm of alumina. Before the observation, in order to acquire electrical conductivity, the sample surface was Pt coated by the thickness of 20 nm using a sputtering device.

In observation of the splat shape for the study of the flattening form of the particles after spray, the splat collection was performed using mirror polished SUS304. For the collection of the splat particles, traverse speed of the substrates was set at 100 mm/s with the dimension of the substrates at 20mm×20mm×5mm.

*3.4.2 Measurement of coating hardness*

The hardness of as-sprayed coatings was measured by micro-hardness measurement device (HMV-1). The micro-hardness measurements were carried out on a polished cross section of the coatings with an applied load of 490.3 mN as a final load and test time was 10 s. The indentation of the Vickers diamond indenter was performed at 7 different places and the average value was calculated. The distance between indentations was large enough to avoid interaction between the work-hardened regions and any micro-cracks caused by the indentations.

### 3.4.3 *X-Ray diffraction analysis*

In this experimentation, X-ray diffraction analysis (XRD) which identifies the composition phase of a coating was performed in order to investigate the coating deposition mechanisms in each coating deposited. XRD was performed using intensified X-ray diffraction equipment (RINT-2500 manufactured by RIKAGAKUDENKIKOGYOU), and the as-sprayed coatings were measured. XRD conditions for this experimentation are shown in Table 3.4.1. XRD analysis measurement was conducted in the diffraction angle range of $20° \leqq 2\theta \leqq 90°$.

Table 3.4.1 Measurement conditions of X-ray diffraction analysis

| Samples | Particles | Coatings |
|---|---|---|
| X-ray generator | 18 kW | |
| Target | CuKα | |
| Power | 30 kV | 30 kV |
| | 80 mV | 160 mV |
| Sampling width | 0.02° | |
| Scanning speed | 4.0°/min | |
| Divergent slit | 0.5° | |
| Scattering slit | 0.5° | |
| Receiving slit | 0.15 mm | |

## 3.5 Deposition of coating and the characteristics evaluations

The experimentation of coating deposition, observation of the morphology of as-sprayed coatings, observation of the splat shape, phase identification of coating by X-ray diffraction, etc. were performed, and the characteristics evaluation of the coatings was conducted.

### 3.5.1 *Deposition of Cr coating onto SUS304 substrates*

In this experimentation, in order to study on the effect antenna outlet diameter towards the deposition of Cr coatings, two sizes of the antenna outlet diameter were used. As the results, at antenna outlet diameter of 2.5 mm, coating deposition within the operation time of 300 s is not able to be observed. As the reason of this phenomenon, the comparison of the characteristics of the plasma was carried out between the two sizes of the antenna and the results is shown in Table 3.5.1. The results of the plasma temperature and plasma structure were derived from the study in second chapter. From the comparison, it is confirmed that by the reduction of antenna outlet diameter, the temperature of the plasma remains almost the same. However, it can be observed that the particle velocity of the Cr particles was accelerated to more than two-fold after the reduction of antenna outlet diameter from 2.5 mm to 1.5 mm. This contributes to the possibility of the deposition of Cr coatings by antenna outlet diameter of 1.5 mm. Furthermore, the structure of the plasma also changed to be fully solid structure at 1.5 mm of antenna outlet diameter which contributes to the increase of the area of the Cr particles to be melted inside the plasma plume. This result also shows that the plasma is more stabilized with the reduction of antenna outlet diameter size.

Table 3.5.1 Comparison between different antenna sizes

| | 1.5 mm | 2.5 mm |
|---|---|---|
| 1) Plasma temperature | Above 4000 K | Above 4000 K |
| 2) Plasma structure | Solid structure even at the upper-stream of the plasma | Hollow structure at the upper-stream of the plasma |
| 3) Maximum particle velocity | 135 m/s | 66 m/s |

The research was then furthered by using only the antenna with 1.5 mm of outlet diameter size. In this experiment, the study on the effect of the change of working gas flow rate was conducted. The photographic view of the Cr coating deposited onto SUS304 substrate is shown in Fig. 3.5.1. Fig. 3.5.2 shows the SEM images of chrome particles and the surface morphologies of sprayed particles. From the result, Cr particles were melted and impinged onto the SUS304 substrate, and the splat was fabricated. The cross-section morphology of the coating under the experimental conditions of working gas flow rate 10 and 20 l/min and spray distance 30, 35, 40 mm is shown in Fig. 3.5.3 and Fig. 3.5.4. From the results, it is clarified that the deposition of high melting point chrome coating is possible at 0.5 kW of input power. From the observation results, the tendency of the increase of coating thickness by the increase of working gas flow rate and the decrease of spray distance is shown. Moreover, dense coatings with low composition of pores were able to be observed. However, in the interface of substrate and coating, the tendency which the pore in the coating increases because working gas flow rate increases is confirmed from the past research findings [16] with the increase in spraying distance in the experiment in which the coating deposition of Cu as a spray particle with antenna inside diameter 1.5 mm, and a spraying distance of 40 mm conditions. On the other hand, when Cr is made into the spray particle, the increase in the pore by the increase in a working gas flow rate was not able to be observed due to the consideration that in this case, only the particles which reached sufficient melting state were flattened and impinged to the substrates. When a coating is deposited by making Cu as the spray particles at the particle diameter the same as the one used in this

experiment, the difference in material characteristics is considered as a cause in which the pores were emerged. Heat transfer coefficients are about 1/4 compared with 93.6 W/m-K of copper at 398 W/m-K, and the chromium currently used in this experiment is considered to be difficult to be cooled during the flight. Therefore, by the case where a heat transfer coefficient is high for the material like Cu, even if it is in the state which carried out enough melting, since it is easy to be cooled during a flight, by the increase in the spraying distance, the solidification takes place during a flight and the flattening of the particles at the moment of impingement to the substrates is difficult to be occurred. However, in the case of Cr, it is thought that the solidification by in-flight cooling does not take place easily, not being influenced with spraying distance, chromium adheres to the substrate while remains in the melting state and flattened to become dense coating with few pores.

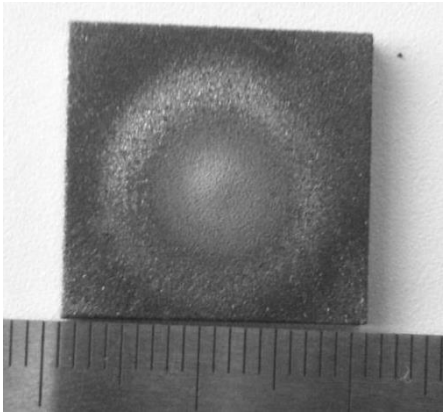

Fig. 3.5.1 Photograph of top view of Cr coating.

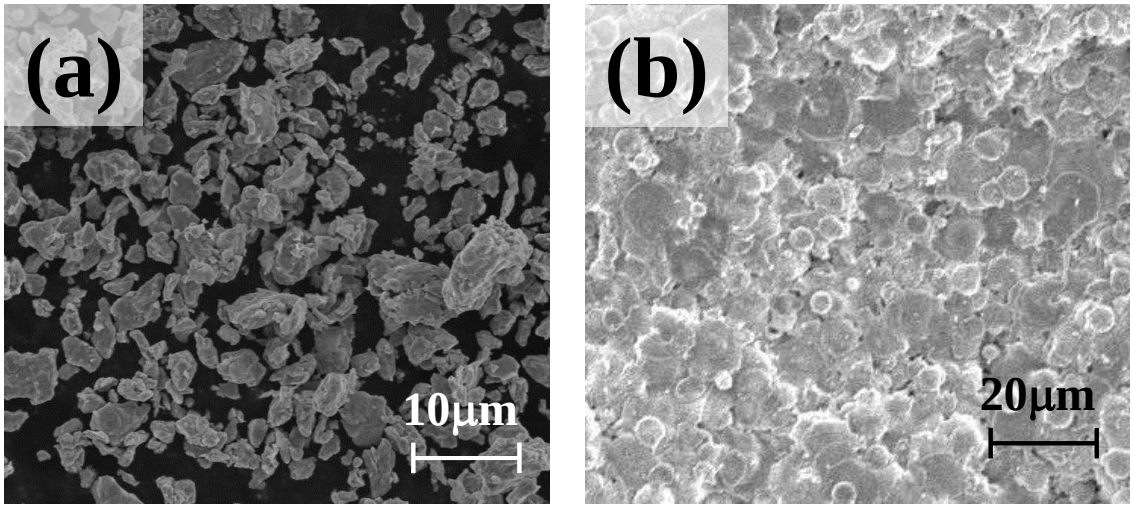


Fig 3.5.2 SEM images of (a) Cr particles and
(b) surface morphology of sprayed (a).

| Spray distance (mm) | Overall view | Enlarged view |
|---|---|---|
| 30 | 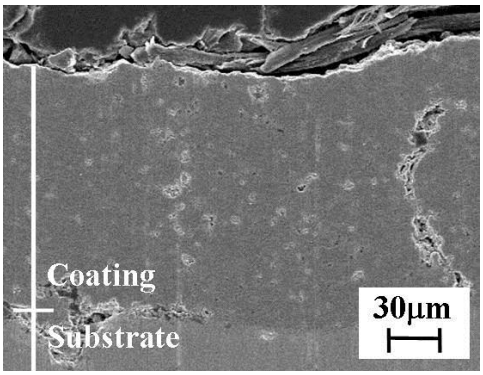 | 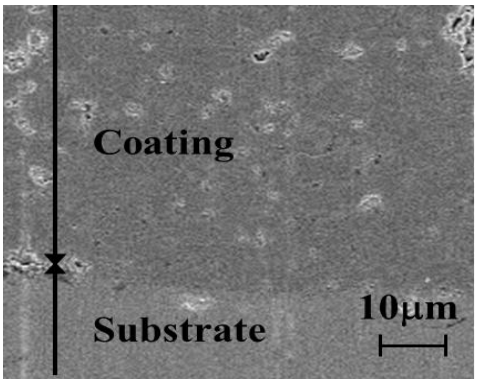 |
| 35 | 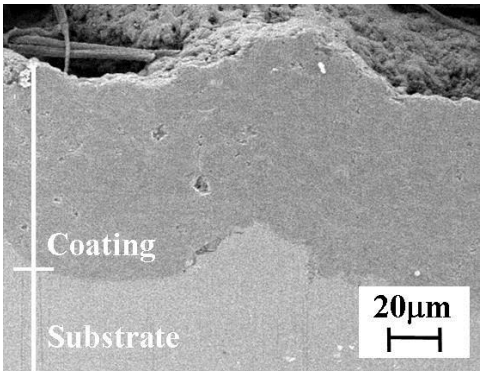 | 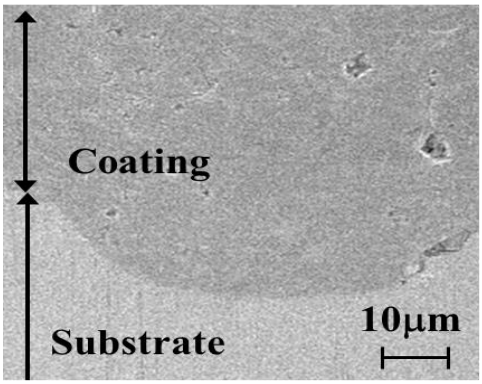 |
| 40 | 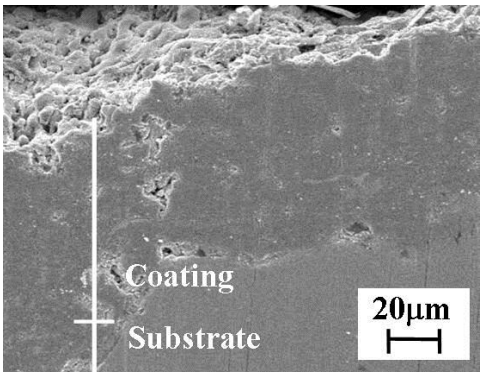 | 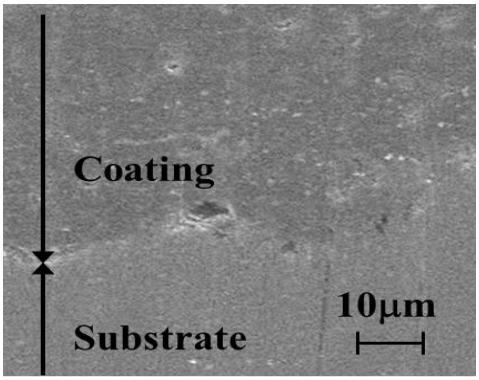 |

Fig. 3.5.3 SEM images of the cross-sectional morphologies of the Cr coatings at working gas flow rate 20 l/min.

| Spray distance (mm) | Overall view | Enlarged view |
|---|---|---|
| 30 | 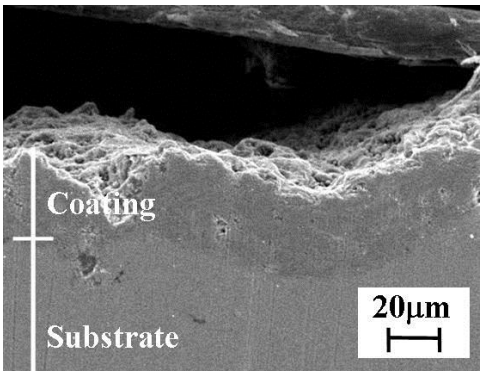 | 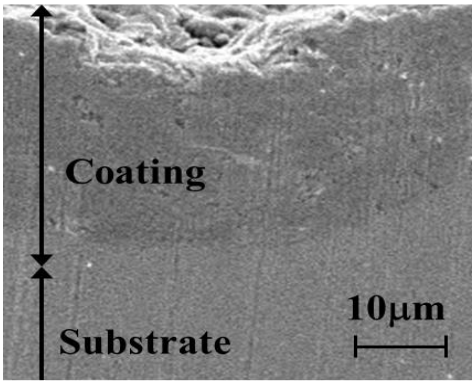 |
| 35 | 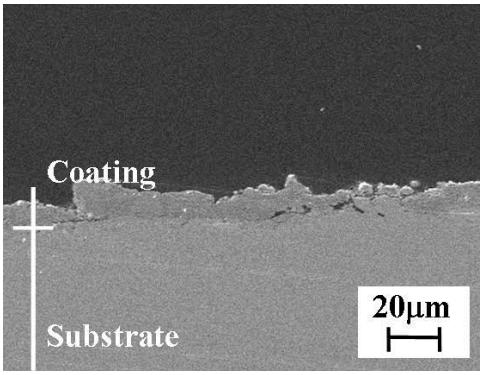 | 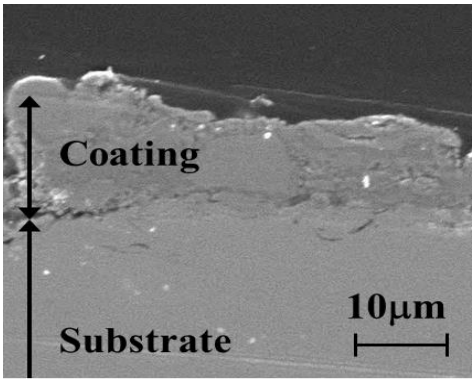 |
| 40 | 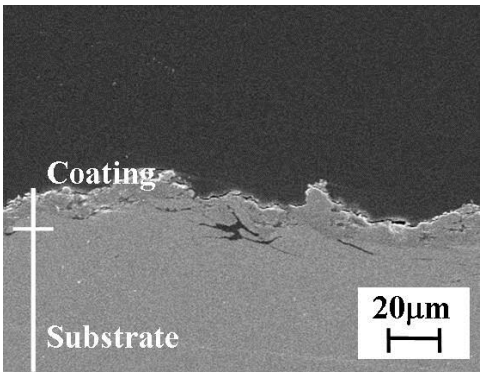 | 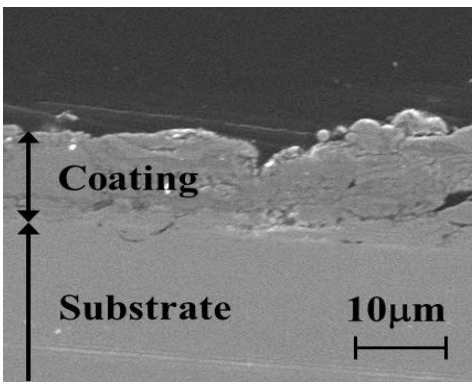 |

Fig. 3.5.4 SEM images of the cross-sectional morphologies of the Cr coatings at working gas flow rate 10 l/min.

### 3.5.2 *Effect of the coating deposition rate*

In this experimentation, the study of the amount of powder supplied and coating deposition rate was conducted as the investigation of the effect to the coating deposition rate by spraying distance and the change in a working gas flow rate. The result of the measurement of the powder feed rate in with the change of working gas flow rate is shown in Fig. 3.5.5. From the results of the investigation, the increase rate of about 50% was shown by a working gas flow rate increasing to 20 l/min from 10 l/min. The results of the investigation of coating deposition rate are shown in Fig. 3.5.6. The coating deposition rate increases with working gas flow rate. As a factor of the increase in coating deposition rate, the increase in the amount of impinged particles to substrate by the increase in the amount of powder supplied by the increase in working gas flow rate and particle velocity can be considered. Coating deposition rate is considered to have risen up not only by the increase in the powder feed rate but also from the rate of increase of the coating deposition rate by the increase in particle velocity by the means of the increase in working gas flow rate in this being by a factor of 5 or more. Moreover, coating deposition rate decreased in all conditions of working gas flow rate with the increase in spraying distance. Since the molten particles which travelled from the plasma plume to collide with the substrate were cooled by the increase of spray distance resulting in the coating was not able to be deposited, due to the reason that only the particles which reached sufficient melting state were impinged onto the substrate, although the coating porosity was improved by this phenomenon, coating thickness was decreased. Therefore, as compared with the conditions of 10 l/min of working gas flow rate, it is possible also on the conditions in working gas flow rate 20 l/min with high particle velocity to have high coating deposition rate.

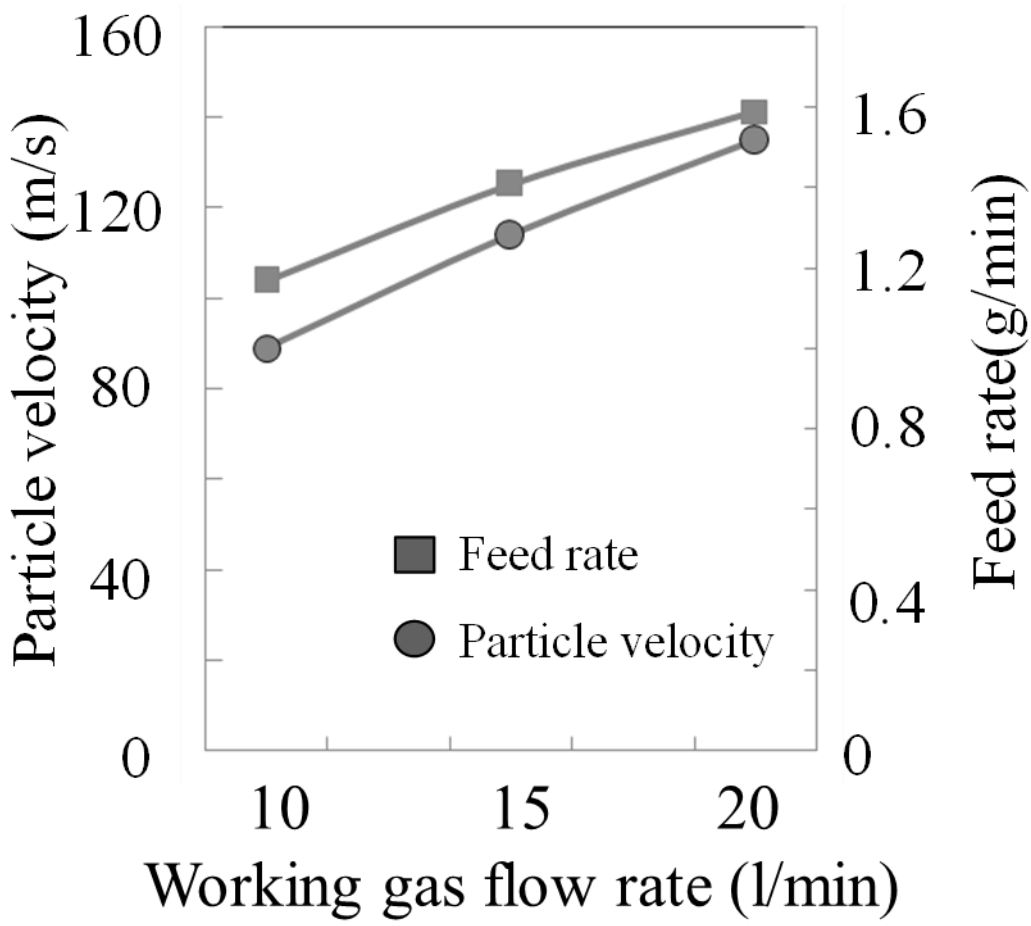


Fig. 3.5.5 Particle velocity and powder feed rate with the change of working gas flow rate.

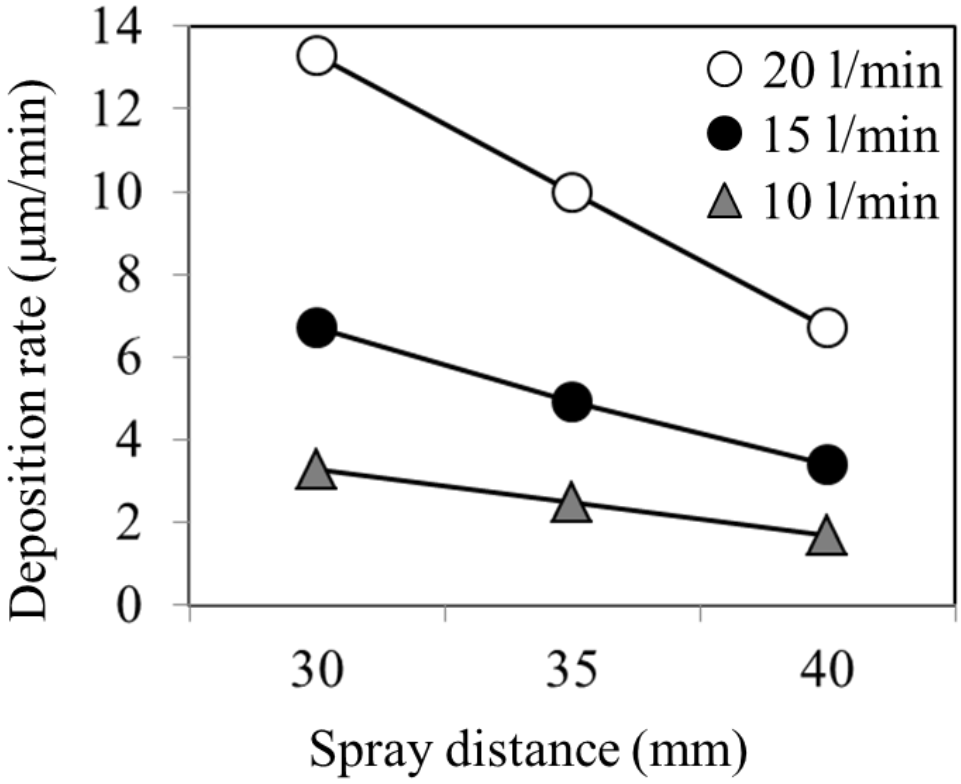


Fig. 3.5.6 Deposition rate of Cr coating deposited onto SUS304.

3.5.3 *Coating hardness and flattening ratio*

The observation of the impinged form of the splat onto the substrates for each experimental condition was conducted, and the appearance ratio of the particle impinged onto the substrates was investigated. Figure 3.5.7 shows the SEM image of the fully-melted and half-melted splat form of the particles impinged onto the substrates. The consideration of the fully melted splat form is defined as the particles which fully impinged onto the substrates and possess splat diameter of more than 10 μm while for the half-melted particles, impinged particles must at least have the size of more than 5 μm. The particles which passed the specifications which defined before will be calculated and the melting percentage is defined as the ratio of the fully-melted and half-melted particles per the sum of the collected particles.

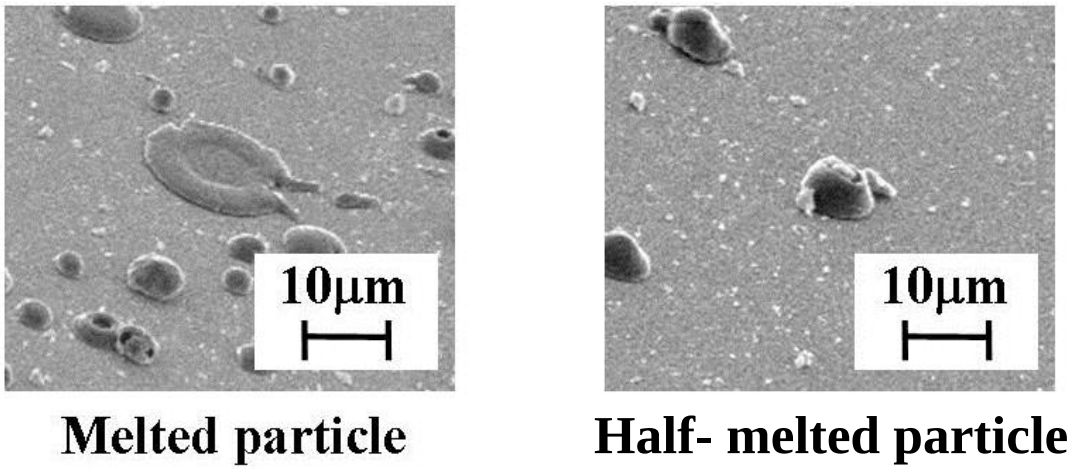


Fig. 3.5.7 SEM image of fully-melted and half-melted splats.

Since sufficient coating thickness was not obtained for the measurement of coating hardness under the conditions of working gas flow rate 15 l/min, only coating deposited under the conditions of working gas flow rate 20 l/min investigation of melting percentage and measurement of coating hardness were performed. The results of SEM images of melted particles under different spray distance are shown in Fig. 3.5.8. Figure 3.5.9 shows the results of coating hardness while Fig. 3.5.10 shows the results of the investigation of melting percentage of Cr particles. From the results of the investigation of melting percentage, it is showed that the rate of melting percentage decreased with by spray distance. In all the spraying distances, the hardness of the coatings is 900 $Hv_{0.05}$ or more. The coating deposited by microwave plasma spray reached the hardness not only comparable as Cr plating but also improved at certain spray conditions. Moreover, coating hardness increased with the reduction in spraying distance, and coating hardness showed the highest value of 1111 $Hv_{0.05}$ under the conditions where the spraying distance is 30 mm. From this, it is thought that since the dense coating was formed of the particles to which sufficient flattening occurred with the increase in melting percentage, coating hardness increased.

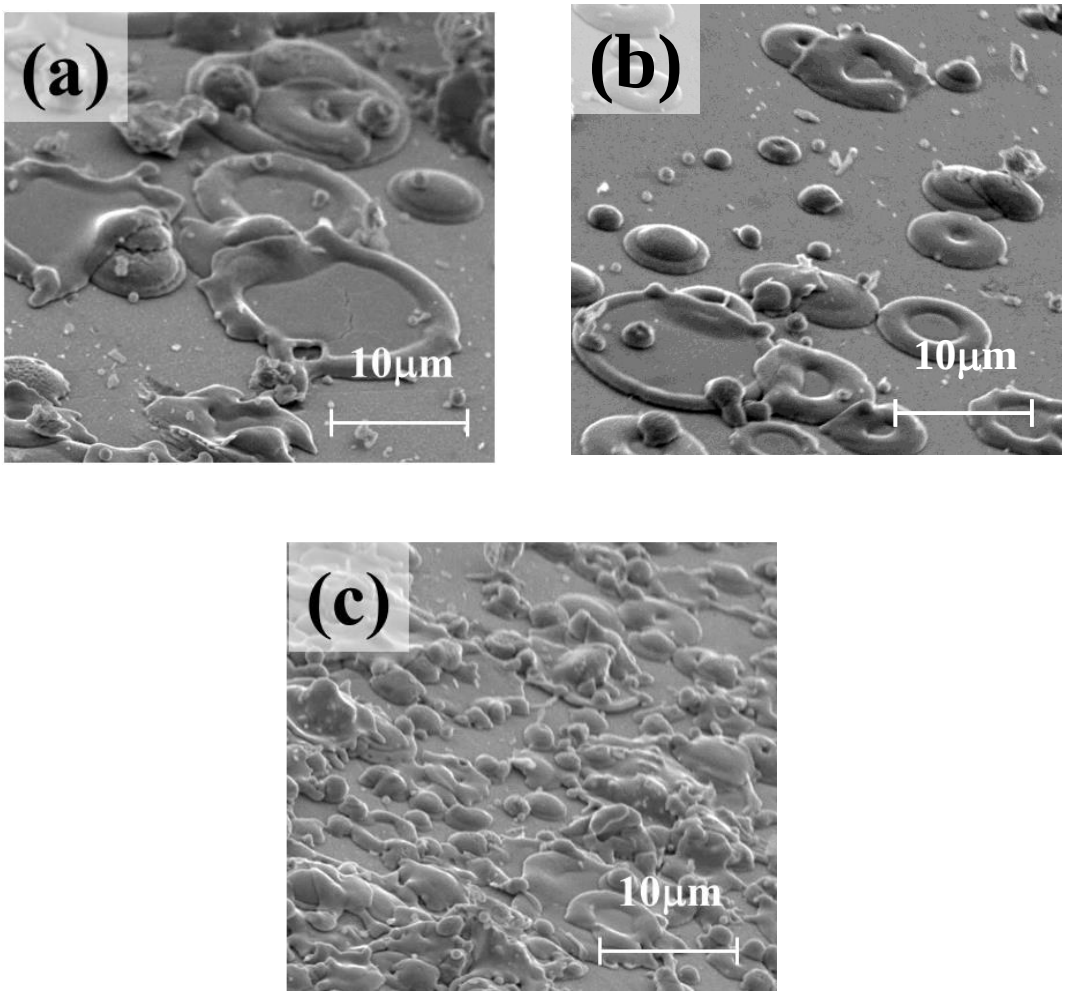


Fig 3.5.8 SEM image of melted particles under different spray distance
(a) 30 mm,(b) 35 mm, (c) 40 mm.

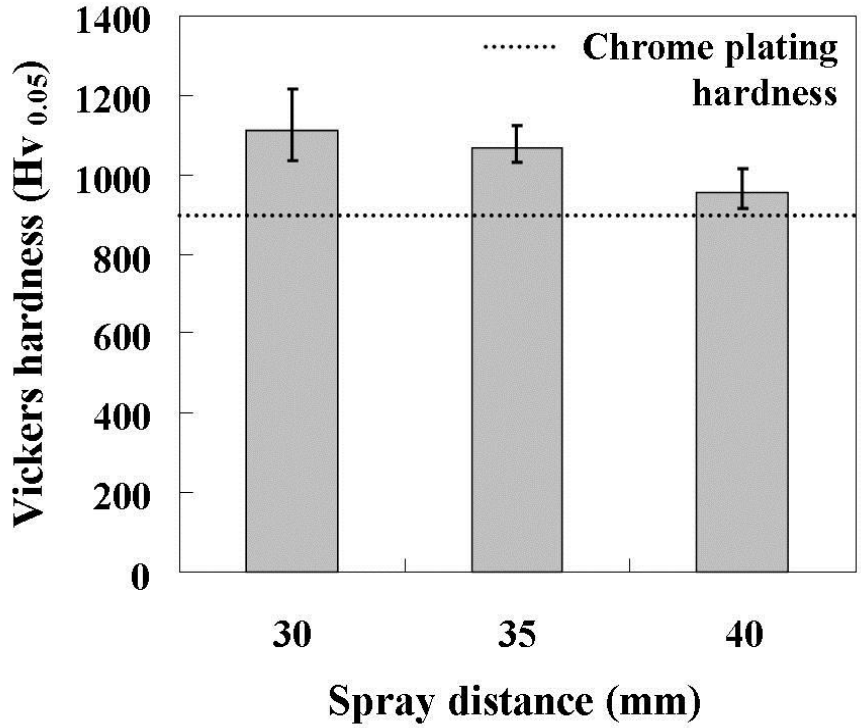


Fig. 3.5.9 Vickers hardness of Cr coatings.

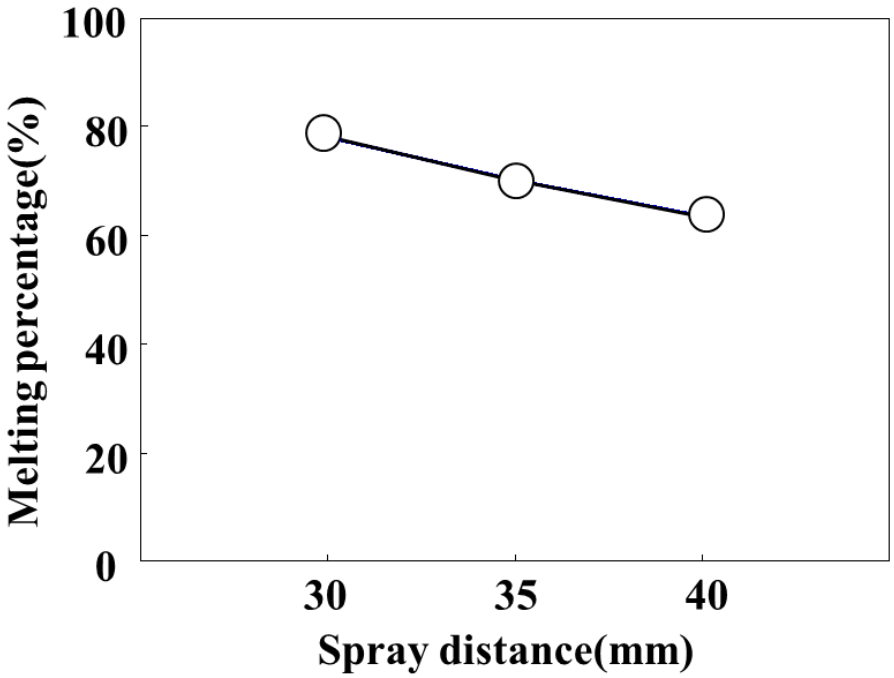


Fig. 3.5.10 Flattening ratio of Cr splat shape with the change of spray distance at 20 l/min of gas flow rate.

### 3.5.4 *X-Ray diffraction analysis*

In this analysis, in order to investigate the effect of working gas flow rate and spray distance to the composition phase of Cr coatings, as-sprayed coatings with different working gas flow rate and spray distance was evaluated. Figure 3.5.11 shows the results of X-ray diffraction patterns of Cr coatings at working gas flow rate 20 l/min and 15 l/min at spray distance 30 mm. In these results, due to the insufficient thickness of the coatings deposited at working gas flow rate 10 l/min, only analysis of coatings deposited at working gas flow rate 15 l/min and 20 l/min were able to be evaluated. From the obtained results, the tendency of the increment of the oxide of chrome, chromium (III) oxide with the increase of the working gas flow rate is confirmed. This is due to the reason that by the increase of the working gas flow rate, plasma length is decreased results in the increase of in-flight time of spray particle in the atmosphere. This will increase the oxidation of the molten spray particles during flight.

Furthermore, composition investigation by the X-ray diffraction of the coating deposited was conducted under the conditions to which spraying distance was changed from 30 to 40 mm at 20 l/min of working gas flow rate in which coating hardness measurement was performed. The results of X-Ray diffraction analysis of the as-sprayed coatings are shown in Fig. 3.5.12. From the result, the peak of chromium (III) oxide which is an oxide of Cr was confirmed inside the coating without the concern of the change of spray distance. From this, it can be thought that the emergence of chromium (III) oxide during spray resulting the increase of the hardness of the coating due to the high hardness of the chromium oxide. Moreover, it turned out that the peak intensity of chromium (III) oxide becomes higher with the increase of spraying distance. Since the in-flight travelling time of the particles exposed into the atmosphere increased with spraying distance, this is considered that oxidization of the Cr particles was increased.

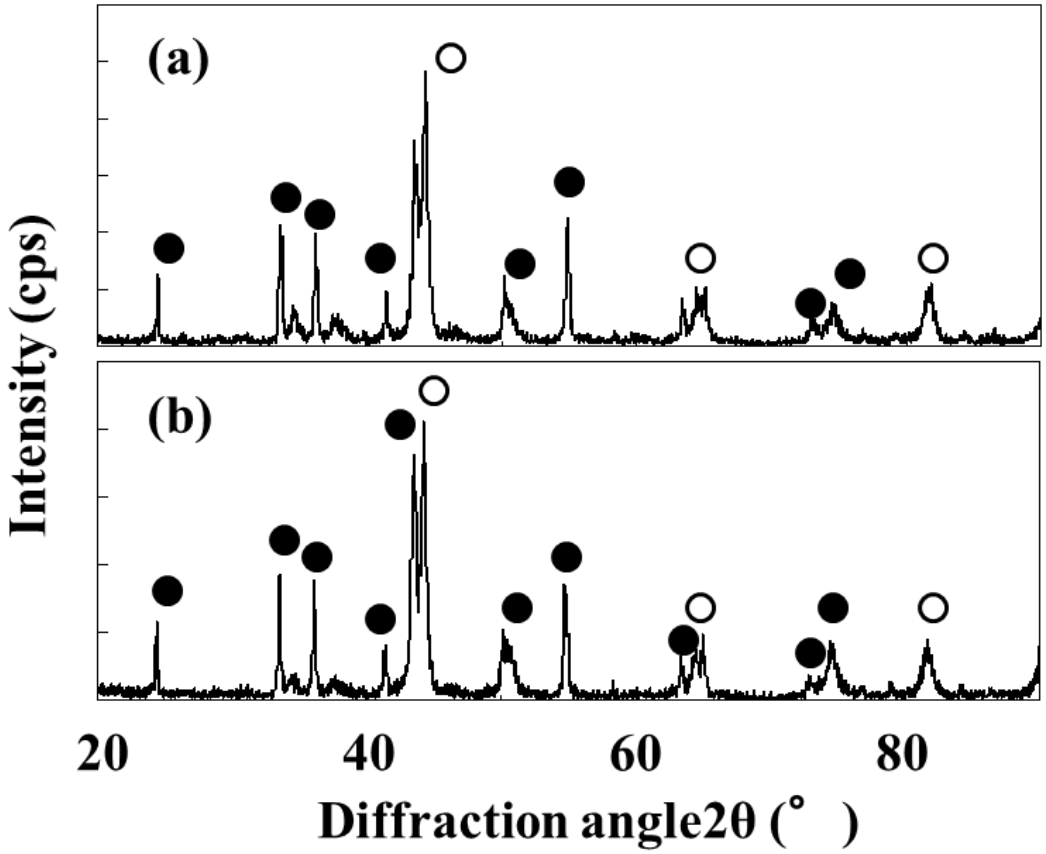


Fig. 3.5.11 X-ray diffraction patterns of Cr coatings at working gas flow rate (a) 20 l/min and (b) 15 l/min.

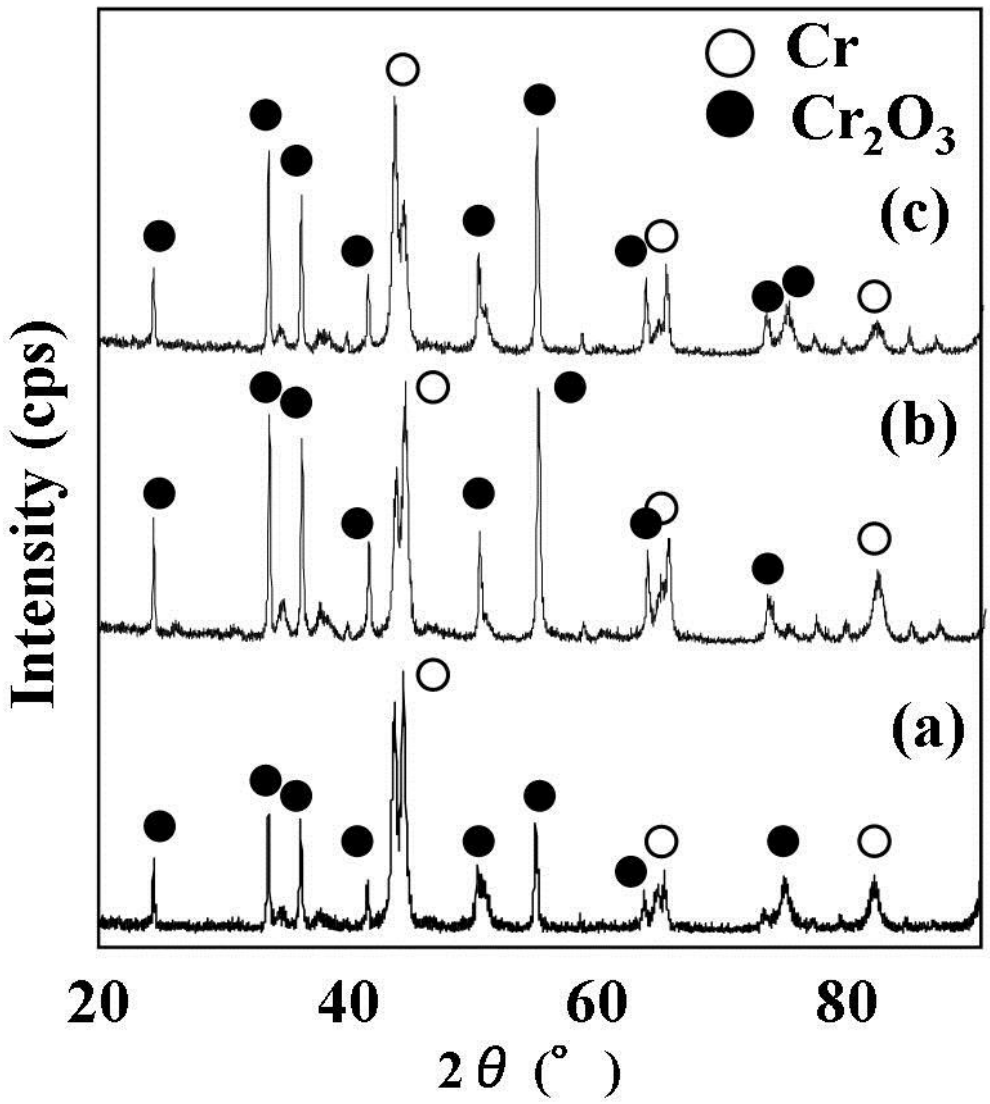


Fig. 3.5.12 XRD patterns of Cr coatings at the spray distance of
(a) 30 mm, (b) 35 mm and (c) 40 mm.

### 3.5.5 *Deposition of Cr coating onto high carbon steel substrates*

The research of depositing high hardness Cr coating was then furthered into the investigation on depositing the coatings onto heat susceptible substrates. The experimentation was first tried onto high carbon steel substrates as the candidate of heat susceptible substrates with higher phase transformation temperature at 973 K. The photographic view of the surface of high carbon steel is shown in Fig. 3.5.13 while Fig. 3.5.14 shows the photograph of the surface of the substrate after the deposition of Cr coating. SEM images of the morphologies of the Cr coatings deposited onto high carbon steel substrates are shown in Fig. 3.5.15. The oblique view of the surface morphology of the coating was also taken in order to observe the impinged particles. The SEM images of the cross-sectional morphologies of Cr coating deposited onto high carbon steel substrates by the change of working gas flow rate and spray distance are shown in Fig. 3.5.16. From these results, it is clarified that the deposition of Cr coating onto high carbon steel is possible. Furthermore, from the result in Fig. 3.5.17, the tendency of the increase of coating thickness by the increase in working gas flow rate and the decrease in spray distance is able to be observed.

Fig. 3.5.13 Photograph of the surface of high carbon steel substrate.

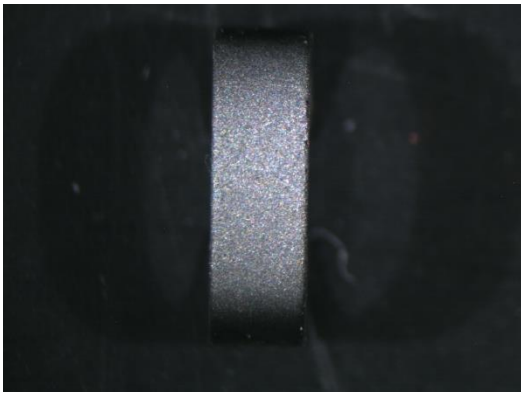

Fig. 3.5.14 Photograph of the surface of the substrate after the deposition of Cr coating.

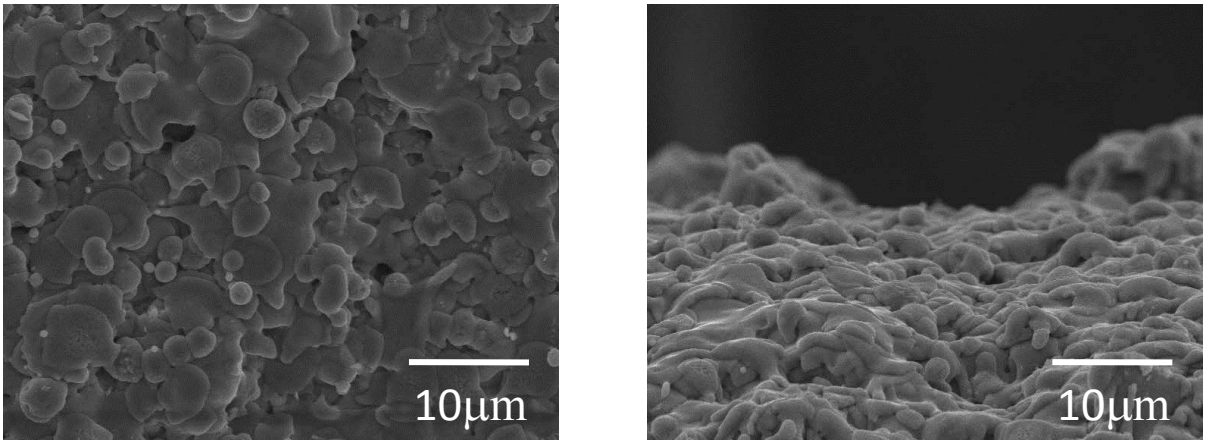


Fig. 3.5.15 SEM images of the morphologies of the Cr coatings deposited onto high carbon steel substrates. (a) surface view ; (b) oblique view.

| Spray distance (mm) | 10 l/min | 15 l/min | 20 l/min |
|---|---|---|---|
| 30 | 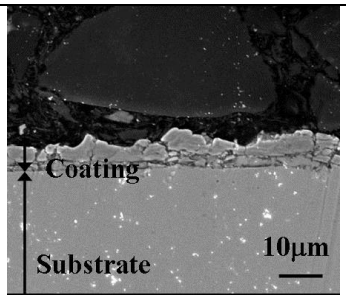  | 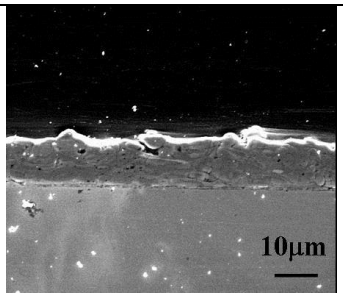  | 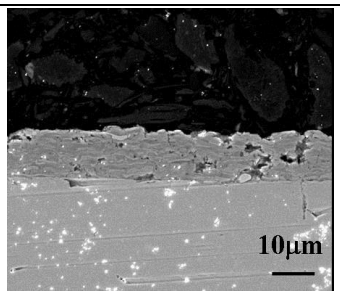  |
| 35 | 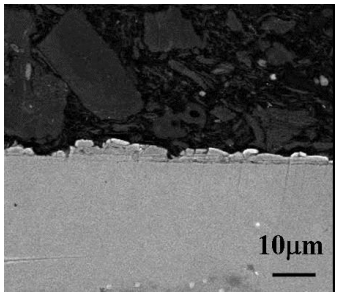  | 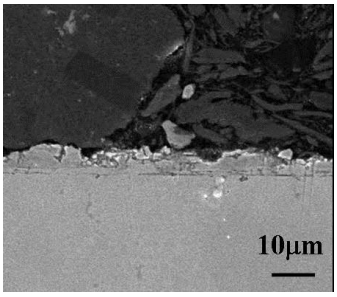  | 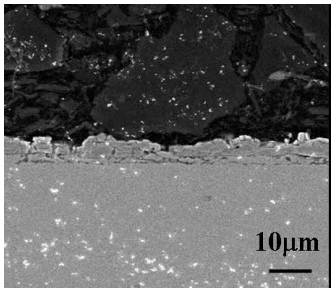  |
| 40 | 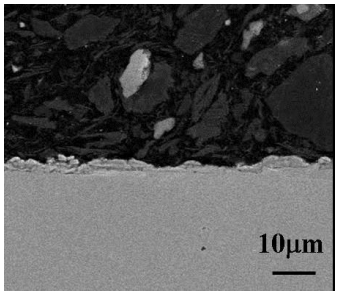  | 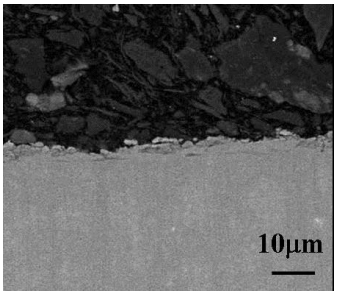  | 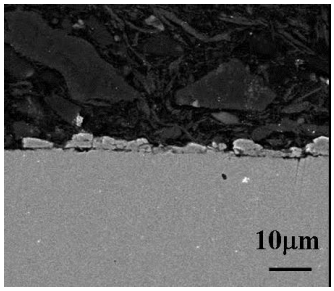  |

Fig. 3.5.16 SEM images of the cross-sectional morphologies of the coatings deposited with the change of working gas flow rate and spray distance.

The results of micro-hardness of coatings and substrates after sprayed at working gas flow rate 20 l/min and spray distance 30 mm are shown in Fig. 3.5.17. From these results, it is clarified that the hardness of the Cr coating deposited onto high carbon steel is also as the same as the result in SUS304 where high hardness coating exceeding the hardness of the coating by chrome plating was able to be obtained. Furthermore, from the investigation of the hardness of the substrates after sprayed, the hardness of the substrates remains at the same level as before sprayed which means that the substrates did not take any damage or softened by the heat input of the plasma during the spray.

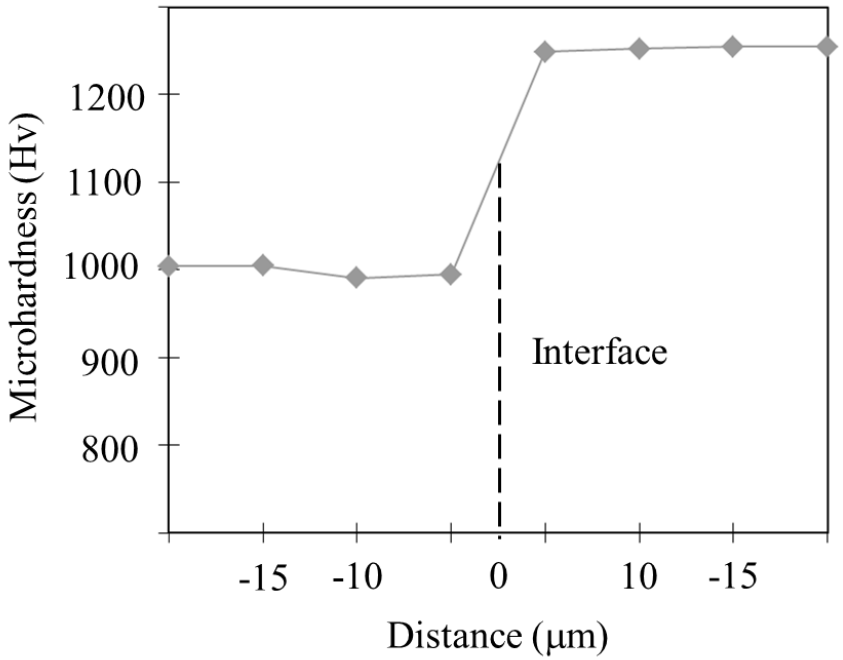


Fig. 3.5.17 Microhardness of coatings and substrates after sprayed at working gas flow rate 20 slm and spray distance 30 mm at the interface area of substrate and coating.

### 3.5.6 *Deposition of Cr coating onto CFRP substrates*

The experimentation of hard Cr coating deposition onto low melting point and heat susceptible substrate which is CFRP after considering the characteristics of coating obtained by the study on SUS304 and high carbon steel substrates was conducted. Deposition of coating was performed under the spray conditions of the spray distance 30 mm which possesses the highest coating thickness and lowest substrates temperature. Figure 3.5.18 shows the photograph of Cr coating onto CFRP substrate. Figure 3.5.19 shows the SEM image of the cross-sectional morphology of CFRP substrate, while the results of cross-sectional morphology of Cr coating deposited under each spray conditions are shown in Fig. 3.5.20 and Fig. 3.5.21. From these results, on the conditions of working gas flow rate 15 l/min, the emergence of the holes inside the substrate by the sublimation of the resin of the matrix of CFRP which was not able to be observed on the substrate before coating deposition was observed. From the result of the study on substrates temperature at Chapter 2.4, under the condition of working gas flow rate 15 l/min, substrates temperature is 560K, and since this temperature is more than the glass transition temperature of CFRP, and the heat input to the substrate material is high, it is thought that the coating deposition is difficult for this condition. On the other hand, on the conditions of working gas flow rate 20 l/min, emergence of the hole by sublimation of resin inside the substrate is not occurred. It is considered that that this due to the reason that the substrates temperature under the conditions of working gas flow rate 20 l/min is 525K, which is near to the heat-resistant temperature of CFRP, and the heat input to the substrates to have been able to be controlled. Moreover, on the condition of working gas flow rate 20 l/min, deposition of Cr coating is possible on CFRP substrates, and it turned out that the thickness of the coating deposited is about 30 μm. However, since the film thickness of the obtained coating is decreased compared with the case where SUS304 is used as the substrate, it is thought that by roughening the surface thick coating was possible to be deposited. As compared with the surface of the substrate before spraying, on the surface of substrate after coating, particles have structure which penetrated into the substrate, it is thought that the resin which is a matrix of the substrate sublimates from the heat effect by the particles impinged onto the CFRP surface part, and it became uneven and bumpy structure. Therefore, from the

concavo-convex field of the surface of substrates made by the impinged particles, it is thought that mechanical bonding becomes a major factor of the bond of the substrates and the coating in order the coating to be deposited. Next, measurement of coating hardness of the Cr coating deposited onto the CFRP substrates was performed. The measurement condition is working gas flow rate 20 l/min and spraying distance of 30 mm. From the hardness measurement result, the hardness of the coating was 1110 $Hv_{0.05}$. From this, it became clear that the hardness of the coating deposited onto the CFRP substrates has coating hardness comparable as the coating deposited on the SUS304 and high carbon steel substrates, and it became clear for the deposition of the hard chrome coating onto CFRP substrates to be possible.

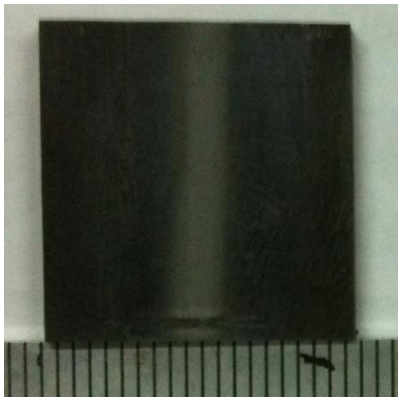

Fig. 3.5.18 Photograph of Cr coating onto CFRP substrate.

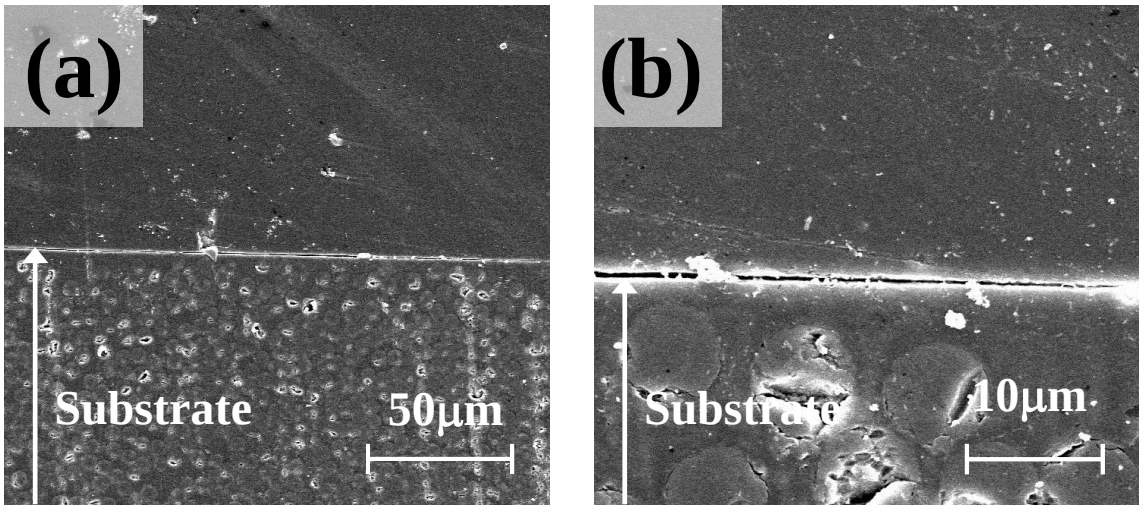


Fig. 3.5.19 SEM images of cross sectional morphologies of substrate
(a) overall view (b) enlarged view.

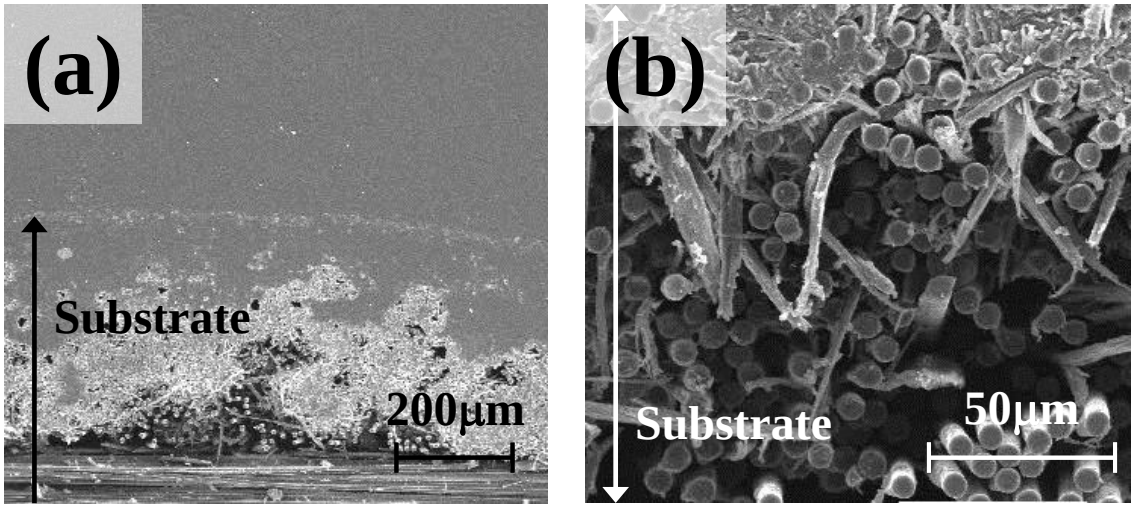


Fig. 3.5.20 SEM images of cross sectional morphologies of substrate (Gas flow rate 15 l/min, spray distance 30mm) (a) overall view (b) enlarged view.

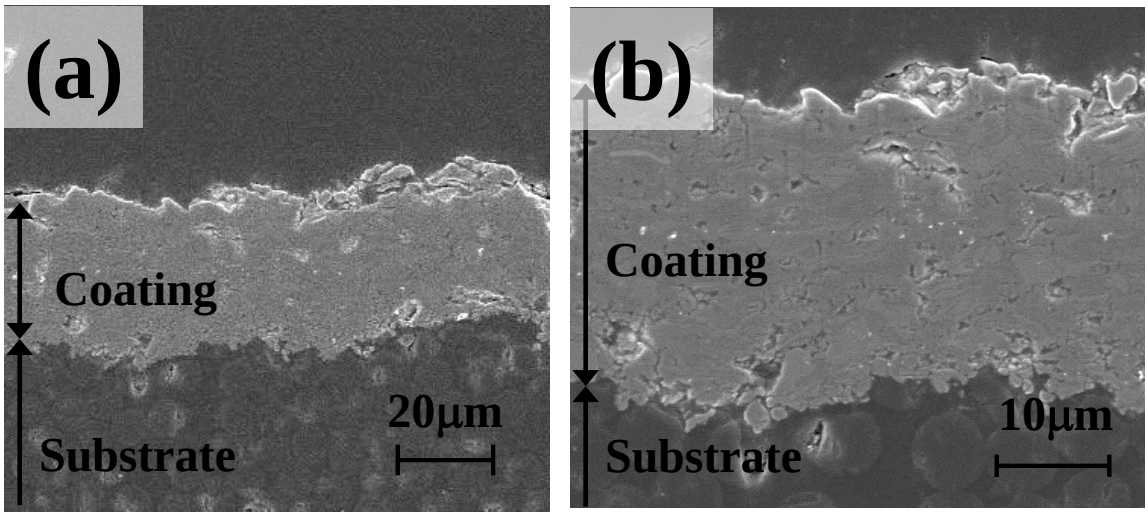


Fig. 3.5.21 SEM images of cross sectional morphologies of Cr coating (Gas flow rate 20 l/min, spray distance 30 mm) (a) overall view (b) enlarged view.

## 3.6 Bonding mechanism

Figure 3.6.1 shows the SEM morphologies of splat collected on CFRP and SUS304 substrates respectively at optimum condition which is at gas flow rate 20 l/min and 30 mm spray distance. Cr coating deposition rate is slower for the coating onto CFRP. This is due to the deposition mechanisms of the coating is different for the particular substrates type. From the observation, it is clear that the surface of SUS304 substrate is not changed during the spray and the fully flattened splat as well as the half molten particles is adhered to substrate surface. While on CFRP, the polymer part of the surface is slightly melted and the spray particles is observed to be more gathered at the area that is appeared to be the carbon fiber. The bonding mechanism of Cr particle onto CFRP substrate is appear to be by mechanical interlocking in between the coating and the carbon fiber which appear on the surface.

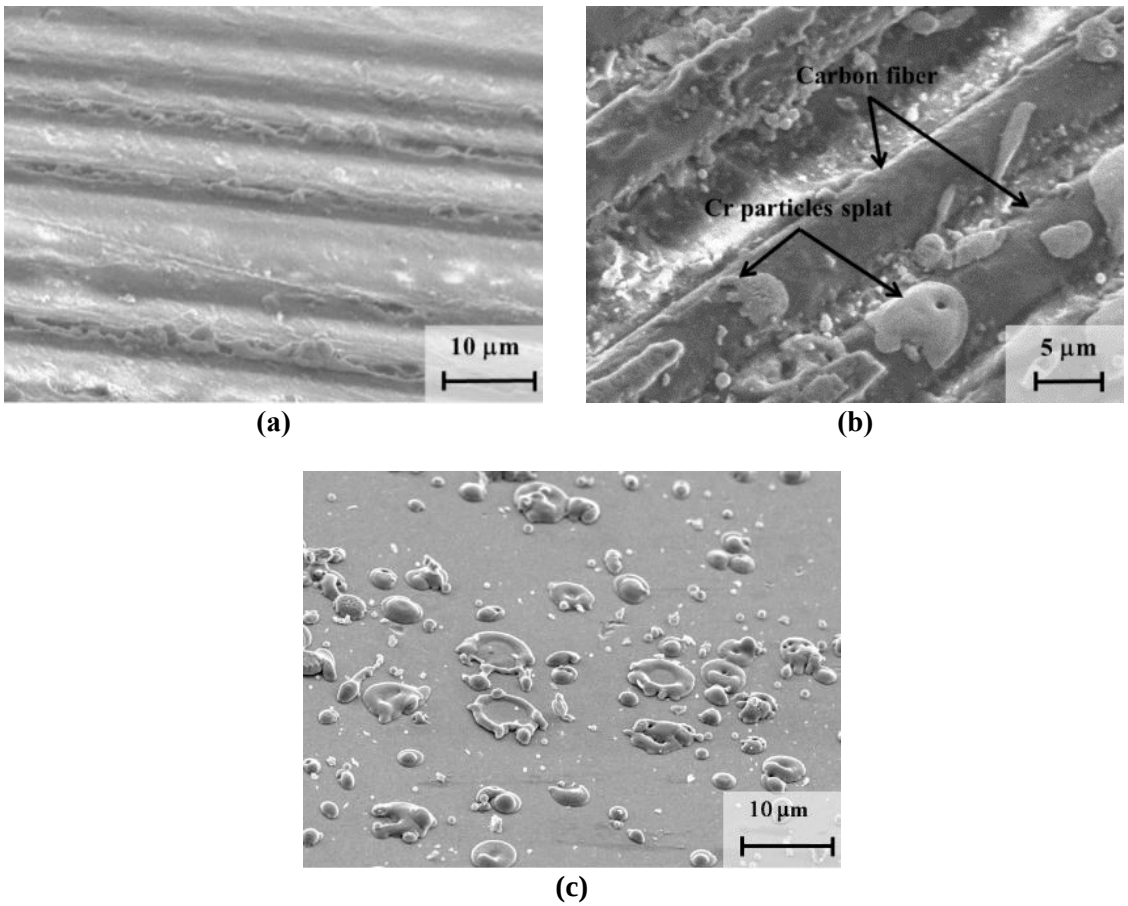


Fig. 3.6.1 Oblique view of SEM morphologies of CFRP substrate (a) before spray, (b) after spray and (c) after spray onto SUS304 substrate.

## 3.7 Conclusions

The summary of the things that had been clarified from the study of the deposition of hard chrome coating by low power atmospheric pressure microwave plasma spray and the characteristics evaluation are listed below.

- The deposition of Cr coating onto SUS304 is possible by using low power atmospheric pressure microwave plasma spray at input power of 0.5 kW.

- The thickness of Cr coatings deposited onto SUS304 increased with working gas flow rate and decreased with spray distance. The deposited Cr coatings are dense at all spray conditions with no influence of spray distance.

- The hardness of the coating obtained at the optimum condition, at working gas flow rate 20 l/min are above 900 $Hv_{0.05}$ which considered superior to the hardness of hard Cr plating.

- Cr coatings deposited by low power atmospheric pressure microwave plasma spray contain the oxide of chrome which contributes to the increase of hardness of the coatings. The composition of chromium (III) oxide inside the coatings increased with spray distance and working gas flow rate.

- Deposition of Cr coatings onto heat susceptible substrates which are high carbon steel and CFRP is possible by using microwave plasma spray device.

# Chapter 4

# Deposition of coating with supress heat input effect onto spray materials

## 4.1 Introduction

Titanium dioxide is a photocatalyst material which has been focused in recent studies because of the magnificent properties of this material where it possesses photocatalytic activity such as the ability to remove the water pollution substance as well as the deodorizing function [1, 2]. Photocatalyst is a material that alters the rate of a chemical reaction when exposed to light. There are various materials that show photocatalytic capability, and titanium dioxide is said to be the most effective [3]. From the high photocatalytic activity that it possesses, this material is being used for wide area of applications, from the construction field to the medical field.

Generally, the deposition method of a titanium dioxide coating is carried out by the fixation of titanium dioxide powder with an organic system binder. However, due to the powerful photocatalytic reaction of a titanium dioxide, it will let the fast degradation of the organic binder [4]. Therefore, from the recent studies, thermal spray is taught to be the alternative method to fabricate titanium dioxide coating with high photocatalytic activities. However, this method will cause high heat input and induces transformation from anatase phase with high photocatalytic activity to rutile phase with low photocatalytic activity [5]. The coatings produced by conventional plasma spray with input power of 28 kW possess low value of anatase content rate at approximately 40 %, and due to this, the study of the coating deposition methods which are able to restrain the phase change of spray particles is advancing [6].

Since our microwave plasma spraying device [7] is operable at low power (below 1 kW) comparing with conventional plasma spraying equipment, the control effect of the heat input to the particles at the time of spraying can be considered, and coating deposition with high rate of anatase phase is expected. Therefore, in this research, the coating deposition by controlling the heat input into the spray particles which can be

resulted in high rate of anatase phase with high photocatalyst activity was conducted. In this study, the objective is to investigate the controlling factor for the change of phase composition of titanium dioxide by using microwave plasma spray.

## 4.2 Experimental procedures

4.2.1 *Process and materials*

4.2.1.1 *Process*

The experimental system of the atmospheric pressure microwave plasma spray used in this research is as explained in Chapter 2. Microwaves of 2.45GHz are transmitted through a rectangular waveguide and oscillated into a cylindrical resonant cavity by a hollow antenna on the axis. Working gas of Ar is mixed with spray particles in an aerosol chamber and supplied axially through the antenna. The system generates high-intensity electric field on the tip of the antenna, induces electrical breakdown of working gas, and plasma plume is generated at the downstream. The spray particles are heated and accelerated by the plasma plume, and the coating is deposited by the impact of spray particles onto substrate surface at downstream. Experimental condition for titanium dioxide coating deposition is shown in Table 4.2.1.

Table 4.2.1 Experimental conditions for $TiO_2$ coating deposition

| | |
|---|---|
| Forward power (kW) | 0.3, 0.5 |
| Working gas | Ar |
| Working gas flow rate (l/min) | 15 |
| Spray distance (mm) | 30, 35, 40 |
| Traverse speed (mm/s) | 5 |
| Deposition time (s) | 210 |
| Antenna outlet diameter (mm) | 1.5 |

4.2.1.2 *Materials*

In this experiment, titanium dioxide, $TiO_2$ powder which possesses the melting point of 2143 K is used as feedstock powder to deposit coatings. $TiO_2$ powder (ATP100-ϕ15μm, KOJUNDOKAGAKU Research Centre) has the average size of 15 μm with the anatase content rate of above 96%. SEM image of $TiO_2$ powder is shown in Figure 4.2.1. The substrate material used in this research is SUS304. As the pre-treatment for the substrates before spraying, the surface of the substrates was grit blasted and then cleaned by ethanol. Size for both kinds of substrates was set at the dimension of 20 x 20 x 3 mm.

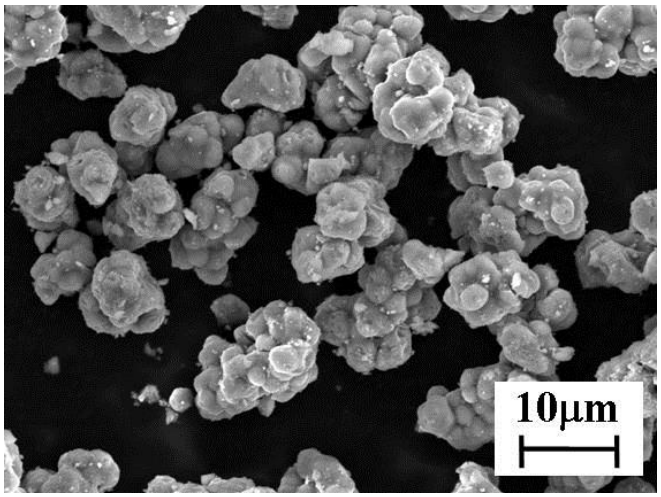


Fig. 4.2.1 SEM image of $TiO_2$ particles.

4.2.2 *Evaluation methods*

Observation of coating surface and cross section was conducted using scanning electron microscope (SEM: JSM-6390TY, JEOL Co. Ltd.). The measurement of the porosity inside the coating was conducted by using the digital image analysis (imageJ software) on the coatings cross sectional morphologies. The area percentage of porosity was calculated from the binary images of the cross-sectional morphologies. Substrate temperature was measured at the position of 1.0 mm from the surface of the substrate by

K-type thermocouple. The phase composition in the deposited coatings was verified by X-ray diffraction analysis (XRD: RINT-2500, Rigaku), with $CuK_{\alpha}$ radiation. The operating conditions were 30 kV and 80 mA for particles and 160 mA for the coatings respectively. The goniometer was set at a scan rate of 4 °/min at the range of $20° \leqq 2\theta \leqq 90°$. The anatase content rate in the coatings was estimated based on the following equation developed by Berger-Keller et al. [8]:

$$A = \frac{1}{1 + 1.265\frac{I_R}{I_A}} \times 100 \qquad (4.2.1)$$

where $I_A$ is defined as the intensity of anatase phase (101), while $I_R$ is defined as the intensity of rutile phase (110).

### 4.2.3 *Investigation of the influence to the anatase content rate by the change of substrate temperature*

This evaluation has been done in order to investigate the influence of substrate temperature to the anatase content rate. During the solidification of titanium dioxide, the nucleation and growth of the rutile phase is formed by usual coagulation process. However, in the case of rapid cooling rate of higher than $1.0 \times 10^6$ K/s, rather than forming the rutile phase, the anatase phase is generated selectively [9, 10]. This experiment is conducted in order to clarify the influence of substrate temperature to the anatase content rate. The substrates were heated on the hot plate on the atmospheric condition and the temperature was set to 473, 573 and 673 K.

### 4.2.4 *Investigation of the anatase phase occurrence by using heat-treated powder*

The generation of anatase phase during the experimentation and the anatase content rate was investigated and evaluated. In order to clarify the rapid cooling rate effect towards the nucleation of anatase phase, the powder particles with the rutile content rate of 99 % were used. The 96% pure anatase phase particles powder was heat treated by using heat furnace. Heat treatment was conducted in low pressure condition with nitrogen environment and the time was set for 30 min. Since the temperature for the phase transformation is 1127 K, the setup temperature for the heat furnace was set at 1223 K to ensure the phase change to be occurred significantly. After the heat treatment, since some of the particles were observed to be agglomerated, sieve with mesh size of 38 μm was used to distribute the powder to smaller size. Figure 4.2.2 shows the SEM images and the XRD patterns of the powder particles before and after the heat treatment. Heat treated particles were changed to 99% of rutile content rate after the treatment. Spray distance of 40 mm and different microwave power of 0.3 and 0.5 kW were set as spray conditions due to the highest possession of anatase content rate in the coating deposition. The coatings deposited by using the heat treated particles were analysed by XRD and the anatase content rate was calculated.

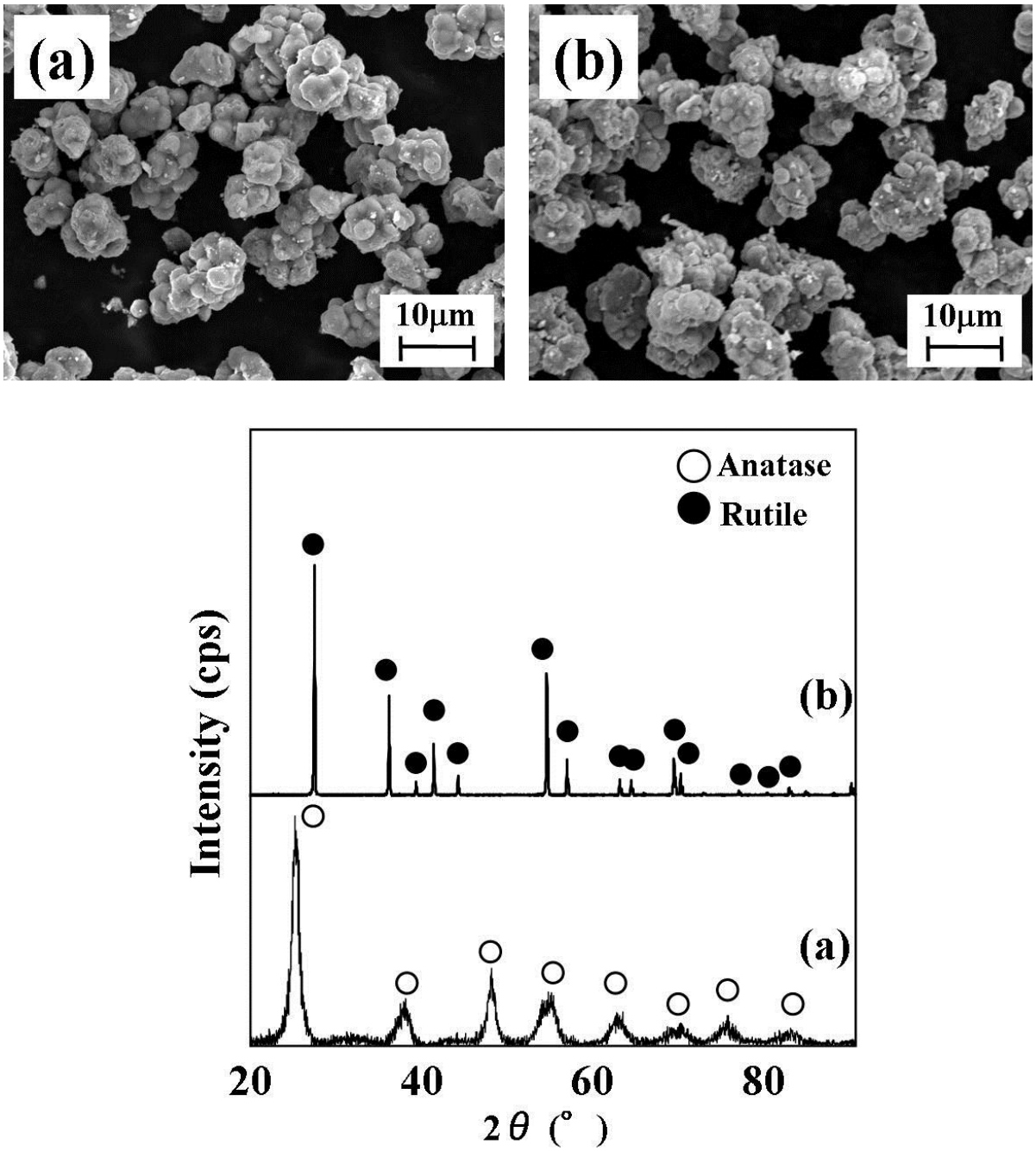


Fig. 4.2.2 Photograph and XRD patterns of (a) before heat treatment (b) after heat treatment.

4.2.5 *Anatase content rate investigation of in-flight particles*

In this study, the change of anatase content rate of the particles during flight was investigated. This is to investigate the mechanisms of anatase phase formation of particles during flight without the effect of substrate temperature. The particles were collected at spray distance of 200 mm. The evaluation was conducted to both heat treated and non-treated powder particles with the anatase content rate of 96 % and 0.02 % respectively.

## 4.3 Results and Discussion

4.3.1 *Deposition of $TiO_2$ coating*

Figure 4.3.1 and Fig. 4.3.2 show the SEM images of cross sectional morphology of $TiO_2$ coating deposited under 0.3 kW and 0.5 kW of input power and the enlarged images respectively. Meanwhile, coating porosity analysis of the coating is shown in Fig. 4.3.3. From the result in Fig. 4.3.1, it can be observed that there is no influence of spray distance to the coating thickness where the thickness is approximately 10 μm irrespective of any spray distance. It is also the same with the appearance porosity that can be observed from the enlarged morphologies in which the spray distance do not contributes much towards the coating porosity and the results of coating porosity analysis also recorded the same. Meanwhile, at 0.5 kW as shown in Fig. 4.3.2, the coating deposition differs much in this spray condition in which the porosity inside the coating is observed to be lower with the decrease of spray distance. At the lowest spray distance of 30 mm, dense coating of approximately 200 μm is able to be fabricated. From the comparison of the coating deposited on 0.3 kW and 0.5 kW, the porosity of the coating is higher in the former. At spray distance of 40 mm, it can be observed that almost same coating thickness was obtained by both input power conditions. On the other hand, at spray distance of 30 and 35 mm, the coating thickness increased with the increase of input power from 0.3 kW to 0.5 kW. This is due to the elongation of plasma length caused by the increase of input power which results in the increase of the dwelling time of particles inside the plasma plume [11]. From this, sufficient melting is

occurred while impacting the surface of the substrate as a result of the increase of energy given from the plasma.

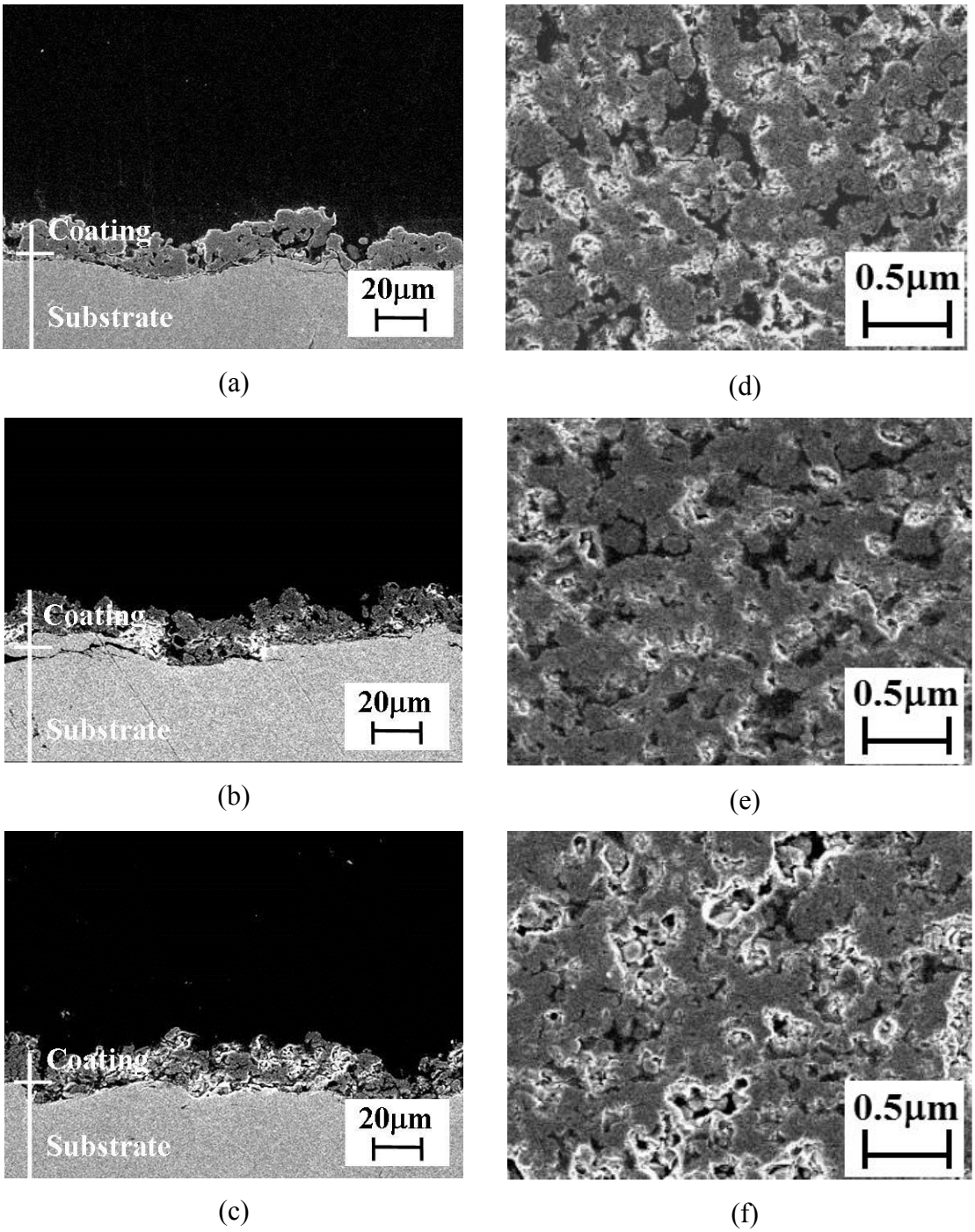


Fig. 4.3.1 Cross sectional SEM images of $TiO_2$ coating at 0.3 kW of input power with spray distance of (a) 30 mm, (b) 35 mm, (c) 40 mm and (d), (e), (f) are the magnified view of (a), (b), (c) respectively.

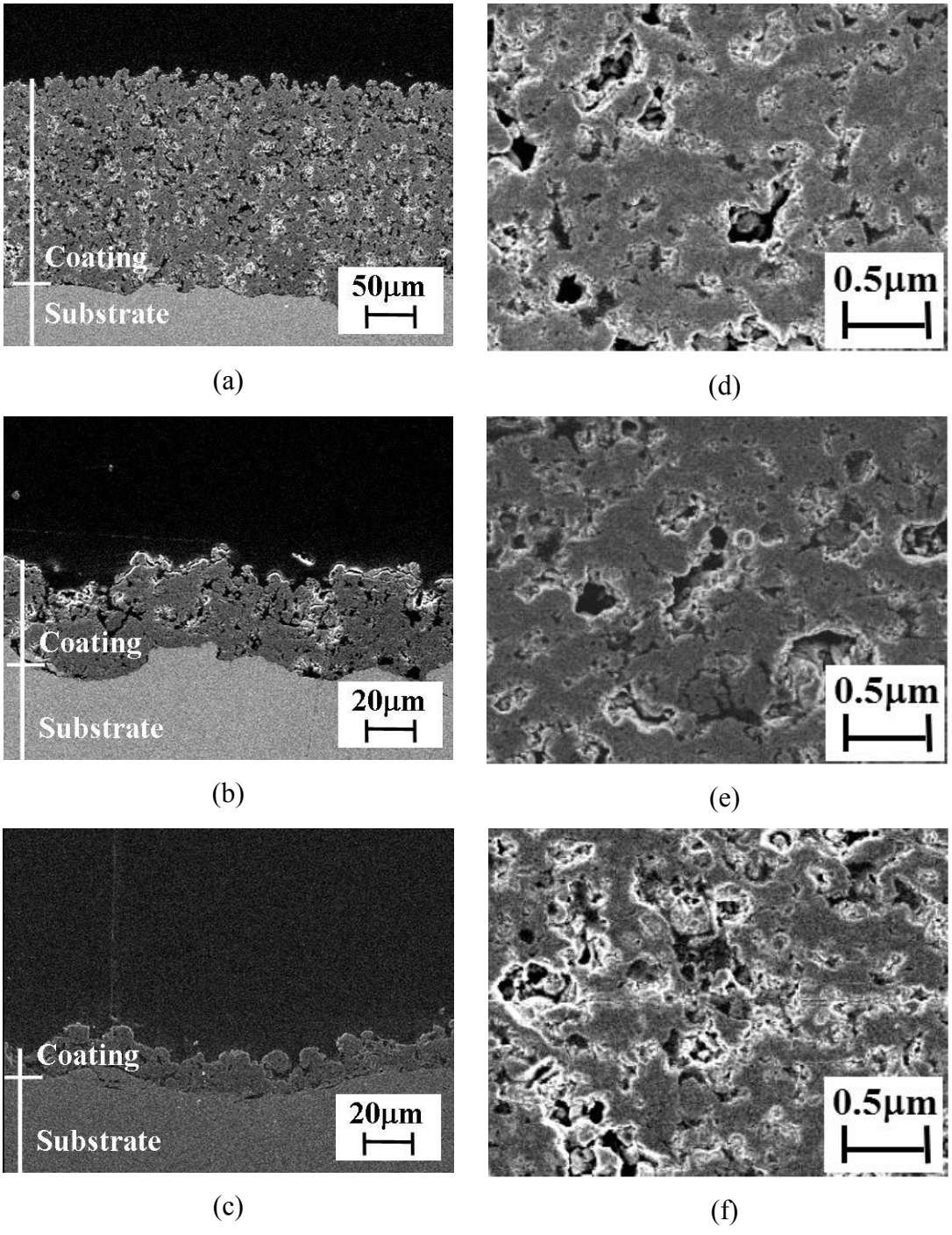


Fig. 4.3.2 Cross sectional SEM image of $TiO_2$ coating at 0.5 kW of input power with spray distance of (a) 30 mm, (b) 35 mm, (c) 40 mm and (d), (e), (f) are the magnified view of (a), (b), (c) respectively.

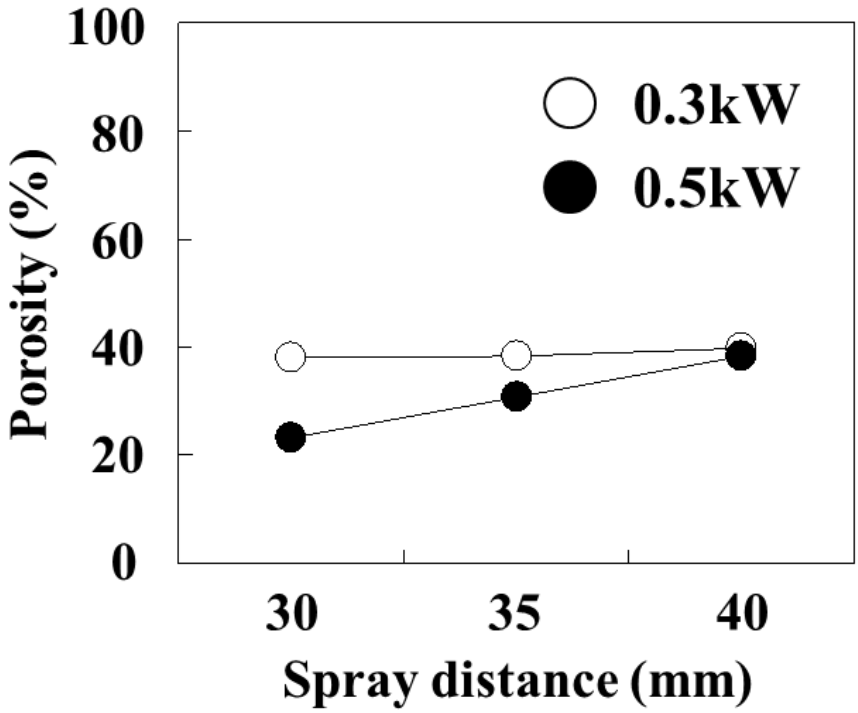


Fig. 4.3.3 Porosity of the coatings at 0.3 kW and 0.5 kW of input power with the change of spray distance.

Figure 4.3.4 shows the correlation of substrate temperature with input power and spray distance. The substrate temperature decreased with the increase of spray distance and irrespective of input power. At a constant spray distance, the substrate temperature was lower with input power of 0.3 kW compared to that of 0.5 kW. This is due to the reduction of the plasma length resulting from higher working gas flow rate. An increase in working gas flow rate induced the reduction of the energy given per unit working gas volume at constant microwave energy, resulting in decrease in plasma length because of the thermal pinching effect [12].

Meanwhile, Fig. 4.3.5 shows the graph of anatase content rate by the change of input power calculated from the results obtained by the XRD analysis. From the results, anatase content rate shows the tendency of increase with the increase of spray distance irrespective of input power conditions. Furthermore, the anatase content rate increases significantly from the lowering of input power and the maximum rate is recorded at spray distance of 40 mm and input power of 0.3 kW. From the decrease of input power

from 0.5 kW to 0.3 kW, it is known that due to the decrease of dwelling time of particles inside the plasma, the controlling factor of heat input towards the particles is obtained.

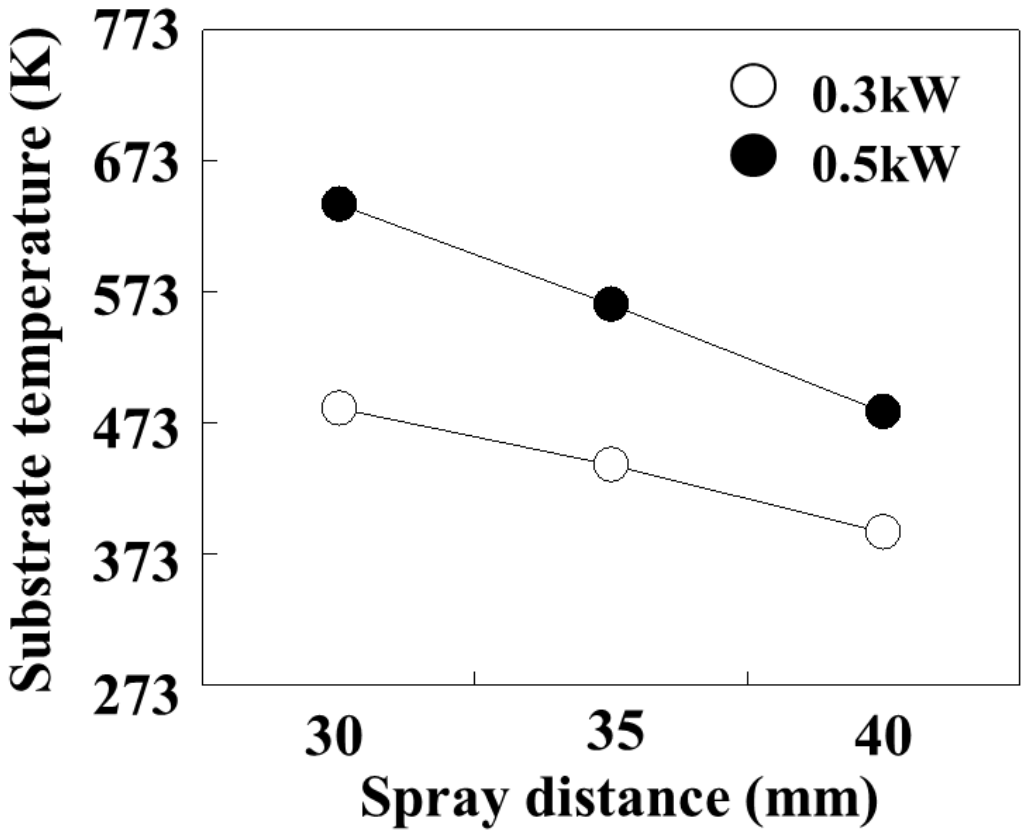


Fig. 4.3.4 Correlation of substrate temperature with input power and spray distance.

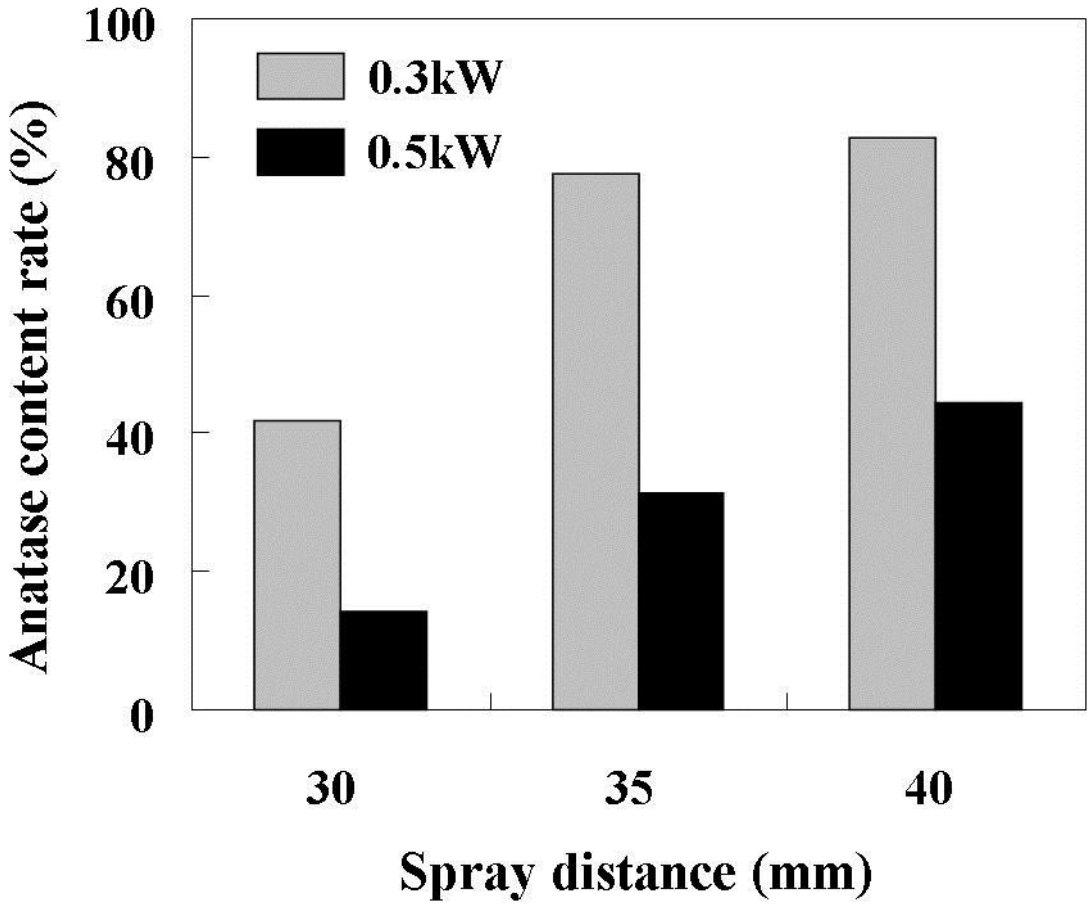


Fig. 4.3.5 Anatase content rate of $TiO_2$ coating by the change of input power and spray distance.

4.3.2 *Effect of substrate temperature to the anatase content rate*

Figure 4.3.6 shows the XRD results of the coating deposited on 473 K, 573 K, and 673 K of preheated substrate temperature at 0.3 kW and 0.5 kW of input power. It can be seen that the intensity peak of rutile phase decreased while the peak of rutile phase is increased by the increase of spray distance irrespective of input power conditions. Table 4.3.1 shows the results of calculated anatase content rate of the deposited coatings by the change of substrate temperature in compare to non-preheated substrate. From the result, it is known that the anatase content rate is decreased with the increase of substrate temperature in the preheated specimens. At input power of 0.5 kW

and spray distance of 40 mm, the non-preheated substrate temperature is 481 K, the anatase content rate of the deposited coating is 43 % while the anatase content rate of preheated at 673 K is 34 %. This shows that the anatase content rate decreased with the increase of substrate temperature. This value is further elevated and became significant in the case of the coatings deposited at input power of 0.3 kW. From the results, it is clarified that by lowering the substrate temperature, the deposition of $TiO_2$ coatings with higher anatase content rate is possible.

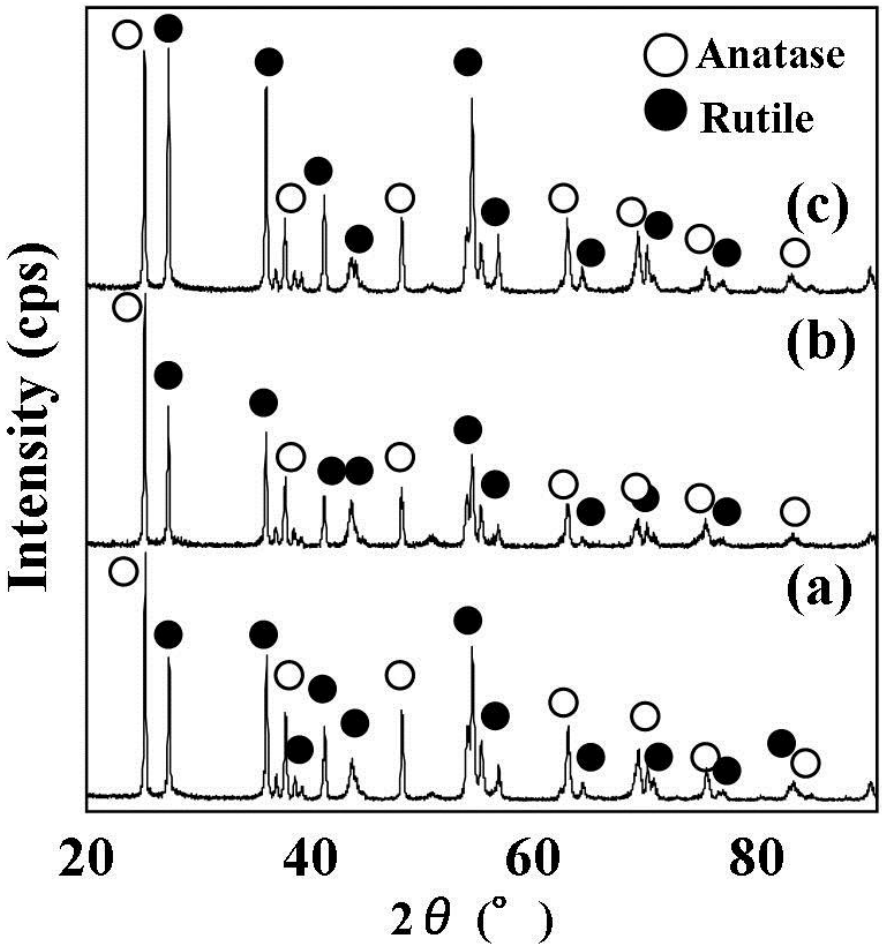

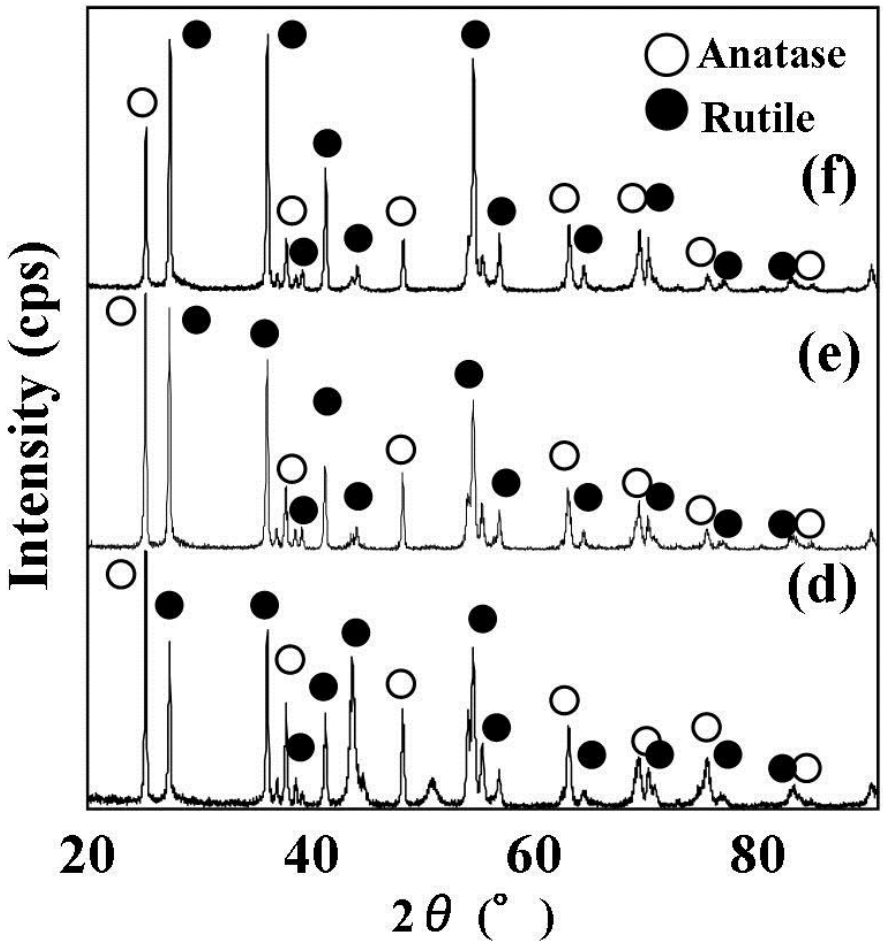


Fig. 4.3.6 XRD results of coatings deposited at input power of (a)-(c) 0.3 kW, (d)-(f) 0.5 kW and preheated substrate temperature of (a),(d) 473 K, (b),(e) 573 K and (c),(f) 673 K

Table 4.3.1 Anatase content rate (%) of $TiO_2$ coating at different substrate temperature

| | | Input power (kW) | |
|---|---|---|---|
| | | 0.3 | 0.5 |
| Without substrate heat (Substrate temperature (K)) | | 83 (389) | 43 (481) |
| Substrate temperature (K) | 473 | 58 | 41 |
| | 573 | 58 | 39 |
| | 673 | 53 | 34 |

4.3.3 *Effect of powder heat treatment to the anatase content rate*

Figure 4.3.7 shows the XRD patterns of the coatings deposited by using heat treated particles at input power of 0.3 kW and 0.5 kW. From the results, it can be seen that the intensity peak of anatase phase is generated irrespective of input power profile and the tendency of the increase of anatase phase peak with the lower input power is observed. The heat treated particles were only consist of the rutile phase before the spray as shown in Fig. 4.2.3, while after the spray, the occurrence of anatase phase is observed means that the phase change were occurred during spray. Table 4.3.2 shows the anatase content rate of deposited $TiO_2$ coatings by using heat treated particles at before and after sprayed at 0.3 and 0.5 kW of input power. It is clarified that the anatase content rate increased after spray irrespective of input power conditions while 0.3 kW shows higher value than 0.5 kW. This is due to the fact that the substrate temperature is lower at input power of 0.3 kW at spray distance 0f 40 mm which recorded 389 K in compare to 481 K in the counterpart. The lowering of the substrate temperature promotes higher cooling rate and this increases the anatase content rate inside the coatings. Moreover, the anatase content rate of the coatings deposited by heat treated particles shows significant decrease in compare to the non-treated ones. Therefore, it is considered that most of the molten particles which travelled inside the plasma plume were not nucleated to rutile phase during spray. Due to the above reasons which including the high porosity (above 40 %), coatings by the non-treated particles are mostly consist of insufficient melting condition which results in the coatings with mainly anatase phase.

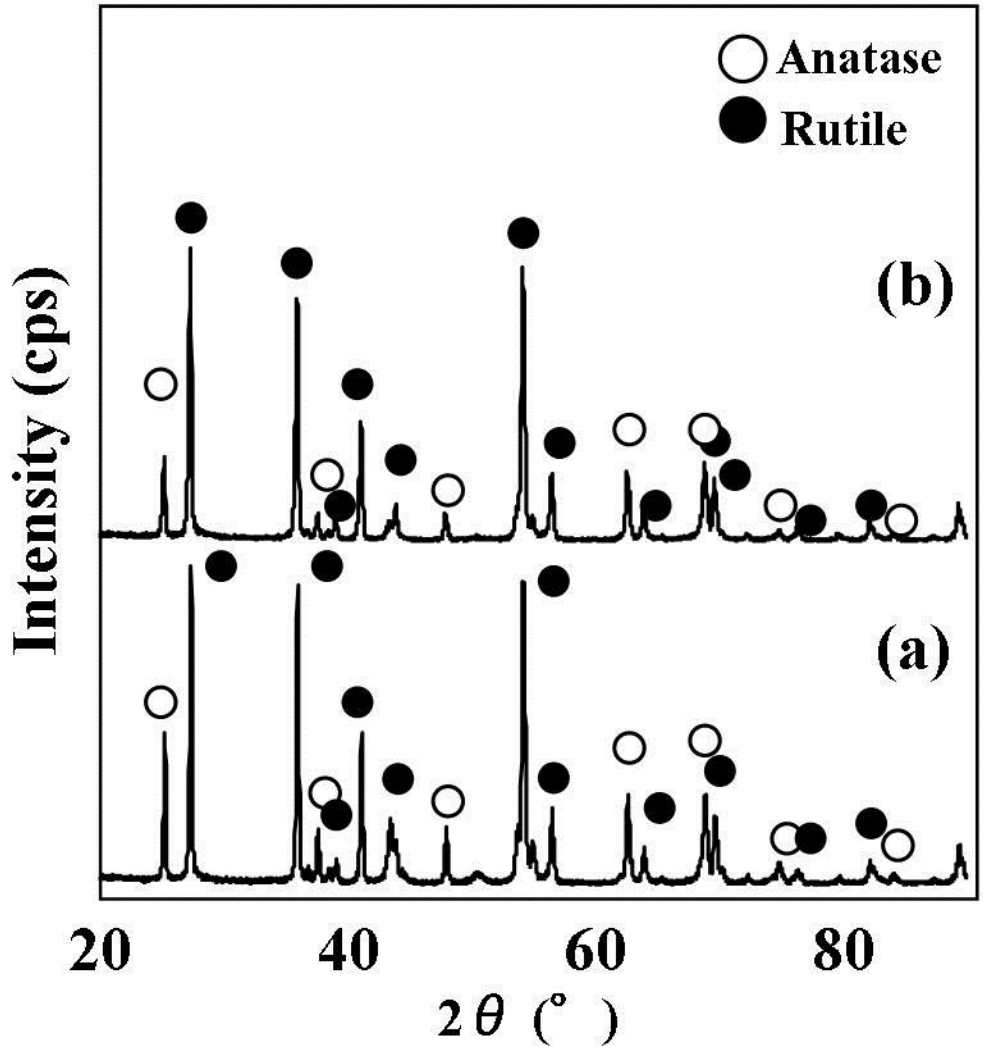


Fig. 4.3.7 XRD patterns of $TiO_2$ coatings at input power of (a) 0.3kW, (b) 0.5kW.

Table 4.3.2 Anatase content rate (%) of deposited $TiO_2$ coatings by using heat treated particles at before and after spray at different input power

| | Before spray | After sprayed at input power (kW) | |
|---|---|---|---|
| | Rutile rich $TiO_2$ particles | 0.3 | 0.5 |
| Anatase content rate (%) | 0.02 | 27.4 | 18.6 |

### 4.3.4 *Investigation of anatase content rate of in-flight particles*

Figure 4.3.8 shows the XRD results of the non-treated particles at different input power. From the results, it is clarified that by lower input power of 0.3 kW, the intensity peak of anatase phase is increased. This is attributed to the increase of heat input per unit power which resulting in increasing number of molten particles during spray. Therefore, it is considered that most of the molten particles which travel inside the plasma are mainly nucleated to rutile phase.

Figure 4.3.9 shows the X-ray diffraction results of the heat treated particles at different input power. It is known from the results that the rutile phase of the collected particles is high. However, the peak of anatase phase which is not existed before spray can be observed irrespective of any input power conditions. By lowering the input power, the intensity peak of anatase phase is increased. The calculated anatase content rate from the XRD results is shown in Table 4.3.3. From this, it is already known that some of the melted particles are solidified during flight resulting in the phase transformation. However, on the same condition as the collected particles, the anatase content rate are higher in the deposited coatings on substrates is to be inferred as mainly the effect of cooling occurred on the surface of the substrate as the generation of the anatase phase nucleation.

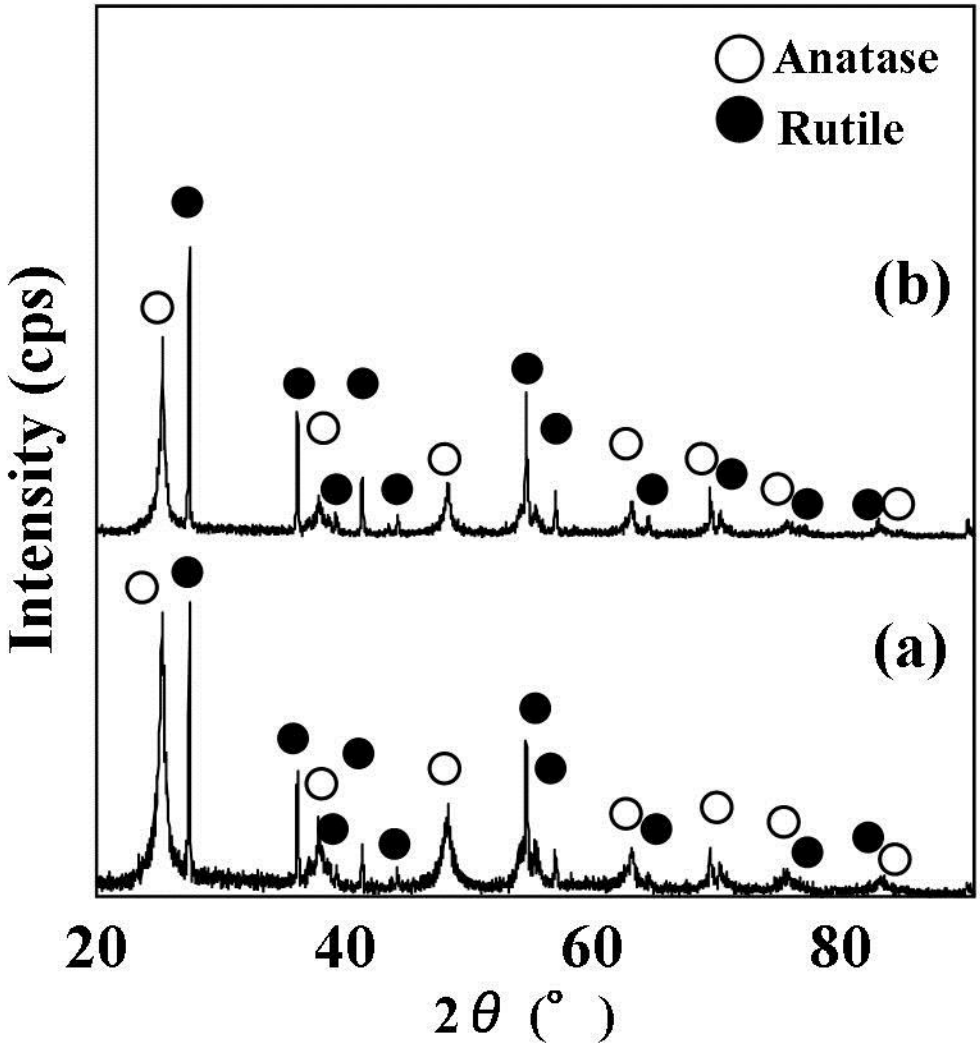


Fig. 4.3.8 XRD patterns of $TiO_2$ coatings by using non-treated particles at input power of (a) 0.3 kW, (b) 0.5 kW.

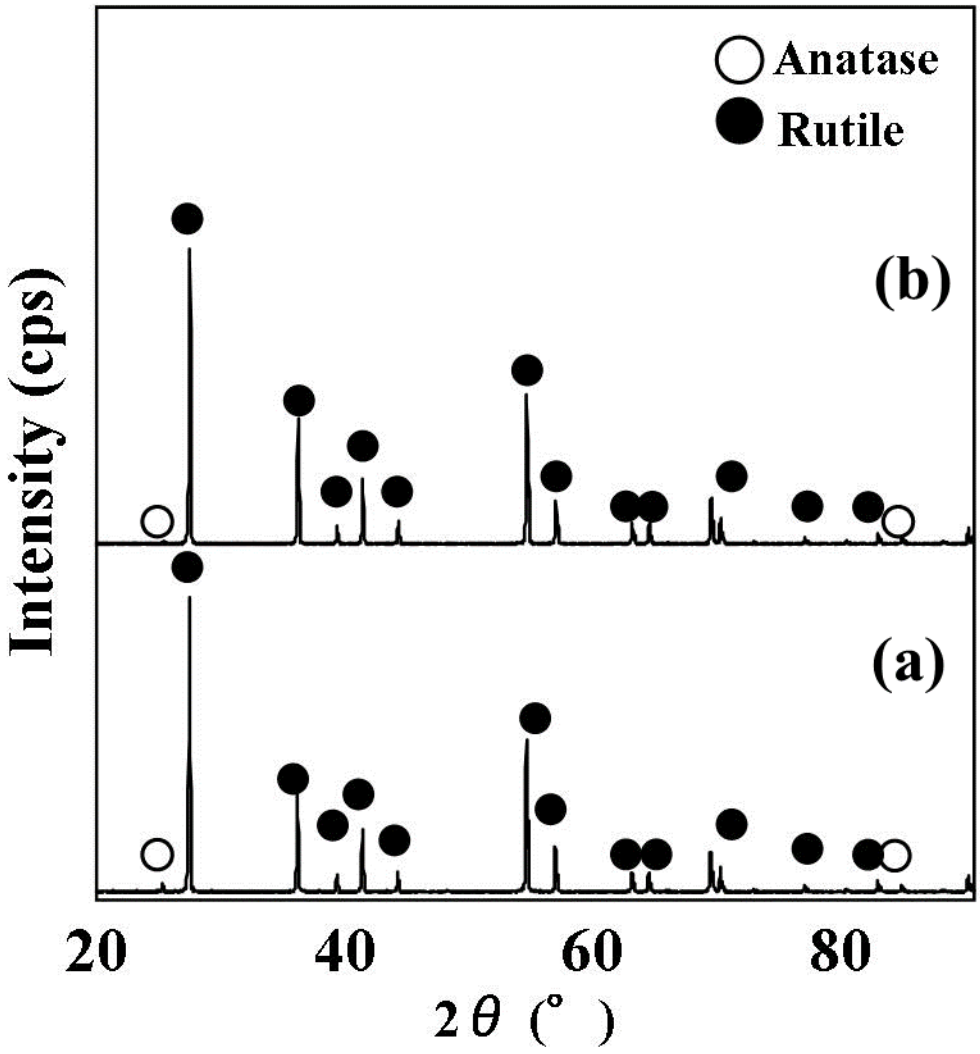


Fig. 4.3.9 XRD patterns of $TiO_2$ coatings by using heat treated particles at input power of (a) 0.3 kW, (b) 0.5 kW.

Table 4.3.3 Anatase content rate (%) of in-flight non-treated and heat treated particles at different input power

| | Particles type | |
|---|---|---|
| | Non-treated | Heat treated |
| 0.3 kW | 43.3 | 2.3 |
| 0.5 kW | 35.3 | 0.7 |

## 4.4 Conclusions

The summary of the things that had been clarified from the study of the deposition of titanium dioxide coating by low power atmospheric pressure microwave plasma spray and the characteristics evaluation are listed below.

- The deposition of titanium dioxide coating onto SUS304 is possible by using low power atmospheric pressure microwave plasma spray at input power of 0.5 kW.
- The anatase content rate of the titanium dioxide coating increased with the reduction of the input power and by the increment of spray distance. The highest anatase content rate of 83 % is recorded at the spray condition of input power 0.3 kW and at spray distance of 40 mm.
- From the coating deposited by 99 % of rutile content rate titanium dioxide powder, the anatase content rate increased inside the as-sprayed coating proved that the nucleation of anatase phase occurred during the spray.
- The anatase content rate inside the as-sprayed coating is increased with the decrease of substrate temperature.

# Chapter 5

# Research tasks and future perspectives

## 5.1 Introduction

In the study presented in this thesis, the low power atmospheric pressure microwave plasma spray device which is able to be operated at input power of lower than 1.0 kW was successfully experimented. Furthermore, it is clarified that the deposition hard chrome coating onto heat susceptible substrates with the controllable heat effect is made possible by using our device. It is also clarified that the deposition of $TiO_2$ coating with high anatase content rate is possible by this microwave plasma spray device. From this, the deposition of various kinds of materials as the coatings including ceramics materials, and the possibility to be applied as a new technique of plasma spray method is expected. However, there are a lot of the characteristics of this device which need to be clarified and the improvement of the coating deposition is also needed.

## 5.2 Research tasks regarding the microwave plasma device

There are a lot of things regarding the characteristics of the generated plasma and functions of our microwave plasma spray device that has yet to be explained. It is thought that the breakthrough of the process of coating deposition and the characteristics of the device in order to optimize the spray conditions is really important to be conducted. The investigations that are thought to be most important in particular of the characteristics of the device are listed below.

1. Improvement of powder feeding method
2. Improvement of the structure of the plasma torch
3. The simulation of heat input into spray particles

1. The spray powder feed rate by the aerosol chamber of the microwave plasma spray device are relatively are not constant resulting in difficulties in depositing uniform coatings. As an improvement of this, the use of micro-feeder machine as a feeding system can be thought. By using this system, it is thought that the constant feed rate is able to be supplied which will improve the deposition of coatings.

2. The antenna that is used as the plasma torch for the microwave plasma spray device has the structure that will trap the spray particle and decrease the amount of particles during spray. The nozzles of the plasma torch that are widely used by the conventional plasma spray method consist of converging parts to prevent the trapping of the spray powder during spray. It is thought that by applying this structure to the plasma torch microwave plasma spray will improve the coating efficiency.

3. As the characteristics of the device, the microwave plasma possess a special structure and the particle velocity is relatively slow compare to conventional plasma spray. These mean that the heating mechanisms toward the spray particles are also expected to be more sophisticated. From the research findings, working gas flow rate, spray distance, size of antenna outlet diameter will influence a lot to the organization of the coatings. The experimentations and evaluations by changing the spray parameters to derive the optimum conditions will take a lot of times and also acquire experiences. Therefore, if the simulation of heat input by applying the detail data of the plasma temperature and the particle velocity is able to conducted, it is thought that the optimum conditions are able to be derived faster and more efficient.

## 5.3 Research tasks regarding the deposition of coatings

In this research, the deposition of Cr and $TiO_2$ coatings are able to be deposited by the microwave device of our laboratory. However, due to the existence of some problems on the coatings as well as some evaluation tests, some improvements are thought to be necessary. The things that are thought to be particularly important for the improvement are as below.

Deposition of hard chrome coating

1. The evaluation of the coating
    - Wear resistant test
    - Adhesion strength
2. Evaluation and the comparison to the coating deposited by other coating method (plating, other thermal spray method : HVOF, APS)

Deposition of $TiO_2$ coating

1. Photocatalytic efficiency of the coating deposited by microwave plasma spray.

## 5.4 Research tasks regarding the enhancement of microwave plasma spray

### 5.4.1 *Introduction*

In Chapter 2, it is known from the operational characteristics of microwave plasma spray device is low in particle velocity. Particle velocity is one of the important reasons to achieve coating with low porosity and excellent mechanical properties where the particle velocity of conventional plasma spray is above 200 m/s [1]. By increasing the particle velocity, the porosity in the coating as well improvement of particle flattening ratio can be expected. The heat source of Ar plasma generated by low power microwave plasma spray is consists of the accumulation of electric charges, electron and ion. When an electric charge particle crosses in the magnetic field, Lorentz force operates on a direction perpendicular to the movement of electric charge particle and the magnetic force [2]. Lorentz force acts on the central axial direction of an electric charge particle in the plasma (ion electron) by impressing a magnetic field on circumferential direction to plasma, and the plasma diameter can be expected to be shrunk by the pinch effect [3]. It is expected that by reduction of plasma diameter through pinching effect, the plasma flow velocity will be increased. Thus, this magnetic field is called magnetic

nozzle. With this principal, the particle velocity improvement is able to be achieved without the increase of microwave power.

From the above mentioned principal, by implementing the magnetic field in microwave plasma spray, due to the unchanged heat input, the improvement of mechanical properties of coating deposition onto low melting point substrate can be expected. In this research, the magnetic nozzle is produced by permanent magnets and applied to low power microwave plasma spray. The plasma temperature, particle velocity, and the behaviour of the deposited coating are investigated.

### 5.4.2 *Experimental procedures*

Figure 5.4.1 shows the schematic diagram of plasma system with magnetic nozzle. As shown in the figure, magnetic nozzle is set to the circumferential part of the plasma in order to study the effect of magnetic field towards plasma and coating behaviour. Table 5.4.1 shows the parameters of the magnet used in this study. Sm-Co permanent magnets were used due to the excellence of this magnet material with regards to heat and the magnetic field by these magnets is also high. Spraying condition is shown in Table 5.4.2. Working gas with lower flow rate at 10 l/min and 2.5 mm of antenna outlet diameter is used because the effect of magnetic field to the plasma is better to be achieved at lower gas velocity. Spray distance was changed from 40 to 50 mm. Cu particle used in the study in spray particles behaviour in Chapter 2 was used to deposit coating. Figure 5.4.2 and Fig. 5.4.3 show the dimension and setup of the magnets in magnetic nozzle. Two types of setting were used to study the effect of increasing magnetic field.

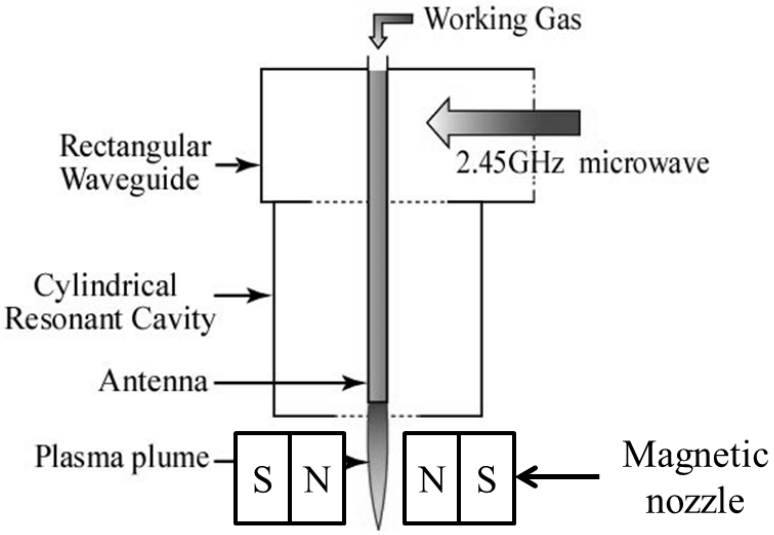


Fig. 5.4.1 Schematic diagram of the plasma torch with magnetic nozzle.

Table 5.4.1 HICOREX Magnet parameters

| Type | H-22A |
|---|---|
| Material | Sm-Co |
| Curie point | 710℃ |
| Maximum allowable working temperature | 200℃ |
| Dimension | 20×10×5 mm |
| Thermal conductivity | 0.025cal/cm・s・℃ |
| Temperature coefficient | -0.04%/℃ |

Table 5.4.2 Spraying conditions

| Input power | 1 kW |
|---|---|
| Working gas rate | Ar 10 l/min |
| Traverse speed | 30 mm/s |
| Spray distance (S.D.) | 40, 50 mm |
| Antenna outlet diameter | 2.5 mm |
| Substrate | SUS304 |
| Powder material | Cu ; φ20 μm |
| Number of spray | 10 pass |
| Nozzle type | Normal, MN4, MN8 |

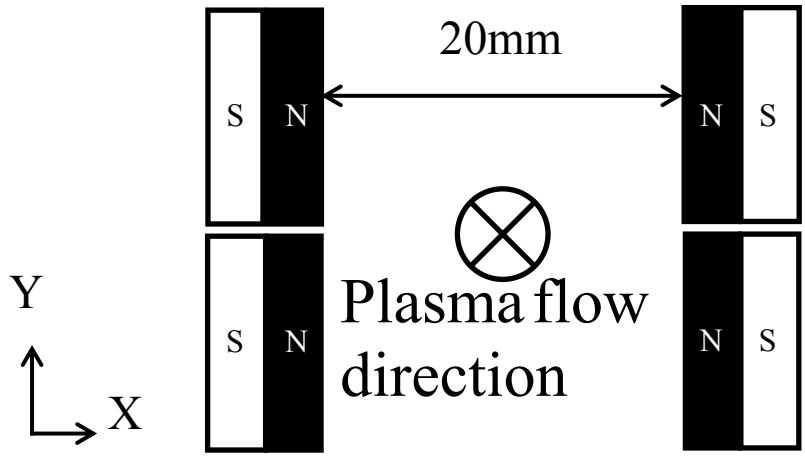


Fig. 5.4.2 Dimensions of the magnetic nozzle with 4 permanent magnets (MN4).

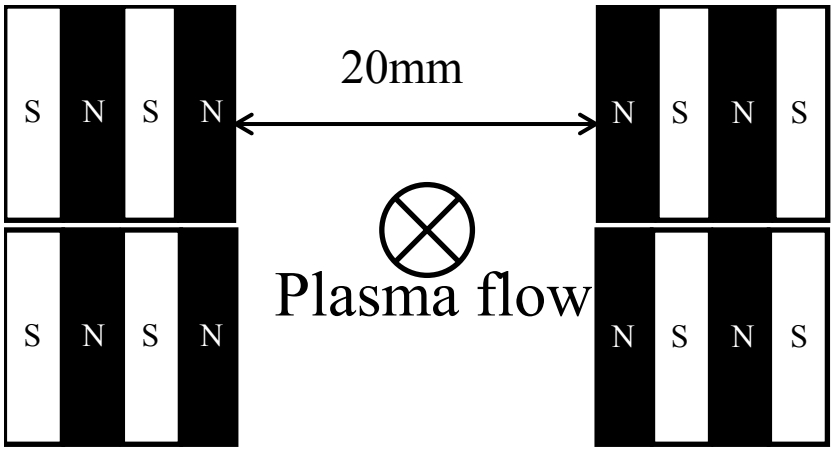


Fig. 5.4.3 Dimension of the magnetic nozzle with 8 permanent magnets (MN8).

5.4.3 *Evaluation methods*

Magnetic flux density of the magnetic field created by each magnetic nozzle was measured by Gaussmeter (Model 6010) manufactured by FW Bell. The position of the center of the magnetic nozzle is assumed as [0,0], the measurement of the magnetic field strength at the position of [0,0], [0,-5], [0,5], [-5,0], [5,0] mm are collected.

Plasma temperature distribution was measured by optical emission spectroscopy at Z=15 mm position. The details of this measurement method already been discussed in

Chapter 2. The effect of increasing the number of permanent magnets to the behaviour of the plasma is studied. Particle velocity of Cu particles with the use of magnetic nozzle is measured by DPV-2000 [3]. Cu coating was deposited onto SUS304 substrates and the evaluation of the coating was conducted by SEM.

5.4.4 *Results and discussion*

Figure 5.4.4 and Fig. 5.4.5 show the measurement results of magnetic field strength of MN4 and MN8 respectively. From the results, it can be understood that the magnetic field of both magnetic nozzle setting shows the value of almost zero at the center of the nozzle. The magnetic field shows the tendency of higher strength at positions near to the magnets. However, the value of the upper and the lower parts at [0, 5] and [0, -5] mm respectively, decrease in compare to the position near the magnets. The magnetic field strength increases as the number of the magnets increased at almost two fold from MN4 with 4 magnets to MN8 with 8 magnets shows the linear relationship of magnetic field strength with increasing magnets.

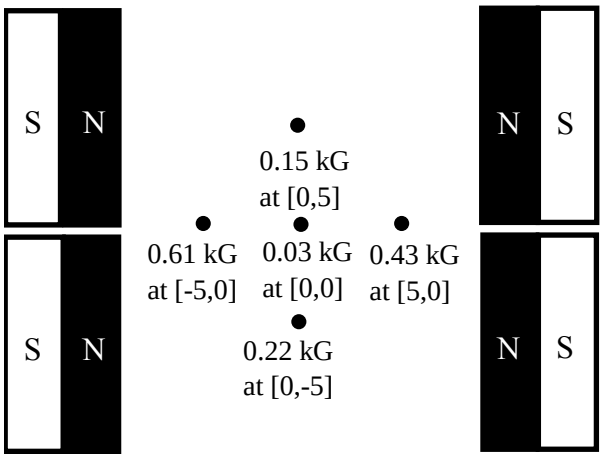


Fig. 5.4.4 Measured magnetic field strength distribution of MN4.

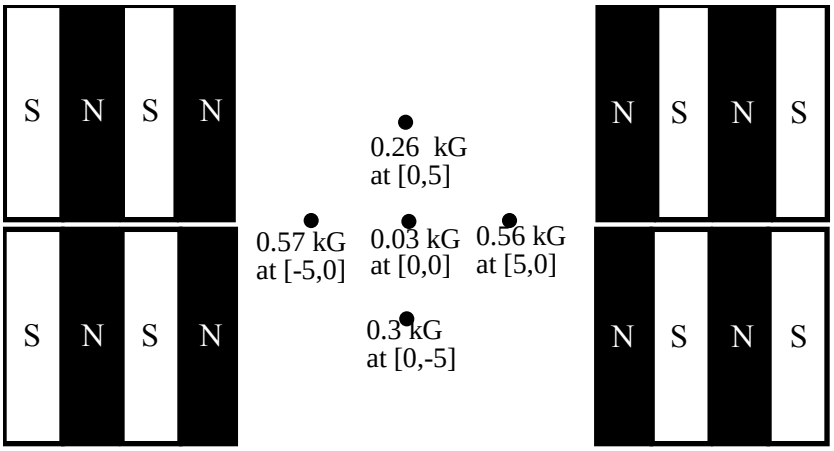


Fig. 5.4.5 Measured magnetic field strength distribution of MN8.

Figure 5.4.6 shows the plasma temperature distribution with the use of different magnetic nozzle at Z=15 mm. From the result, it can be understood that the plasma temperature was increased by the use of magnetic nozzle. Furthermore, it can also be observed that the radial size of the plasma is decreased slightly with magnetic nozzle. This is due to the thermal pinching effect that occurred by the magnetic field contributes towards the increase in plasma temperature. By using much higher number of magnets, the pinching effect of the plasma is thought to be increased which results in increasing plasma temperature. The particle velocity of Cu particles with the use of magnetic nozzle is shown in Table 5.4.3. From the results, it is known that the improvement of particle velocity is achievable by the use of magnetic nozzle. However, the particle velocity that has been accelerated by the magnetic nozzle is still low in compare to the conventional plasma spray method which is at least higher than 100 m/s.

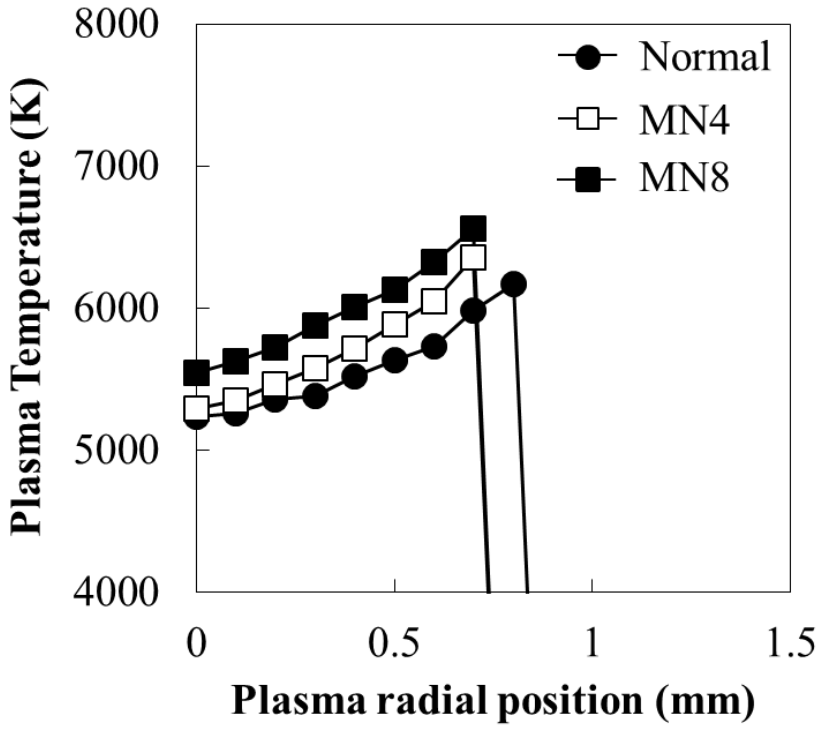


Fig. 5.4.6 Plasma temperature distribution with the use of different magnetic nozzle at Z=15 mm.

Table 5.4.3 Particle velocity of Cu particle with the use of each magnetic nozzle

| | Normal | With magnetic nozzle |
|---|---|---|
| MN4 | 25.46 m/s | 30.12 m/s |
| MN8 | 23.75 m/s | 40.93 m/s |

Due to the effect of magnetic nozzle is much achievable in higher number of magnets in magnetic nozzle, the coating deposition was deposited by the use of magnetic nozzle with 8 magnets setting. Figure 5.4.7 shows the results of the cross-sectional morphology of Cu coating with the change of spray distance. From the results, it can be observed that the coating produced with the use of magnetic nozzle if lower in thickness in compare with the ones without. This can be thought due to the further flattening of the particles. From the apparent porosity of the coating, it can be observed that the porosity decrease with the use of magnetic nozzle at spray distance 40 and 50 mm.

| S.D. | Without magnetic nozzle | With magnetic nozzle (MN8) |
|---|---|---|
| 40 mm | 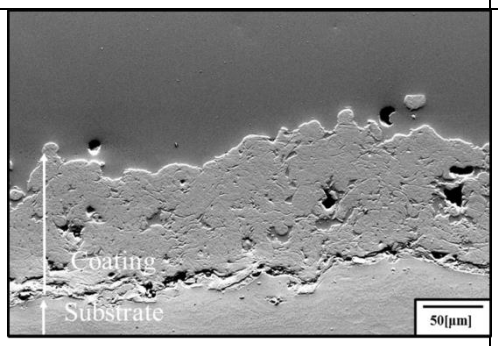  | 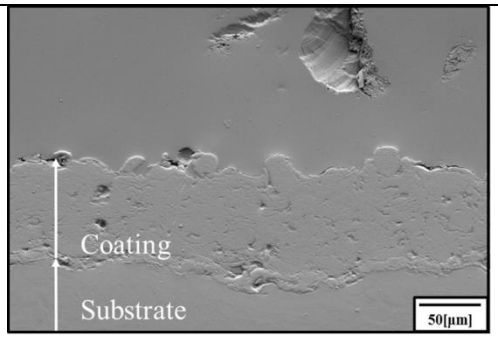  |
| 50 mm | 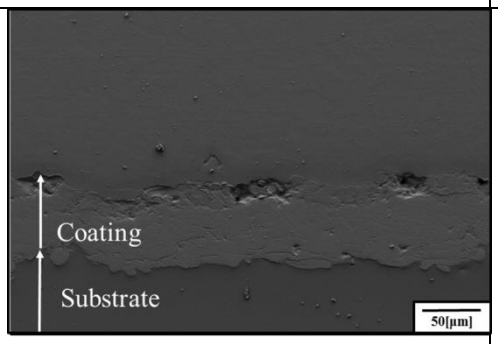  | 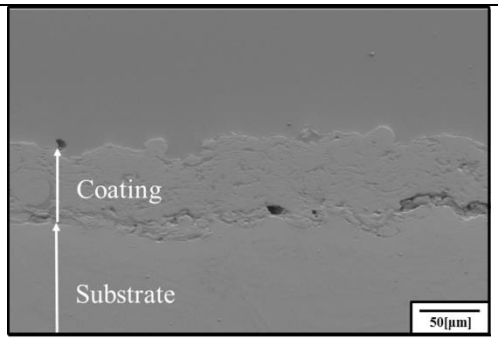  |

Fig. 5.4.7 Cross-sectional morphology of Cu coating with and without the use of magnetic nozzle at 40 and 50 mm of spray distance.

# Chapter 6

# General conclusions

## 6.1 Conclusion remarks

In this research, the study on the operational characteristics evaluation of the low power microwave plasma spraying device as well as the investigation of the deposition of coatings with suppress heat input toward substrate and spray materials was conducted. The conclusions of the things that had been clarified from these studies are listed below.

[Characteristics evaluation of low power atmospheric pressure microwave plasma spray device]

1. On the input power 0.5 kW of the plasma production conditions, it became clear that for the generation and maintenance of plasma to be possible. However, on 0.1 kW of input power, plasma production and maintenance cannot be performed and the maintenance of plasma becomes difficult on the input power of 0.3 kW, antenna outlet diameter 1.5 mm, and the ignition conditions of working gas flow rate 19 l/min.

2. Substrate temperature decreased by the increase in working gas flow rate, and the reduction of the antenna outlet diameter, in which the substrate temperature in 0.5 kW of input power, working gas flow rate 20 l/min, and antenna outlet diameter 1.5 mm was 381K.

3. It is clarified that the influence of the reduction of antenna outlet diameter towards the plasma temperature is little and 4000 K of high temperature plasma field was produced uniformly at the distance of 13 mm from the antenna apical portion. At 3.5 mm from antenna apical portion, In the case of antenna outlet diameter 1.5 mm, the

structure of the plasma is solid compare to the hollow structure at antenna outlet diameter 2.5 mm.

4. From particle velocity measurement and a gas velocity analysis results, the increase in a gas velocity and the increase in particle velocity were shown with the reduction of the antenna outlet diameter and the increase in working gas flow rate. The maximum particle velocity of Cr particle is recorded by using antenna outlet diameter of 1.5 mm at 135 m/s.

[Deposition of coating with suppress heat input onto substrate materials]

5. The deposition of Cr coating onto SUS304 and heat susceptible substrates is possible by using low power atmospheric pressure microwave plasma spray at input power of 0.5 kW.

6. The thickness of Cr coatings deposited onto SUS304 increased with working gas flow rate and decreased with spray distance. The deposited Cr coatings are dense at all spray conditions with no influence of spray distance.

7. The hardness of the coating obtained at the optimum condition, at working gas flow rate 20 l/min are above 900 $Hv_{0.05}$ which considered as the same level of the hardness of hard Cr plating. Cr coatings deposited by low power atmospheric pressure microwave plasma spray contain the oxide of chrome which contributes to the increase of hardness of the coatings.

8. The bonding mechanism of Cr coating onto CFRP substrate's surface is mainly mechanical interlocking in between Cr particles with carbon fiber which surfaced after heated by microwave plasma.

[Deposition of coating with suppress heat input onto substrate materials]

9. The deposition of titanium dioxide coating onto SUS304 is possible by using low power atmospheric pressure microwave plasma spray at input power of 0.5 kW.

10. The anatase content rate of the titanium dioxide coating increased with the reduction of the input power and by the increment of spray distance. The highest anatase content rate of 83 % is recorded at the spray condition of input power 0.3 kW and at spray distance of 40 mm.

11. From the coating deposited by 99 % of rutile content rate titanium dioxide powder, the anatase content rate increased inside the as-sprayed coating proved that the nucleation of anatase phase occurred during the spray.

12. The anatase content rate inside the as-sprayed coating is increased with the decrease of substrate temperature.

## 6.2 Significance of the study

The significance of the results obtained in this research and its contribution towards academic and industrial sectors is summarized and discuss as follows:

### 6.2.1 *Contribution towards academic sector*

The research regarding thermal spray technology especially in plasma spray method had been conducted through recent years. A lot of researches are also focusing on suppressing the heat input towards spray materials with low power plasma spray method which already been discussed in detail in Chapter 1. This low power plasma spray method is deemed important due to the reason that it can benefit the versatility of plasma spray method in depositing various kinds of materials as well as to lower the excessive heat input towards the spray materials.

For the contribution of this research in academic sectors, firstly is the success of our research group on applying microwave plasma in thermal spray technology. In current research report, there is actually very few successful example of microwave

plasma to be applied as plasma spray due to its reported plasma instability after spray material insertion as well as lots of unknown features. Microwave plasma spray by our research has been studied towards deposition of various kinds of materials and the efficiency of this method is comparable to conventional plasma spray methods.

In this research, the application of microwave plasma spray at extremely low power (0.5 kW) has been achieved successfully for the deposition of hard chrome coating onto thermally sensitive substrate materials, CFRP. What is important in this achievement is that not only coating can be fabricated onto CFRP, the interlayer coating is not needed by the use of this method. In conventional plasma spray, the Cu or Ni interlayer is needed in order to fabricate the coating and the same goes to hard chrome plating where Cu interlayer by electroplating is needed prior to plating with hard chrome.

Nonetheless, the coating deposition of $TiO_2$ with high anatase content rate which is beneficial for photocatalytic activity can also be achieved. By using this newly developed low power microwave plasma spray method, the applicability of thermal spray in thermally sensitive materials (both substrates and spray materials) can be achieved.

### 6.2.2 *Contribution towards industrial sector*

From this study, it is known that the hard chrome coating can be deposited by extremely low power by low power plasma spray method. This can be an alternative method for hard chrome plating which produces harmful exhaust. This coating technology also has the benefit over electroplating due to it being dry process where the process can be much simpler and easy to be setup. For many years, the research on using thermal spray as an alternative for hard chrome plating has been and the method which is focused is HVOF (high velocity oxy fueled) spray. However, as been discussed in detail in Chapter 3, this method is not applicable to heat susceptible substrate due to the excessive heat and the low power microwave plasma spray will make an appeal in this matter profoundly successful.

# References

## Chapter 1

[1] J. R. Davis, Handbook of surface engineering for corrosion and wear resistance, ASM International (2001).

[2] J. Hasui, New Publication, Thermal Spraying Engineering, Sanpo Publication, (1990) (in Japanese).

[3] C. Verdon, A. Karimi, J. L. Martin, A Study of High Velocity Oxy-Fuel Thermally Sprayed Tungsten Carbide Based Coatings, Part 1: Microstructures, Materials Science Engineering A, 246 (1998) 11-24.

[4] M. I . Boulos, ,P. Fauchais, E. Pfender, Thermal Plasmas: Fundamentals and Applications, Plenum Press, New York, (1994).

[5] T. Yasui, D. Yamaguchi, Y. Kimura and M. Fukumoto, Application of Atmospheric Pressure Microwave Discharge to Plasma Spray, Industrial Application of Plasma Process, 2 (2009) 1-7.

[6] S. Dyshlovenko, B. Pateyron, L. Pawlowski, D. Murano, Numerical simulation of hydroxyapatite powder behaviour in plasma jet, Surface and Coatings Technology, 179 (2004) 110-117.

[7] J. S. Cho, D. S. Jung, J. M. Han, Y. C. Kang, Nano-sized α and β-TCP powders prepared by high temperature flame spray pyrolysis, Materials Science and Engineering: C, 29 (2009) 1288-1292.

[8] E. Lugscheider, P. Remer, C. Herbst, K. Yushchenko, Thermal Spraying: Current Status and Future Trends, High Temperature Society of Japan, (1995) 273-282.

[9] J. Karthikeyan, C. C. Berndt, J. Tikkanen, S. Reddy, H. Herman, Plasma spray synthesis of nanomaterial powders and deposits, Materials Science and Engineering: A, 238 (1997) 275-286.

[10] C.-J. Li, B. Sun, Microstructure and property of micro-plasma-sprayed Cu coating, Materials Science and Engineering: A, 379 (2004) 92-101.

[11] C. -J. Li, T. Wu, C. -X. Li, Effect of spray particle trajectories on the measurement signal of particle parameters based on thermal radiation, Journal of Thermal Spray Technology, 12 (2003) 80-94.

[12] A. Minenaga, Master's Thesis of Toyohashi University of Technology, (2004).

[13] M. I. Boulos, RF induction plasma spraying: State-of-the-art review, Journal of Thermal Spray Technology, 1 (1992) 33-40.

[14] T. Yasui, Study of plasma generation method by the microwave for process applications, Doctoral Thesis of Osaka University, (1994).

[15] S. Sato, Microwave plasma investigation ad hoc committee, Institute of Electrical Engineers of Japan, Technology of microwave plasma, Ohmsha, (2003) (in Japanese).

[16] K. Tsujimoto, Master's Thesis of Toyohashi University of Technology, (2006).

[17] A. Ganguli, R. D. Tarey, Understanding plasma sources, Current Science, 83 (2002) 279-290.

[18] C. Joseph, Handbook of Plasma Processing Technology, Noyes Publications, Park Ridge, New Jersey, (1990).

[19] A. L. Michael, J. L. Allan, Principles of Plasma Discharges and Materials Processing, John Wiley, New York, (1994).

[20] A. Seyed, Co-spraying of alumina and stainless steel by d.c. plasma jets, Doctoral Thesis of University of Limoges France and GIK Institute, (2004).

[21] M. Yamada, T. Inamoto, M. Fukumoto, T. Yasui, Fabrication of Silicon Nitride Thick Coatings by Reactive RF Plasma Spraying, Materials Transactions, 45 (2004) 3304-3308.

[22] Y. L. Li, T. Ishigaki, Spheroidization of Titanium Carbide Powders by Induction Thermal Spray Processing, Journal of the American Ceramic Society, 84 (2012) 1929-1936.

[23] P. Linke, K. H. Weiss, G. Nutsch, New manufacturing technologies of two phase tungsten carbide. Materialwissenschaft und Werkstofftechnik, 34 (2008) 613-617.

[24] J. Noelte, ICP Emission Spectrometry – A Practical Guide, Wiley-VCH, Weinhem, (2002).

[25] Commission Directive 2013/28/EC, Official Journal of the European Union, (2013).

[26] J. A. Picas, HVOF coatings as an alternative to hard chrome for pistons and valves, Wear, 261 (2006) 477–484.

[27] D. Startwell, Thermal Spray Coatings as Alternative to Hard Chrome Plating, Welding Journal (2000) 39-43.

[28] J. Weng, M. Wang, J. Chen, Plasma-sprayed calcium phosphate particles with high bioactivity and their use in bioactive scaffolds, Biomaterials, 23 (2002) 2623-2629.

[29] O. Yukio, High-sensitivity microwave-induced plasma mass spectrometry for trace element analysis, Journal of Analytical Atomic Spectrometry, 9 (1994) 745-749.

[30] T. Yasui, D. Yamaguchi, Y. Kimura and M. Fukumoto, Proceedings of 18th International Symposium on Plasma Chemistry, Kyoto (2007) CD.

[31] T. Yasui, K. Tsujimoto, T. Kondo, and M. Fukumoto, Operational characteristics of atmospheric pressure microwave plasma spraying onto low melting point materials, Proceedings of 19th International Symposium On Plasma Chemistry, Bochum (2009) USB.

[32] A. Fujishima, K. Honda, Electrochemical Photolysis of Water at a Semiconductor Electrode, Nature, 238 (1972) 37-38.

[33] M. R. Hoffmann, S.T. Martin, W. Choi, D. W. Bahnemann, Environmental Applications of Semiconductor Photocatalysis, Chemical Reviews, 95 (1995) 69-96.

[34] A. Bumajdad, M. Madkour, Understanding the superior photocatalytic activity of noble metals modified titania under UV and visible light irradiation, Physical Chemistry Chemical Physics, 16 (2014) 7146-7158.

[35] A. Fujishima, K. Hashimoto, T. Watanabe, $TiO_2$ Photocatalysis: fundamentals and application, BKC, Tokyo (1999).

[36] C. Lee, H. Choi, C. Lee, H. Kim, Photocatalytic properties of nano-structured $TiO_2$ plasma sprayed coating, Surface and Coatings Technology, 173 (2003) 192-200.

## Chapter 2

[1] M. J. Moran, H. N. Shapiro, D. D. Boettner, M. B. Bailey, Fundamentals of Engineering Thermodynamics, Wiley, (2010).

[2] Y. Arata , Thermal Spray of Ceramics and the applications, Nikkan Kogyo Shimbun, (1999) (in Japanese).

[3] K. Mitsuharu, Fundamental of Plasma and Coating Deposition, Nikkan Kogyo Shimbun, (1991) (in Japanese).

[4] S. Lee, Energy balance and the radius of electromagnetically pinched plasma columns, Plasma Physics, 25 (1983) 571–576.

[5] H. Daidoji, Atomic spectra measurement and its application, Society Publishing Center, (1989) (in Japanese).

[6] P. Fauchais, A.Vardelle, Heat, mass and momentum transfer in coating formation by plasma spraying, International Journal of Thermal Sciences, 39 (2000) 852-870.

[7] M. L. Thorpe, Thermal Spray: Industry in Transition, Advanced Material Processing, 143 (1993) 50–56.

[8] O. Yukio, High-sensitivity microwave-induced plasma mass spectrometry for trace element analysis, Journal of Analytical Atomic Spectrometry, 9 (1994) 745-749.

[9] S. Sato, Microwave plasma investigation ad hoc committee, Institute of Electrical Engineers of Japan, Technology of microwave plasma, Ohmsha, (2003) (in Japanese).

[10] T. Yasui, D. Yamaguchi and M. Fukumoto, Proceedings of 5th International Symposium on Microwave Science and Its Application to Related Fields, Tsukuba, (2005) 52-53.

[11] T. Yasui, D. Yamaguchi, Y. Kimura and M. Fukumoto, Proceedings of 2nd Asian Thermal Spray Conference, Korea, (2006) 62-63.

[12] T. Yasui, D. Yamaguchi, Y. Kimura and M. Fukumoto, Proceedings of 18th International Symposium on Plasma Chemistry, Kyoto, (2007) CD.

[13] A. Redza, T. Yasui, M. Fukumoto, Deposition of Hard Chrome Coating onto Heat Susceptible Substrates by Low Power Microwave Plasma Spray, IOP Conference Series: Material Science Engineering, 114 (2016) 01230, 1-10.

[14] A. Redza, T. Kondo, T. Yasui, M. Fukumoto, High Anatase Rate Titanium Dioxide Coating Deposition by Low Power Microwave Plasma Spray, IOP Conference Series: Material Science Engineering, 114 (2016) 01231, 1-9.

[15] R. Alvarez, A. Rodero, M.C. Quintero, An Abel inversion method for radially resolved measurements in the axial injection torch, Spectrochimica Acta Part B: Atomic Spectroscopy, 57 (2002) 1665-1680.

[16] S. Y. Moon, W. Choe, H. S. Uhm, Y. S. Hwang, J. J. Choi, Characteristics of an atmospheric microwave-induced plasma generated in ambient air by an argon discharge excited in an open-ended dielectric discharge tube, Physics of Plasmas, 9 (2002) 4045-4051.

[17] M. S. Bronet, Particle velocity measurements in induction plasma spraying, Plasma Chemistry and Plasma Processing, 9 (1989) 343-353.

[18] M. Vardelle, A. Vardelle, P. Fauchais, K.-I. Li, B. Dussoubs, N. J. Themelis, Controlling Particle Injection in Plasma Spraying, Journal of Thermal Spray Technology, 10 (2001) 267-284.

[19] M. Pasandideh-Fard, V. Pershin, S. Chandra, and J. Mostaghimi, Splat Shapes in a Thermal Spray Coating Process: Simulations and Experiments, Journal of Thermal Spray Technology, 11 (2002) 206-217.

[20] M. Fukumoto, T. Yamaguchi, M. Yamada, T. Yasui, Splash Splat to Disk Splat Transition Behavior in Plasma-Sprayed Metallic Materials, Journal of Thermal Spray Technology, 16 (2007) 905-912.

[21] C. Mundo, M. Sommerfeld, and C. Tropea, Droplet-wall Collisions: Experimental Studies of the Deformation and Breakup Process, International Journal of Multiphase Flow, 21 (1995) 151-173.

## Chapter 3

[1] M. Breitsameter, Thermal Spraying versus Hard Chrome Plating, Materials Australasia, 32 (2000) 11-13.

[2] Commission Directive 2013/28/EC, Official Journal of the European Union, (2013).

[3] J. A. Picas, HVOF coatings as an alternative to hard chrome for pistons and valves, Wear, 261 (2006) 477–484.

[4] B. D. Startwell, Thermal Spray Coatings As an Alternative to Hard Chrome Plating, Welding Journal, (2000) 39-43.

[5] M. L. Thorpe, Thermal Spray: Industry in Transition, Advanced Materials Processing, 143 (1993) 50–56.

[6] J. Karthikeyan, C. C. Berndt, J. Tikkanen, S. Reddy, H. Herman, Plasma spray synthesis of nanomaterial powders and deposits, Materials Science Engineering: A, 238 (1997) 275-286.

[7] C. J. Li, B. Sun, Microstructure and property of micro-plasma-sprayed Cu coating, Materials Science and Engineering: A, 379 (2004) 92-101.

[8] C. J. Li, T. Wu, C. X. Li, B. Sun, Effect of spray particle trajectory on the measurement signal of particle parameters based on thermal radiation, Journal of Thermal Spray Technology, 12 (2003) 80-94.

[9] T. Yasui, D. Yamaguchi, Y. Kimura and M. Fukumoto, Application of Atmospheric Pressure Microwave Discharge to Plasma Spray, Industrial Application of Plasma Process, 2 (2009) 1-7.

[10] O. Yukio, High-sensitivity microwave-induced plasma mass spectrometry for trace element analysis, Journal of Analytical Atomic Spectrometry, 9 (1994) 745-749.

[11] S. Sato, Microwave plasma investigation ad hoc committee, Institute of Electrical Engineers of Japan, Technology of microwave plasma, Ohmsha, (2003) (in Japanese).

[12] T. Yasui, D. Yamaguchi, Y. Kimura and M. Fukumoto, Procedings of 18th International Symposium on Plasma Chemistry, Kyoto (2007) CD.

[13] T. Yasui, K. Tsujimoto, T. Kondo, and M. Fukumoto, Operational characteristics of atmospheric pressure microwave plasma spraying onto low melting point materials, Proceedings of 19th International Symposium on Plasma Chemistry, Bochum (2009) USB.

[14] J. S. Cho, D. S. Jung, J. M. Han, Y. C. Kang, Nano-sized α and β-TCP powders prepared by high temperature flame spray pyrolysis, Materials Science and Engineering: C, 29 (2009) 1288-1292.

[15] K. Tsujimoto, Master's Thesis of Toyohashi University of Technology, (2011) (in Japanese).

[16] T. Kondo, Master's Thesis of Toyohashi University of Technology, (2011) (in Japanese).

## Chapter 4

[1] A. Fujishima, K. Honda, Electrochemical Photolysis of Water at a Semiconductor Electrode, Nature, 238 (1972) 37-38.

[2] M. R. Hoffmann, S. T. Martin, W. Choi, D. W. Bahnemann, Environmental Applications of Semiconductor Photocatalysis, Chemical Reviews, 95 (1995) 69-96.

[3] A. Bumajdad, M. Madkour, Understanding the superior photocatalytic activity of noble metals modified titania under UV and visible light irradiation, Physical Chemistry Chemical Physics, 16 (2014) 7146-7158.

[4] A. Fujishima, K. Hashimoto, T. Watanabe, $TiO_2$ Photocatalysis: fundamentals and application, BKC, Tokyo (1999).

[5] C. Lee, H. Choi, C. Lee, H. Kim, Photocatalytic properties of nano-structured TiO2 plasma sprayed coating, Surface and Coatings Technology, 173 (2003) 192-200.

[6] T. Yasui, D. Yamaguchi, Y. Kimura and M. Fukumoto, Application of Atmospheric Pressure Microwave Discharge to Plasma Spray, Industrial Application of Plasma Process, 2 (2009) 1-7.

[7] N. Berger-Keller, G. Bertrand, C. Filiatre, C. Meunier, C. Coddet, Microstructure of plasma-sprayed titania coatings deposited from spray-dried powder, Surface and Coatings Technology, 168 (2003), 281–290.

[8] M. Bozorgtabar, M. Rahimipour, M. Salehi, Novel photocatalytic $TiO_2$ coatings produced by HVOF thermal spraying process, Materials Letters, 64 (2010) 1173-1175.

[9] Y. Li, T. Ishigaki, Thermodynamic analysis of nucleation of anatase and rutile from $TiO_2$ melt, Journal of Crystal Growth, 242 (2002) 511-516.

[10] A. McDonald, C. Moreau, S. Chandra, Effect of substrate oxidation on spreading of plasma-sprayed nickel on stainless steel, Surface and Coatings Technology, 202 (2007) 23-33.

[11] T. Yasui, K. Tsujimoto, T. Kondo, and M. Fukumoto, Operational characteristics of atmospheric pressure microwave plasma spraying onto low melting point materials, Proceedings of 19th Inernational Symposium on Plasma Chemistry, Bochum (2009), USB.

[12] S. Lee, Energy balance and the radius of electromagnetically pinched plasma columns, Plasma Physics, 25 (1983) 571–576.

## Chapter 5

[1] P. Gougeon, C. Moreau, A New Sensor for On-Line Diagnostic of Particles Under Thermal Spraying Conditions, Advanced Processing Techniques, 6 (1994) 199-210.

[2] M. I. Boulos, P. Fauchais, E. Pfender, Thermal Plasmas: Fundamentals and Applications, Plenum Press, New York, 1994.

[3] H. E. Knoepfel, Magnetic Fields: A Comprehensive Theoretical Treatise for Practical Use, Wiley-VCH, 2000.

# Publication list

## List of Papers/Journals with Referee's Review

1. Ahmad Redza, Toshiaki Yasui and Masahiro Fukumoto, "Deposition of Hard Chrome Coating onto Heat Susceptible Substrates by Low Power Microwave Plasma Spray," Materials Science and Engineering, Vol. 114, No. 1, 01230, pp.1-9, 2016.
2. Ahmad Redza, Toshiki Kondo, Toshiaki Yasui and Masahiro Fukumoto, "High Anatase Rate Titanium Dioxide Coating Deposition by Low Power Microwave Plasma Spray," Materials Science and Engineering, Vol. 114, No. 1, 01231, pp.1-10, 2016.

## List of Papers at International Conference with Referee's Review

1. Ahmad Redza, Toshiaki Yasui and Masahiro Fukumoto, "Mechanism Study of High Hardness Wear Resistant Coating onto Heat Susceptible Substrates Deposited by Low Power Microwave Plasma Spray," Proceedings of the 2014 Asian Thermal Spray, pp. 169-170, 2014.
2. Toshiaki Yasui, Ahmad Redza, Masahiro Fukumoto, "Development of Low Power Plasma Spray Process Using Atmospheric Pressure Microwave Plasma," Proceedings of the 2013 International Thermal Spray Conference, pp. 433-436, 2013.

## International Conference Participation

1. Ahmad Redza, Toshiaki Yasui and Masahiro Fukumoto, "Deposition of high hardness metal coating by using microwave plasma spray," ISPlasma 2012, 2012.3.5, Nagoya, Japan, 2012.
2. Ahmad Redza, Toshiaki Yasui and Masahiro Fukumoto, "Deposition of high hardness coating by using low power atmospheric pressure microwave plasma spray," 2012 Asian Thermal Spray Conference, 2012.11.26, Tsukuba, Japan, 2012.
3. Ahmad Redza, Toshiki Kondo, Toshiaki Yasui and Masahiro Fukumoto, "Deposition of titanium dioxide coating by using low power atmospheric pressure microwave plasma spraying," The 5th International Symposium on

Designing,Processing and Properties of Advanced Engineering Materials ISAEM-2012, 2012.11.5, Toyohashi, Japan, 2012.

4. Ahmad Redza, Toshiaki Yasui and Masahiro Fukumoto, "Mechanism Study of High Hardness Wear Resistant Coating onto Heat Susceptible Substrates Deposited by Low Power Microwave Plasma Spray," 2014 Asian Thermal Spray, 2014.11.25, Hyderabad, India, 2014.
5. Ahmad Redza, Toshiaki Yasui and Masahiro Fukumoto, "Deposition of Hard Chrome Coating onto Heat Susceptible Substrates by Low Power Microwave Plasma Spray," Joint conference of iMEC 2015 (2nd International Manufacturing Engineering Conference & APCOMS 2015 (3rd Asia-Pacific Conference on Manufacturing Systems), Kuala Lumpur, Malaysia, 2015.
6. Ahmad Redza, Toshiki Kondo, Toshiaki Yasui and Masahiro Fukumoto, "High Anatase Rate Titanium Dioxide Coating Deposition by Low Power Microwave Plasma Spray," Joint conference of iMEC 2015 (2nd International Manufacturing Engineering Conference & APCOMS 2015 (3rd Asia-Pacific Conference on Manufacturing Systems), Kuala Lumpur, Malaysia, 2015.

## Local Meeting Participation

1. Ahmad Redza, Toshiaki Yasui and Masahiro Fukumoto, "Deposition of Hard Chrome Coating by Low Power Atmospheric Pressure Microwave Plasma Spraying," Technical Meeting of Plasma Science and Technology, 2012.5.11, Toyohashi, Japan 2012.
2. Ahmad Redza, Toshiaki Yasui and Masahiro Fukumoto, "Study on Plasma and Spray Particles Behavior of Low Power Microwave Plasma Spray," 2016 Japan Thermal Spray Society Spring Meeting, 2016.6.7, Osaka, Japan, 2016.

# Acknowledgements

First and foremost, I would like to express my deepest gratitude and thankfulness to the Absolute Creator of the world and mankind, Allah Subhanahu Wa Taala, The Benefecient the Most Merciful for giving me the strength and will to complete this project.

I take immense pleasure in thanking Associate Prof. Toshiaki Yasui, Prof. Masahiro Fukumoto, and Asst. Prof. Motohiro Yamada, for having permitted me to carry out this project work and especially to Prof. Toshiaki Yasui for continuous supports and ideas as well as guidance in order to complete this project. I also wish to express my deep sense of gratitude to Prof. Takayuki Shibata of MEMS/NEMS Processing Laboratory for the guidance and useful suggestions.

Words are inadequate in offering my thanks to my microwave group colleagues of the Interface and Surface Fabrication Laboratory which are Toshiki Kondo, Keisuke Yamada, Mikiyasu Kamano, and as well as my labmates, Keisuke Atsumi, Takaaki Shimizu, Hiroki Tahara, Daichi Mano, Hiroki Mizushima, Shuta Yoshino and Yuta Watanabe for their encouragement and cooperation in carrying out the project work.

Finally, yet importantly, I would like to express my heartfelt thanks to my beloved parents for their blessings, my wife, children and friends for their help and wishes for the successful completion of this project.